IDENTIFICATION OF INTERACTION PARTNERS OF UNZIPPED,

A NOVEL CELL ADHESION MOLECULE

by

Gamze Akgün

B.S., Molecular Biology and Genetics, Boğaziçi University, 2011

Submitted to the Institute for Graduate Studies in

Science and Engineering in partial fulfillment of

the requirements for the degree of

Master of Science

Graduate Program in Molecular Biology and Genetics

Boğaziçi University

2013

IDENTIFICATION OF INTERACTION PARTNERS OF UNZIPPED,

A NOVEL CELL ADHESION MOLECULE

APPROVED BY:

Assoc. Prof. Arzu Çelik ……………………….
(Thesis Supervisor)

Prof. Neş'e Bilgin ……………………….

Assoc. Prof. Uygar Halis Tazebay ……………………….

DATE OF APPROVAL: 24.10.2013

ACKNOWLEDGEMENTS

Foremost, I would like to thank my advisor Assoc. Prof. Arzu Çelik for her guidance, supervision, and support during my study. I'm grateful for her understanding.

I'm thankful to Prof. Neş'e Bilgin and Assoc. Prof. Uygar Halis Tazebay for devoting their time to evaluate my thesis.

I would like to send my sincere thanks to my labmates; Bahar for answering patiently every question of mine, Ece for bringing constant joy to my days in the lab, Kaan for making me laugh especially with his moustache, Güner, Stefan, Çağrı and Rıdvan for their help and friendship, and everything else. I would also like to thank my sister-lab members: Xalid Bayramlı, Tuba Özaçar, Kerem Uzel and Gizem Sancer.

I'm truly thankful to Duygu Koldere, for her unconditional love and friendship. I really enjoyed our time together. I'm grateful to have such a sincere friend.

A simple 'thank you' is not enough to explain my gratitude towards Kerem Yıldırım. He is the one who thought me true friendship, by being there for me whenever I needed. He did not let me down for even a second during my years in Boğaziçi.

I also want to send my thanks to Merve Sıvacı, Selen Zülbahar, Kaya Akyüz, Merve Kılınç, Burak Tepe and Oğuzhan Kaya for being great friends and many things that cannot be listed here…

My heartfelt thanks go to Yasemin Büyükçolak, Şebnem Zeyveli, Esra Şekerci, Şule Terzioğlu, Özge Yıldız, Hilal Kahraman and Saliha Yıldızhan for their endless support and friendship.

My deepest thanks belong to Mehmet Emin Gönen for being my light and giving my heart peace. Without him, I would not find the strength to bare the difficulties. He was always there to hold my hand. I am so lucky to have him.

And last but not least, I thank my parents, my brother, my sister and my cousin Banu for their everlasting love and support.

ABSTRACT

IDENTIFICATION OF INTERACTION PARTNERS OF UNZIPPED, A NOVEL CELL ADHESION MOLECULE

The brain is unquestionably the most sophisticated organ in bodies of many organisms. Establishment of this complex architecture depends on the ability of axons to find their proper targets. On their way to their synaptic sites axons follow guidance cues, which can be repulsive or attractive. Negative and positive adhesion between these guidance cues and axon guidance molecules on the cell surface of axons determine the path on which axons elongate. While some axons (pioneer axons) are steered by cues, some others (follower axons) follow the previously formed paths. Unzipped (Uzip), a novel cell adhesion molecule is expressed in neurons and glial cells and is involved in proper targeting of *Drosophila* olfactory receptor neurons (ORNs). Unzipped is expressed in pioneer neurons, which are guided by glia-derived Uzip through homophilic interaction. We hypothesize that Uzip localized to pioneer neurons interacts with other adhesion molecules on follower axons through heterophilic interactions. In an attempt to prove our hypothesis and understand the mechanism of Unzipped guidance function, we aimed to identify interaction partners of Uzip. For this purpose we performed co-immunoprecipitation assays followed by Mass spectrometry analysis. Among the proteins that were identified in this analysis, four candidates were selected for more detailed analysis: Hts, dFMR1, EPS15 and Syn. Co-IP experiments performed to validate the MS results did not reveal any physical interaction between these candidates and Uzip. Additionally, analysis of the expression pattern of these four proteins revealed that in most cases these do not co-localize with Unzipped, except for Hts where more detailed analyses are needed before excluding it as an interaction partner. Furthermore, the expression pattern of a Flag-HA-tagged Uzip fusion protein was analyzed throughout *Drosophila* nervous system development to reveal its endogenous expression pattern.

ÖZET

YENİ HÜCRE ADHEZYON MOLEKÜLÜ UNZIPPED'İN ETKİLEŞİM PARTNERLERİNİN BELİRLENMESİ

Beyin, birçok organizmanın vücudundaki en karmaşık organdır. Bu karmaşık yapının oluşumu aksonların doğru hedeflerini bulma yeteneğine bağlıdır. Aksonlar sinaptik bölgelerine doğru ilerlerken çekici veya itici olabilen işaretler tarafından yönlendirilmektedir. Akson hücre yüzeyindeki akson yönelim molekülleri ile rehber işaretler arasındaki negatif ve pozitif adhezyon, aksonların üzerinde uzadığı yolu belirlemektedir. Bazı aksonlar (öncü aksonlar) işaretler tarafından yönlendirilirken, diğerleri (takipçi aksonlar) önceden oluşmuş yolları takip etmektedir. Nöron ve glia hücrelerinde anlatılan yeni bir hücre adhezyon molekülü olan Unzipped (Uzip) *Drosophila* koku reseptör nöronlarının (KRN) doğru hedeflerine ulaşmalarında görev almaktadır. Unzipped, öncü nöronlarda anlatılmaktadır ve bu nöronlar gliadan gelen Uzip ile homofilik etkileşimle yönlendirilmektedir. Öncü nöronlarda bulunan Uzip'in, takipçi aksonlar üzerindeki diğer adhezyon molekülleri ile heterofilik etkileşimlerde bulundukları tahmin edilmektedir. Hipotezimizi kanıtlamak ve Unzipped'in yönelim işlevinin mekanizmasını anlamak amacıyla, Uzip'in etkileşim partnerlerini bulmayı amaçladık. Bu amaçla, ko-immünopresipitasyon deneyini takiben, kütle spektrometresi analizi gerçekleştirdik. Bu analizle bulunan proteinler arasında, dört aday ileri incelemeler için seçilmiştir: Hts, dFMR1, EPS15 ve Syn. Kütle spektrometresi sonuçlarını doğrulamak için yapılan ko-immünopresipitasyon deneyleri, bu adaylar ve Uzip arasında hiçbir fiziksel etkileşim göstermemiştir. Ayrıca, bu dört proteinin anlatım örüntüsünün incelenmesi, çoğu durumlarda, Hts dışındakilerin Unzipped ile kolokalize olmadıklarını ortaya koymuştur ve Hts'nin de etkileşim partneri olmadığı sonucuna varılması için daha fazla inceleme gerekmektedir. Bunun yanında, Uzip'in *Drosophila* sinir sistemi gelişim aşamalarındaki endojen anlatım örüntüsü, Flag-HA-işaretli Uzip füzyon proteinin anlatım örüntüsü incelenerek ortaya çıkarılmıştır.

TABLE OF CONTENTS

LIST OF FIGURES

LIST OF TABLES

LIST OF ACRONYMS/ABBREVIATIONS

AL	Antennal Lobe
APF	After Puparium Formation
BAC	Bacterial Artificial Chromosome
CAMs	Cell Adhesion Molecules
CNS	Central Nervous System
DCC	Deleted in Colorectal Cancer
Dscam	Down Syndrome Cell Adhesion Molecule
ECM	Extracellular Matrix
EGFR	Epidermal Growth Factor Receptor
EPS15	Epidermal Growth Factor Receptor Pathway Substrate Clone 15
FMRP	Fragile X Mental Retardation Protein
GFP	Green Fluorescent Protein
GO	Gene Ontology
HRP	Horse Radish Peroxidase
kD	Kilo Dalton
Ig	Immunoglobulin
LG	Longitudinal Glia
LH	Lateral Horn
LN	Local Interneuron
MB	Mushroom Body
MS	Mass Spectrometry
N-Cad	N-cadherin
NGS	Normal Goat Serum
OR	Olfactory Receptor
ORN	Olfactory Receptor Neuron
PBS	Phosphate Buffered Saline
PFA	Paraformaldehyde
pH	Power of Hydrogen
PN	Projection Neuron
PR	Photoreceptor

RBG   Retinal Basal Glia

RNA   Ribonucleic Acid

Uzip   Unzipped protein

1. INTRODUCTION

The brain, which perceives and processes information coming from the outside world or inside the body, is the most complex organ in most organisms. What makes it so complex and unique is its special structure and connections of neurons. In adult humans, for example, each neuron makes synapses with over a thousand target cells. The correct establishment of this complex circuit pattern is essential for the proper functioning of the nervous system.

The fruit fly, *Drosophila melanogaster*, is a popular model organism since Morgan has started genetic analyses on it (Morgan, 1910), and his discoveries earned him the Nobel Prize for Medicine in 1933. *Drosophila* is a powerful experimental organism since it can be cultured in mass, has a short life-time, and advanced molecular genetic tools are readily available. The fruit fly has a simple and well-defined nervous system and its structure and development are similar to that of vertebrates (Reichert, 2009; Sprecher, 2012). Thus, in order to understand the development and function of the nervous system *Drosophila* is preferably and widely used.

1.1. Visual and Olfactory Systems of *Drosophila melanogaster*

1.1.1. Organization of the *Drosophila* Visual System

The visual system of *Drosophila* consists of the compound eye and the optic lobe, which is the visual information processing center. The optic lobe is composed of four ganglia: the lamina, the medulla, the lobula, and the lobula plate. The compound eye is formed by approximately 800 units of eye-like structures called 'ommatidia' (Fischbach and Hiesinger, 2008). The ommatidia are composed of 8 photoreceptor (PR) cells and 12 supporting cells. PRs are separated into two subsets depending on their position within the ommatidia as inner and outer PRs. The outer PRs (R1-R6) are similar to rod cells of humans in detecting motion in dim light and the inner PRs (R7 and R8) are detecting color

as cone cells of mammals. The outer and inner PRs can again be divided based on their opsin gene expression pattern. R1-R6 neurons express the opsin Rh1, which responds to a broad light spectrum. R7 cells express either UV-sensitive Rh3 or Rh4; in contrast R8 cells express either Rh5 or Rh6, which are blue-sensitive and green-sensitive, respectively (*reviewed in* Ting and Lee, 2007).

While PRs differentiate, their axons project to the optic ganglion (Figure 1.1) (*explained in detail in* 1.2.2.). The R8 cells are the first cells to differentiate and send their axons out of the retina. Then the outer PRs differentiate, their axons bundle and elongate along R8 axons. The axons of the outer PRs follow the R8 axons through the optic stalk to the first optic ganglion, the lamina. Lastly, R7 neurons differentiate and project to the medulla. The outer PRs terminate in the lamina, whereas R7 and R8 axons terminate in the M6 and M3 layers of the medulla, respectively. Stopping at the lamina, outer PR axons distribute themselves into six different lamina cartridges for the establishment of a correct visuotopical map (Clandinin and Zipursky, 2000). The PRs make synapses with the interneurons in the lamina and medulla, which then project to higher processing centers, the lobula and the lobula plate (*reviewed in* Hadjieconomou *et al*., 2011).
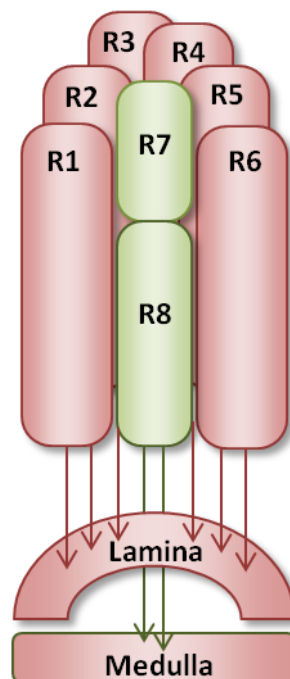
Figure 1.1. Schematic drawing of an ommatidium. Outer PRs (R1-R6) surround inner PRs (R7 and R8). R7 is distal and R8 is proximal.

Throughout the establishment of a correct retinotopical map in the fruit fly eye, axons of PRs are lead to their final destinations. This leading process occurs through interactions of molecules on the axon membrane with the other cells or the environment. Therefore, the visual system has been a good model for axon guidance studies as well.

1.1.2. Organization of the *Drosophila* Olfactory System

The olfactory organs of *Drosophila* include the third segment of the antenna and the maxillary palp. Olfactory stimuli coming from these organs are processed in the brain, in a region called the antennal lobe (AL) (Figure 1.2).
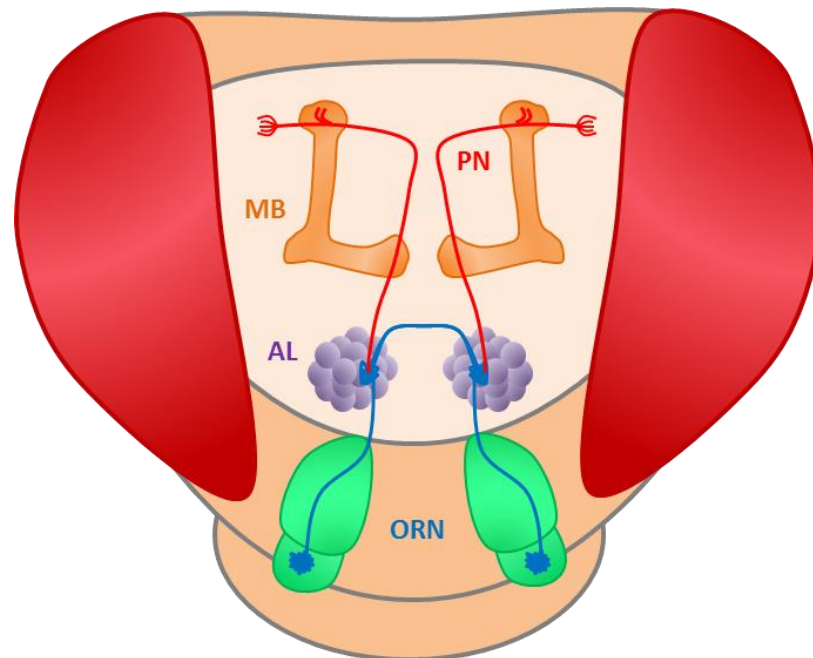
Figure 1.2. Schematic presentation of the fly olfactory system. ORNs project from the antenna and maxillary palp (not shown) to the AL and synapse with PNs. PNs, in turn, project to the MBs and lateral horn. AL: Antennal lobe, PN: Projection neuron, MB: Mushroom body. (adapted from Hansson *et al.,* 2009).

The sensory neurons of the olfactory system are called olfactory receptor neurons (ORN). There are approximately 1200 ORNs in the main olfactory organ antenna and 120 ORNs in the maxillary palp. Cell bodies of ORNs are found in hair-like structures, called sensilla, on these organs together with non-neuronal support cells (Shanbhag *et al.*, 2000; Hallem and Carlson, 2004). There are three distinct morphological types of sensilla: basiconic, trichoid, and coeloconic. All three classes of sensilla are found on the antenna;

however, the maxillary palp houses only basiconic sensilla (Vosshall *et al.*, 1999). Each sensillum usually contains two ORNs, but there are some exceptional sensilla that house three or four ORNs (Hallem and Carlson, 2004).

ORNs expressing one of the ~60 olfactory receptor (OR) genes project their axons to the antennal lobe. Axons of ORNs that are expressing the same OR gene synapse to a region on the antennal lobe called 'glomerulus' (Figure 1.2). The antennal lobe, the *Drosophila* counterpart of the olfactory bulb in vertebrates, is the first olfactory processing center (Mombaerts, 2001). When ORN axons reach the AL, they form the glomerular structure by synapsing with higher order neurons: local interneurons (LNs) and projection neurons (PNs). LNs branch and synapse with neurons in multiple glomeruli, providing information transfer between them. Olfactory stimuli coming through ORNs are sent to the higher olfactory processing centers in the brain, the mushroom bodies (MB) and the lateral horn (LH), by PNs (Hallem and Carlson, 2004).

Antennal ORNs elongate their axons, before they start to express OR genes, through the antennal nerve to the newly forming AL during pupation (Figure 1.3) (*Explained in detail* in 1.2.3). Glomerular pattern formation of the AL begins before ORN axons reach their targets, by PNs and glial cells (Jefferis *et al.*, 2004). ORN axons expressing the same OR converge into the same glomerulus. The position of each glomerulus that houses a distinct class of ORNs is detectable. Axons of the maxillary palp ORNs extend in a different way than antennal ORNs, through the labial nerve by passing across the suboesophageal ganglion (SOG). After ORN axons project to the ipsilateral side of the AL, they cross the midline and connect to symmetrical glomeruli on the contralateral side. Axons of olfactory sensory neurons make synapses in glomeruli with their targets: higher order LNs and PNs (Stocker *et al.*, 1990).

During these targeting processes, axons are guided by many cues to the antennal lobe and to their appropriate glomerulus. This highly regulated system constitutes a good model for pathfinding and axon targeting research.
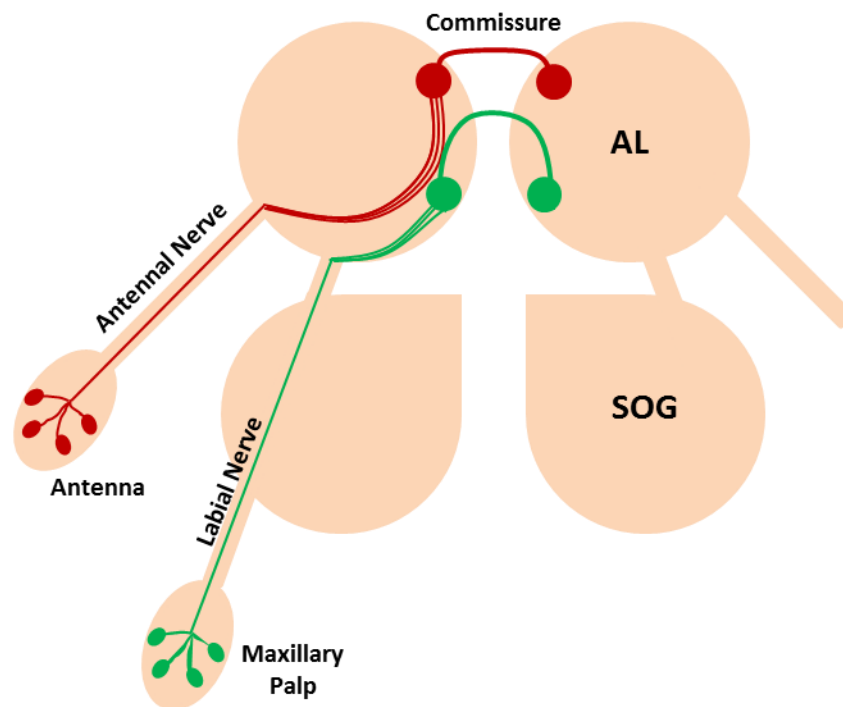
Figure 1.3. Projection of ORNs to the AL. ORNs that project from the antenna and the maxillary palp follow different paths. In order to reach the destined glomeruli, axons of antennal ORNs fasciculate and pass through the antennal nerve. In contrast, maxillary palp neurons project to the AL through the labial nerve by passing through the SOG (adapted from Hummel *et al.*, 2003).

1.2. Axon Guidance

The accurate functioning of a nervous system depends on the establishment of correct connections of neurons. The assembly of the neuronal circuitry requires axons to travel along precise pathways and synapse to their appropriate targets. The guidance of axons is a complex process, which can happen in two ways: axons can follow the paths formed by pioneering axons or they can find their path individually by responding to guidance cues. The growth cone of the axons navigates over long distances by responding to extracellular guidance cues. The ability of growth cones to track down attractive cues and escape from the repulsive ones facilitates the formation of appropriate connections.

1.2.1. Axon Guidance Molecules

Extracellular cues can enlighten the way to the elongating axons in four different mechanisms: chemoattraction, chemorepulsion, contact-mediated attraction and contact-mediated repulsion (Cook *et al*., 1998; Stoeckli *et al*., 1998). These four mechanisms work in a combined manner in order to form the intricate structure of the nervous system. Growth cones can be guided by long-range chemoattractans or chemorepellents that are secreted by intermediate or final target cells. In addition to these diffusible long-range cues, short-range cues coming from nearby cells and the extracellular matrix (ECM) have also an important role on the guidance of axons. These contact-mediated mechanisms involve cell surface molecules and non-diffusible ECM molecules (Hynes and Lander, 1992). Genetic and biochemical studies have led to the identification of several conserved axon guidance molecule families.

1.2.1.1. Netrins. Netrins are an extracellular chemotropic guidance protein family that has functions in cell migration and axon guidance during embryonic development. They are conserved among species that have bilateral symmetry. Netrins can attract or repel axons from short or long distances, depending on the circumstances (Sun *et al*., 2011). The family has membrane bound members as well as secreted proteins. Secreted Netrins are the ligands of three types of receptor families: Deleted in Colorectal Cancer (DCC), UNC-5 and Down Syndrome Cell Adhesion Molecule (DSCAM) (Rajasekharan and Kennedy, 2009). In *Drosophila* two receptors are present, Frazzled and UNC-5, for two Netrin ligands Netrin-A and Netrin-B. They attract and direct axons to the nervous system midline (Harris *et al*., 1996; Kolodziej *et al*., 1996; Keleman and Dickson, 2001).

1.2.1.2. Slits. Slits are secreted bifunctional guidance molecules that can act as chemorepellents or chemoattractants (Long *et al*., 2004)). Slit was first identified as a repellent factor for the Roundabout (Robo) receptor, mutations of which cause midline guidance defects in the fruit fly (Seeger *et al*., 1993; Kidd *et al*., 1998). *Drosophila* has one Slit protein and 3 Robo receptors. Slits form repulsive corridors in the ventral midline and prevent ipsilateral axons from crossing the midline and commissural axons from re-crossing (Kidd *et al*., 1999; Battye *et al*., 1999).

1.2.1.3. Semaphorins. Semaphorins are a large protein family that is composed of secreted and transmembrane guidance molecules. The family is divided into eight classes of proteins that share a Sema domain at their N-termini. Invertebrates express classes 1 and 2, vertebrates have classes 3 to 7 and the last class is found in viruses (Raper, 2000). Plexins are the receptors of Semaphorins, however, they sometimes form multimeric receptor complexes including Neuropilin and L1CAM (Tamagnone *et al*., 1999; Castellani *et al*., 2000; Raper, 2000). Semaphorins mainly act as repulsive cues, but in some circumstances they have an attractive ability. Surprisingly, the same Semaphorin protein may function as chemoattractant in one situation and chemorepellent in another (Bagnard *et al*., 1998; Tran *et al*., 2007). In the *Drosophila* nervous system three Semaphorins have been characterized: transmembrane Sema-1a and Sema-1b and secreted Sema-2a. Transmembrane Semaphorins binds to PlexA while secreted Semaphorin functions through PlexB (Winberg *et al*., 1998; Ayoob *et al*., 2006).

1.2.1.4. Ephrins. Ephrins are membrane-bound guidance proteins that have two subfamilies: class A Ephrins are attached to the membrane with GPI-anchorage and class B Ephrins are transmembrane molecules (Wilkinson, 2001). Ephrins function in a contact-dependent manner via binding to Eph receptor tyrosine kinase family members (Drescher *et al*., 1995). Ephrins have a repulsive role in establishing the anterior-posterior topographic map and an attractive role in mapping along the dorsal-ventral axis in the retina (Wilkinson, 2001; Hidges *et al*., 2002). Ephrins have a reverse signaling ability in which they function as a receptor (Hidges *et al*., 2002). In contrast to animals that have several Eph/Ephrin proteins, fruit flies have a single Eph receptor for a single Ephrin ligand.

1.2.1.5. Cell Adhesion Molecules. Cell adhesion molecules (CAMs) are cell surface proteins that function in cell to cell or cell to ECM communication. CAMs provide contact-dependent regulation of axon guidance and they regulate fasciculation/ defasciculation of axons at specific choice points. There are three major families of CAMs: Cadherins, Integrins and the Immunoglobulin (Ig) superfamily. The members of these families have three common domains: an intracellular domain for mediating the signaling processes, a transmembrane domain and an extracellular domain for homophilic or

heterophilic interactions (Sun and Xie, 2011). N-cadherin (N-Cad) is the most studied cadherin that regulates axonal pattern formation and fasciculation (Iwai *et al*., 1997). Down syndrome cell adhesion molecule (DSCAM), an Ig superfamily protein, is required for dendritic self-avoidance and is important for precise neuronal connections in the brain (Schmucker *et al*., 2000; Soba *et al*., 2007). Integrins are heterodimeric proteins that provide adhesion between neurons and ECM. Loss of Integrins causes phenotypes like defasciculation, fascicle displacement and midline axon guidance errors (Hynes and Lander, 1992; Stevens and Jacobs, 2002).

1.2.1. Axon Targeting in the *Drosophila* Visual System

The precise connection pattern of the *Drosophila* visual system is formed through a sophisticated series of cell-cell interactions. These adhesive interactions can be between axons and their targets and also among axons themselves.
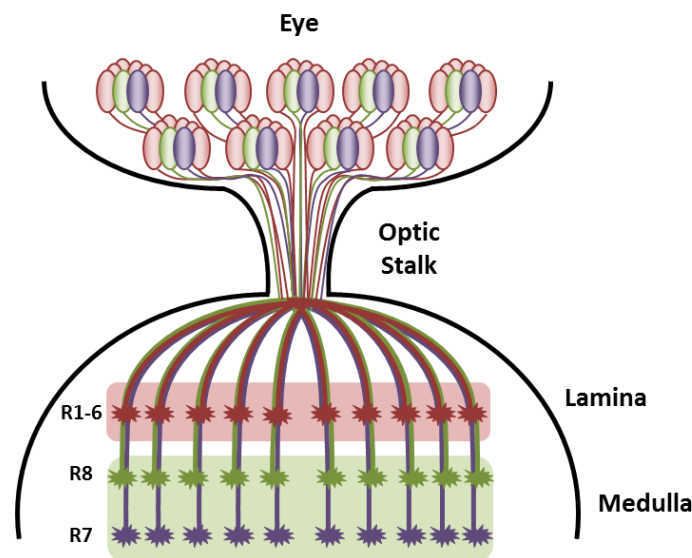
Figure 1.4. Schematic representation of PR projection to their respective ganglia in the fly visual system.

During development, differentiating PRs send their axons from the eye disc through the optic stalk to the brain (Figure 1.4.). In order to enter the optic stalk, PRs need guidance cues coming from the retinal basal glia (RBG). These glial cells migrate from the optic stalk, where they originate, to the eye disc (Choi and Benzer, 1994). Within each ommatidium, R8 axons are the pioneer axons to project out of the eye disc followed by the

outer PR axons and finally by R7 axons. Lamina-glia serve as intermediate targets for the outer PRs, providing a 'stop' signal. After reaching the lamina, axon bundles of outer PRs are separated from each other and project to appropriate cartridges. This lateral projection requires N-cadherin (N-Cad) expression in both afferent axons and lamina neurons. N-Cad is required for R1-R6 axons to defasciculate and to project into correct lamina cartridges (Lee *et al*., 2001). Lateral movement of axons also depends on two other molecules: the synaptic scaffolding molecule Liprin-α and the receptor tyrosine phosphatase LAR (Choe *et al.*, 2006; Schwabe *et al*., 2009). Flamingo (Fmi) is another important factor for the establishment of the lamina pattern. In Fmi mutant flies, R1-R6 form lamina cartridges with a variable number of terminals (Lee *et al*., 2003).

The R8 and R7 axons initially extend adjacent to each other through the lamina and terminate at the M3 and M6 layers of the medulla, respectively. Layer-specific projection of inner PRs occurs in two steps: first, during early pupal stages R7 and R8 axons project to their temporal layers; second, during the mid-pupal stage axons of inner PRs regain their motility and project to their final layers (Ting *et al*., 2005; Hadjieconomou *et al*., 2011).

The projection of R8 axons is based on the presence of three cell-surface proteins: Fmi, Golden Goal (Gogo), and Capricious (Caps). Fmi is dynamically expressed in all PRs, in addition to the lamina and medulla neurons. R8 cells express Fmi transiently while they enter the medulla. Loss of Fmi in PRs disrupts synaptic patterning of the medulla (Lee *et al.*, 2003). Gogo helps to maintain the proper spacing between R8 axons by repulsive axon-axon interactions and allow R8 axons to find their temporary layer during the mid-pupal stage (Tomasi *et al*., 2008). Caps is a homophilic cell surface molecule, which is expressed in R8 axons and M3 layer neurons of the medulla. By mediating axon-target interactions, Caps provides layer-specific targeting of R8 axons. In the absence of Caps, R8 axons extend into deeper layers of the medulla and into adjacent columns (Shinza-Kameda *et al*., 2006).

In each ommatidium R7 cells are the last PRs to differentiate and project their axons to the medulla. Genetic screens have revealed several cell-surface molecules that are important for the targeting of R7 axons: N-Cad, LAR, PTP69D and Liprin-α (Ting and

Lee, 2007; Hadjieconomou *et al.*, 2011). Loss of N-Cad in R7 axons and in target neurons in the medulla cause similar defects of mistargeting. Therefore, N-Cad mediated axon-target interactions are required for proper layer-specific targeting of R7 axons (Ting *et al.*, 2005; Yonekura *et al.*, 2007). Mutations in the receptor tyrosine phosphatases PTP69D and LAR cause mistargeting of R7 axons to the M3 layer (Clandinin *et al.*, 2001). Liprin-α is thought to work together with LAR to modulate the actin cytoskeleton during axon elongation (Choe *et al.*, 2006).

1.2.2. Mechanisms of ORN Targeting

In the mammalian olfactory system, OR expression begins before ORNs project to a distinct glomerulus. In contrast, *Drosophila* ORNs do not depend on the OR expression to find their final targets (Jefferis *et al.*, 2004). Various axon guidance molecules that contribute to the proper targeting of ORN axons via neuron-neuron or neuron-glia interaction to their specific places within the AL have been identified.

At the time that ORN axons reach the newly developing antennal lobe, they form a transient structure called protoglomerulus. Protoglomeruli are formed by the interactions of ORN axons and glial cells (Oland *et al.*, 1990). Formation of protoglomeruli depends on the function of N-Cad. In *N-Cad* mutant flies, ORN axons fail to form protoglomeruli and to synapse with their targets at the AL (Hummel and Zipursky, 2004).

Dscam is another cell adhesion molecule that is required for the specific classes of ORN axons to synapse in appropriate target glomeruli. In *Dscam* null mutants, some ORNs project to ectopic glomeruli and some others fail to form a commissure. These findings suggest a role for Dscam in promoting adhesion between growth cones of axons and their targets (Hummel *et al.*, 2003).

In addition to neuron-neuron interactions, ingrowing axons interact with glial cell on the way to their final targets. These interactions are again mediated by guidance cues. An example for neuron-glia interactions is seen in the case of Wnt5 and its receptors Derailed (Drl) and Drl2. Wnt5, expressed in ORNs, is modulated by Drl which is

introduced by glia during the organization of the glomerular pattern. In *wnt5* overexpression mutant flies, the AL architecture is disrupted with ectopic glomeruli and defects in commissure formation. *drl* mutants show similar defects with *wnt5* mutant flies, however ectopic glomeruli tend to form at the midline. The similarity between the loss-of-function phenotype of *drl* and the overexpression phenotype of *wnt5* suggests that Drl functions as an antagonist of Wnt5 (Yao *et al*., 2007). In another study (Sakurai *et al*., 2009), Drl2, expressed in a subset of ORNs, is found to be a positive regulator of Wnt5 signaling. Thus, the correct wiring of the *Drosophila* olfactory system is established by cooperative functioning of these two receptors of Wnt5 (Sakurai *et al*., 2009).

1.3. Unzipped, A Novel Cell Adhesion Molecule

Unzipped is a recently identified gene, which codes for a novel cell adhesion protein (Ding *et al*., 2011).

The Uzip protein is composed of 488 amino acids, which correspond to a molecular weight of 55 kD. However, endogenous Uzip in wild-type fly extracts is observed in two forms: 80 kD and 65 kD. Further investigation showed that these differences result from post-translational modifications, mainly glycosylation, since Uzip has 5 N-glycosylation sites (Figure 1.5). The 65 kD Uzip represents the secreted form and lacks the C-terminus and 80 kD Uzip is the membrane-bound form, which is attached to the membrane through a GPI moiety. Only the membrane-bound form has the adhesive ability and can cause cell aggregation (Ding *et al*., 2011).
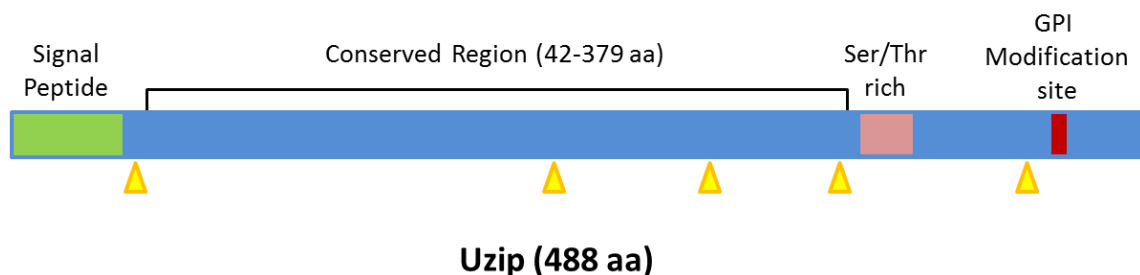
Figure 1.5. Representation of the Uzip protein structure.

(adapted from Ding *et al*., 2011)

Uzip shares no homology with known cell adhesion molecule families and it has no homolog in vertebrates. Nevertheless, it is highly conserved among insects (up to 94% similarity). The most conserved domain of Uzip within insects is the region between amino acids 42-379, which was shown to be important for the adhesive ability of the protein. On the other hand, deletion of the region between amino acids 401-450 appears to have no effect on the function of Uzip (Ding *et al*., 2011).

Uzip mRNA was observed to be present in the ventral nerve cord (VNC) of fruit fly embryos with an enriched expression in longitudinal glia (LG). Axons also express Uzip but in lower amounts. Uzip expression was absent in both glia and axons when a mutant line that lacks glial cells was investigated. Thus, glial cells are the main source of Uzip. Although Uzip null mutants showed no phenotypic defect in longitudinal axonal tracts, loss of Uzip enhances the severity of breaks in the tracts in NCad and Wnt5 mutants (Ding *et al*., 2011).

In our lab Uzip was identified in an enhancer-trap screen and shown to be expressed in third instar larval eye imaginal discs (Öztürk, 2010). Closer examination of Uzip expression showed colocalization of Unzipped expression with the R8-specific marker Senseless (Zülbahar, 2012). Further investigation revealed that Uzip is expressed in the olfactory system during the pupal stage and adulthood by one subset of antennal ORNs, some of maxillary palp ORNs and glia (Zülbahar, 2012).

In an *uzip* null mutant background axons of antennal and maxillary palp ORNs fail to project to glomeruli located on the contralateral side of the antennal lobe. Besides commissure formation defects, mistargeting defects were observed in some of the maxillary palp ORN axons, while some others could not reach the antennal lobe since they were stuck in the SOG (Zülbahar, 2012).

These findings together suggest a role for Uzip in axonal targeting of ORNs.

2. PURPOSE

The proper functioning of the nervous system relies on the ability of axons to find their way to their targets. In this journey, some axons are guided by a large number of guidance cues and others follow previously created paths. In order to detect different cues, axons possess molecules on their membranes that can recognize these cues.

A novel cell adhesion molecule, Uzip, is a candidate guidance cue identified in our laboratory that has no homology to previously identified guidance molecules. Loss-of-function analyses of Uzip reveal guidance defects in the olfactory system and mushroom body. These guidance defects are thought to arise from the disruption of homophilic and heterophilic interactions of Uzip with other guidance molecules. Thus, to get insight into the mechanisms of how Uzip exerts its guidance function in the framework of this study we aimed to identify and analyze interaction partners of Uzip.

In order to achieve our aim we used following strategy:

- Co-immunoprecipitation of proteins that interact with Uzip,
- Mass spectrometry analysis of these proteins,
- Determination of candidate proteins,
- Validation of MS results using Co-IP
- Expression analysis of the candidates in the *Drosophila* nervous system.

Furthermore, we analyzed the endogenous expression profile of Uzip throughout development of the fly nervous system using a transgenic fly line.

3. MATERIALS AND METHODS

3.1. Biological Material

All fly stocks were kept in incubators with 80% humidity and a 12:12 day:night cycle at 25°C, unless stated otherwise. Commercially available fly food (Nutri-Fly^{TM} Bloomington Formulation) was prepared weekly with the addition of 4.8 ml of propionic acid per liter of the fly food.

Drosophila melanogaster lines used in the experiments are listed and described in Table 3.1.

Table 3.1. *Drosophila melanogaster* strains used throughout this study.

Name of line	Chr. No	Description
FH::Uzip	III	Uzip transgenic construct with Flag and HA tags at the N-terminal
w^{1118}	X	Wild type

3.2. Chemicals and Supplies

Unless stated otherwise, all chemicals used in this study were purchased from Fisher Scientific, Sigma, Molecular Probes or Roche.

3.2.1. Chemical Supplies

Table 3.2. Chemical Supplies.

Acrylamide/bis-Acrylamide	: Sigma Aldrich (A3574)
PageBlue Staining Solution	: Thermo Scientific (24620)
NaCl	: Sigma Aldrich (S7653)
Protease Inhibitor Cocktail	: Roche (11836153001)
Protein Ladder	: Precision Plus Protein (161-0374)
Sodium Deoxycholate	: Sigma (30970)
Tris	: Sigma (T6066)
Triton X-100	: AppliChem (A4975)
Tween 20	: Sigma Aldrich (S36285-326)

3.2.2. Buffers and Solutions

Table 3.3. Buffers and Solutions.

Buffer/Solution	Content
Blocking Solution	5% non-fat milk in TBS-T
Blue Loading Buffer	New England BioLabs, USA (B7703S)

Table 3.3. Buffers and Solutions (cont.).

Fly Head Lysis Buffer (Denaturing)	50 mM Tris-Cl pH 8.0 150 mM NaCl 1% SDS 5 mM DTT 1X Roche Protease Inhibitor Cocktail®
Fly Head Lysis Buffer (Ionic)	50 mM Tris-Cl pH 8.0 150 mM NaCl 1% NP-40 0.5% Na-DOC 0.1% SDS 1X Roche Protease Inhibitor Cocktail®
Fly Head Lysis Buffer (Non-ionic)	20 mM Tris-Cl pH 8.0 50 mM NaCl 1% NP-40 2 mM EDTA 1X Roche Protease Inhibitor Cocktail®
Monoclonal Anti-HA Agarose Beads	Sigma, USA (A2095)
Mouse IgG-Agarose Beads	Sigma, USA (A0919)
Laemmli's Sample Buffer (3X)	50 mM Tris-Cl pH 7.5 2% SDS 10% Glycerol 0.1% Bromophenol blue 100 mM DTT
LumiGlo® Western Blotting Substrate	Cell Signaling, USA
Normal Goat Serum	Millipore, Germany
PAXDG	10 g BSA 3 g Sodium Deoxycholate 3 ml Triton X-100 50 ml Normal Goat Serum 100 ml 10X PBS in 1 L
PBS (1x)	137 mM NaCl 2.7 mM KCl 10 mM Na_2HPO_4 1.8 mM KH_2PO_4
PBT	0.2% Triton X-100 in 1X PBS
PBX3	0.3% Triton X-100 in 1X PBS
PEM	0.1 M PIPES, pH 6.95 2 mM EGTA 1mM $MgSO_4$
PFA (16%)	8 g paraformaldehyde in 50 ml 1 N NaOH until it dissolves completely

Table 3.3. Buffers and Solutions (cont.).

PIPES (0.2 M, pH 6.9)	64.87 g PIPES monosodium salt in 1 L
Ponceau Staining Solution	1 g Ponceau 50 ml Acetic acid in 1 L
Protein G Agarose Beads	Roche (11719416001)
Running Buffer	25 mM Tris Base 190 mM Glycine 0.1% SDS pH adjusted to 8.3 with HCl
TBS-T	20 mM Tris Base 150 mM NaCl 0.1% Tween-20 pH adjusted to 7.6 with HCl
Transfer Buffer	25 mM Tris Base 190 mM Glycine 20% Ethanol/Methanol
Western Blot Developer Solution (Rapid Developer)	Ilford, UK 1/10 Diluted in Water
Western Blot Fixer Solution (Rapid Fixer)	Ilford, UK 1/5 Diluted in Water

3.2.3. Antibodies

Antibodies used throughout the Western blot experiments are listed in Table 3.3. Antibodies used during immunohistochemistry experiments are listed in Table 3.4.

Table 3.4. Antibodies used in the Western blotting experiments.

Name	Antigen	Species	Dilution	Source
Primary Antibodies				
Anti-EPS-15	EPS-15	Mouse	1:100	DSHB (DEPS15-1)
Anti-HA	Hemagglutinin	Rat	1:1000	Roche
Anti-dFMR1	dFMR1	Mouse	1:200	DSHB (5A11)
Anti-Hts	Hts	Mouse	1:10	DSHB (1B1)
Anti-Syn	Synapsin	Mouse	1:200	DSHB (3C11)

Table 3.4. Antibodies used in the Western blotting experiments (cont.).

Secondary Antibodies				
Anti-mouse IgG, HRP linked	IgG	Mouse	1:1000	Cell Signaling Tech/

Table 3.5. Antibodies used in the immunohistochemistry experiments.

Name	Antigen	Species	Dilution	Source
Primary Antibodies				
Anti-dFMR1	Fmr1	Mouse	1:50	DSHB (5A11)
Anti-Elav	Elav	Rat	1:50	DSHB
Anti-Elav	Elav	Mouse	1:20	DSHB
Anti-EPS-15	EPS-15	Mouse	1:2	DSHB (DEPS15-1)
Anti-Flag	Flag tag	Rabbit	1:800	Cell Signaling Tech.
Anti-HA	Hemagglutinin	Rat	1:200	Roche
Anti-Hts	Hts	Mouse	1:5	DSHB (1B1)
Anti-NCad	N-Cadherin	Rat	1:20	DSHB
Anti-Repo	Repo	Mouse	1:20	DSHB
Anti-Syn	Synapsin	Mouse	1:100	DSHB (3C11)
Secondary Antibodies				
Alexa 488	Mouse	Goat	1:800	Invitrogen
Alexa 488	Rabbit	Goat	1:800	Invitrogen
Alexa 546	Rat	Goat	1:800	Invitrogen
Alexa 555	Mouse	Goat	1:800	Invitrogen
Alexa 647	Rat	Donkey	1:800	Invitrogen
Alexa 647	Mouse	Goat	1:500	Invitrogen

3.2.4. Disposable Labware

Table 3.6. Disposable labware used during this study.

Filter Tips	Greiner Bio-One, Belgium
Microscope cover glass	Fisher Scientific, UK
Microscope slides	Fisher Scientific, UK
Petri Dish	Greiner Bio-One, Belgium

Table 3.6. Disposable labware used during this study (cont.).

Pipette Tips	VWR, USA
Test Tubes, 0.5 ml	Citotest Labware Manufacturing, China
Test Tubes, 1.5 ml	Citotest Labware Manufacturing, China
Test Tubes, 2 ml	Citotest Labware Manufacturing, China
Test Tubes, 15 ml	Becto, Dickinson and Company, USA
Test Tubes, 50 ml	Becto, Dickinson and Company, USA

3.2.5. Equipment

Table 3.7. Equipment used during this study.

Autoclave	Astell Scientific Ltd., UK
Centrifuges	Eppendorf, Germany (Centrifuge 5424, 5417R)
Cold Room	Birikim Elektrik Soğutma, Turkey
Confocal Microscope	Leica Microsystems, USA (TCS SP5)
Electrophoresis Equipment	Bio-Rad Labs, USA (ReadySub-Cell GT Cells)
Environmental Test Chamber	Sanyo, Japan (MLR 351H)
Freezers	Arçelik, Turkey
Heating Block	Fisher Scientific, France (Dry-bath incubator)
Heating magnetic stirrer	IKA, China (RCT Basic)
Homogenizer	Kontes, USA (749540-0000)
Incubator	Weiss Gallenkamp, USA (Incubator Plus Series)
Inverted Microscope	Zeiss, USA (Axio Observer, Z1)
Laboratory Bottles	Isolab, Germany
Micropipettes	Eppendorf, Germany
pH meter	WTW, Germany (Ph330i)
PVDF Membrane Visualization	Stella, Raytest, Germany
Refrigerators	Arçelik, Turkey
SDS-PAGE Electrophoresis System	Bio-Rad Labs, USA (Mini PROTEAN® Tetra Cell)
SDS-PAGE Transfer System	Bio-Rad Labs, USA (Mini Trans-Blot® Electrophoretic Transfer Cell)
Stereo Microscope	Olympus, USA (SZ61)
Vortex Mixer	Scientific Industries, USA (Vortex Genie2)

3.3. Biochemical Methods

3.3.1. Protein Extraction

Young adult flies were used to extract total protein. Total protein was extracted from fly heads. For each round of co-immunoprecipitation experiment, heads of 6 FH::Uzip flies were homogenized thoroughly in 60 µl lysis buffer with the help of a homogenizer and kept on ice for 30 min in order to let the tissues dissolve in buffer. The protein extract was centrifuged at 4°C and 10000 rpm for 10 min. 50 µl of the supernatant was transferred into a clean tube (while performing co-IP different amounts of fly heads and lysis buffer were used, and supernatant was transferred into a tube filled with α-HA or IgG agarose beads) without disturbing the pellet of hard tissue debris and the upper layer rich in lipids. 25 µl of 3X Laemmli's buffer was added to the supernatant. The proteins were heated at 99°C for 5 min in order to denature them and reduce their disulfide bonds.

3.3.2. Co-Immunoprecipitation

α-HA and IgG Agarose beads were prepared by washing them 3 times with 1 ml of 1X PBS. Then 200 µl of the supernatant, obtained as described in 3.3.1, were added onto 60 µl of Agarose beads. 200 µl of lysis buffer was added on top of the bead-supernatant mix. The mixture was incubated overnight on a 4°C shaker. On the next day, the tube was centrifuged for 2 min at 200 g at 4°C. The supernatant was taken into a fresh tube and the beads were washed 4 times with 1 ml of PBS. At each round, the tube was centrifuged for 2 min at 2000 g at 4°C and supernatant of each spin down was collected in a fresh tube. Bound proteins were eluted twice using 2X Laemmli's sample buffer. In the first elution step, the sample was heated to 70°C for 20 min with agitation and in the second elution step the beads were boiled at 99°C for 10 min with agitation. Each elution was followed by 2 min centrifugation at 200 g at 4°C. Afterwards the supernatant was transferred into a fresh tube. Samples were then loaded on a SDS-PAGE gel.

3.3.3. Cross Co-Immunoprecipitation

50 µl protein G agarose beads were prepared by washing with ice-cold PBS as section 3.3.2. Beads were incubated with 2 µg of α-Hts antibody, diluted in 200 µl PBS, for 4 hours at 4°C by shaking. After incubation beads were washed three times with PBS by centrifuging for 1 min at 12000 g each time. Protein extract of 80 FH:Uzip adult fly heads was added on the beads and they were incubated overnight at 4°C by shaking. The following day, beads were spinned down and the supernatant kept frozen for further analysis. The beads were washed with 1X PBS three times. Bound proteins were eluted twice using 2X Laemmli's sample buffer. In the first elution step, the sample was heated to 70°C for 20 min with agitation and in the second elution step the beads were boiled at 99°C for 10 min with agitation. Afterwards the supernatants were transferred into a fresh tube. Samples were then loaded on a SDS-PAGE gel.

3.3.4. SDS-PAGE

Polyacrylamide gel was poured in a standard way. In order to be able to separate the proteins better an 8% gel was preferred. 4 µl of a ready-to-use protein ladder and 15-20 µl of protein extract were loaded. The gel was run in 1X running buffer under 30 mA constant current.

Table 3.8. Polyacrylamide Gel Materials.

	Resolving gel, 5 ml	Stacking gel, 3 ml
ddH$_2$O	1.7 ml	2.175 ml
Tris-Cl	1.875 ml (pH 8.8)	375 µl (pH 6.8)
Acrylamide-Bisacrylamide 29%-1%	1.35 ml	397.5 µl
SDS 20%	25 µl	15 µl
APS 10%	50 µl	30 µl
TEMED	3 µl	7.5 µl

3.3.5. Western Blotting

The PVDF membrane was activated in methanol for 1 min and stabilized in 1X transfer buffer. Transfer to the PVDF membrane was performed under 200 mA constant current in cold 1X transfer buffer for 2 hours. Transfer was confirmed by reversible staining of the membrane with Ponceau's Red. After the membrane was destained with TBS-T, it was blocked in 5% non-fat dry milk dissolved in TBS-T for 1 hour at room temperature by shaking. The primary antibody was dissolved in 1% milk (in dilutions stated in Table 3.3) in TBS-T. The membrane was incubated with the primary antibody solution overnight at 4°C while shaking. The next day, unbound and non-specifically bound antibodies were removed by washing 3 times with TBS-T for 10 min. HRP coupled secondary antibody (host species stated in Table 3.3) was dissolved in 1% milk at a dilution of 1:1000 and incubated with the membrane at room temperature for 2 hours. The washing step was performed as previously. The membrane was incubated with HRP revealing kit 20X LumiGlo® diluted to 1X in ddH$_2$O for 3 min. Chemiluminescent detection film was placed onto the membrane and exposed for sufficient amount of time. The film was washed in the developer solution, dipped into water for a few seconds and washed with fixer solution. The film was allowed to dry and scanned (In the WT blots the Stella documentation system was used to record the chemiluminescent signal.). Images were processed with Adobe Photoshop.

3.3.6. Sample Preparation for Mass Spectrometry

In order to use in Mass Spectrometry (MS) analysis, the supernatant of the first elution step in co-immunoprecipitation was loaded on pre-cast Tris-Glycine gel. The samples were run under 160 V constant Voltage until the dye front leaves the gel. For detecting the presence of proteins, the gel was stained with PageBlue protein dye for 60 min and destained by washing 3 times with distilled water. The gel was cut into fractions of interest with scalpel. Fractions were transferred into a microcentrifuge tube and washed

with HPLC water, ammonium bicarbonate and acetonitrile until all the stain is removed. Then the proteins were reduced, alkylated and digested with Trypsin treatment.

3.3.7. Mass Spectrometry and Data Analysis

LC-MS/MS analysis of the peptides was carried out using Q Exactive Benchtop Orbitrap LC-MS/MS Mass Spectrometer by Koç University Proteomics Facility, İstanbul. The peptides were ionized by the spectrometer and they were separated and detected by their mass-to-charge ratio. Amino acid sequences of the peptides were identified from their mass-to-charge spectra by using SEQUEST Software. These peptide sequences were matched to Drosophila proteins with the help of Mascot Software. The proteins that matched with the peptide sequences were filtered by considering 'protein coverage percent' and 'number of unique peptides/number of peptides ratio' as parameters. These filtered proteins were categorized by their gene ontology (GO) term with the help of GeneCodis tool.

3.4. Histological Methods

3.4.1. Preparation of *Drosophila* Tissues for Immunohistochemistry

3.4.1.1. <u>Preparation of larval eye imaginal discs.</u> Larvae of selected genotype are dipped into ice-cold PBS. A hole was made on the body with the forceps right below the third-most anterior segment. Then, pulling from the mouth hook by one pair of forceps and from the body with the other, eye-antennal disc attached to the brain was dissected out and transferred into cold PBS.

3.4.1.2. Preparation of pupal eye discs. Pupae of the desired stage were carefully removed from the vials and transferred into PBS on silicon plate. Carefully, the operculum was grabbed and the puparium was removed. A little hole was pinched in the anterior and enlarged carefully to take out the eye-brain complex and the tissue was transferred into PBS on ice.

3.4.1.3. Preparation of adult brains. Flies of selected genotype were anesthetized with CO_2 and killed by transferring into 70% ethanol in a glass dish. They were washed 3 times with PBS and dissected on a silicon plate in a drop of ice-cold PBS. While dissecting, first the proboscis was removed. Then, the hole that the proboscis left was used to grab and remove the head exoskeleton. After residual trachea was cleaned, the brain was detached from the body and placed into ice-cold PBS.

3.4.2. Immunohistochemistry

The following protocol was used for all the immunohistochemistry experiments in all tissues with minor differences, except for those stained with α-HA antibody.

- Tissues were fixed in 4% PFA in PBS with variable timing periods changing according to the tissue.
- Tissues were washed three times for 15 min with PBX3.
- Tissues were blocked in PAXDG for 2 h at room temperature.
- Tissues were incubated in primary antibody solution overnight at 4°C. Primary antibodies were diluted in PAXDG.
- Tissues were washed three times for 15 min with PBX3.
- Tissues were incubated in secondary antibody solution prepared with PAXDG for 2 h at room temperature.
- Tissues were washed three times for 15 min with PBX3.
- Tissues were mounted in Vectashield embedding medium, and stored at 4°C in dark.

- The samples were visualized using confocal microscopy.

3.4.2.1.   Antibody staining of Flag::HA::Uzip transgenic flies. Immunohistochemical staining of tissues with anti-HA polypeptide may require some modifications to commonly used antibody staining protocols, so the following protocol was performed to detect expression of Flag::HA::Uzip transgenic protein.

Adult brains, pupal eye discs and larval eye discs were dissected and fixed in 4% PFA in PEM buffer for 2 h at 4°C. Tissues were washed in PBT for 15 min three times. Blocking was performed in normal goat serum (NGS), which was diluted to 10% in PBT, at room temperature for 1 h. Tissues were incubated overnight at 4°C in primary antibodies which were diluted in 10% NGS in PBT. Next day, tissues were washed in PBT for 15 min three times. Secondary antibodies were diluted in 10% NGS and the tissues were incubated overnight at 4°C. After three 15 min washing steps in PBT, the tissues were mounted in Vectashield medium and stored at 4°C in dark until they were visualized with confocal microscopy.

4. RESULTS

Unzipped is a novel cell adhesion molecule, which is expressed in embryonic longitudinal glial (LG) cells and ventral nerve cord (VNC) axons of fruit flies, and takes part in axonal targeting. It is a 488 amino acid protein, which is expressed in two forms: a 80 kD membrane-bound form and a 65 kD secreted form. Uzip triggers cell adhesion by homophilic binding (Ding *et al*., 2011). Uzip expression is also detected in the *Drosophila* visual and olfactory systems, both in neurons and glial cells (Zülbahar, 2012). While its distribution in glial cells in the brain is very broad, Uzip is expressed in only one subset of olfactory receptor neurons (ORNs). Loss of Uzip however affects midline crossing of all ORNs. Thus, we hypothesize that Uzip protein in the ORN subset mediates guidance of all other ORNs through heterophilic interactions (Zülbahar, 2012). The aim of this project was to get insight into the mechanism of Unzipped action by identifying the interaction partners of Uzip. For this purpose we chose to make an unbiased approach and perform mass spectrometry analysis.

4.1. Determination of the Endogenous Expression Pattern of *Uzip* using the Flag::HA::Uzip Transgenic Line

Unzipped was identified in an enhancer-trap screen searching for genes that are expressed in PRs and was shown to be expressed in neurons and glia in third instar larval imaginal eye discs (Öztürk, 2010). The expression of this enhancer-trap line has been analyzed in detail (E. Terzioğlu-Kara, unpublished). In order to confirm that this enhancer-trap line reflects endogenous Uzip expression, a transgenic line expressing Unzipped under its own regulatory region was generated. Using BAC recombineering technology both forms of the Uzip protein (membrane-bound and secreted forms) were tagged at the N-terminus right after the signal peptide sequence with Flag and HA tags (Zülbahar, 2012). In parallel our lab is in the process of generating an Uzip-specific antibody (E. Terzioğlu-Kara, unpublished).

4.1.1. Uzip is Expressed in the Eye Imaginal Disc in the 3rd Instar Larval Stage

The Flag-HA-tagged transgenic Uzip line (FH::Uzip) described above was used to analyze endogenous Uzip expression and its cellular localization. The analysis was started with third instar larval eye imaginal discs using an antibody against HA and the neuronal marker Elav that stains the nuclei of all neurons. Several protocols were tested as it is known that the detection of HA in tissues is difficult. Uzip expression in the eye imaginal disc was observed after many trials (Figure 4.1).
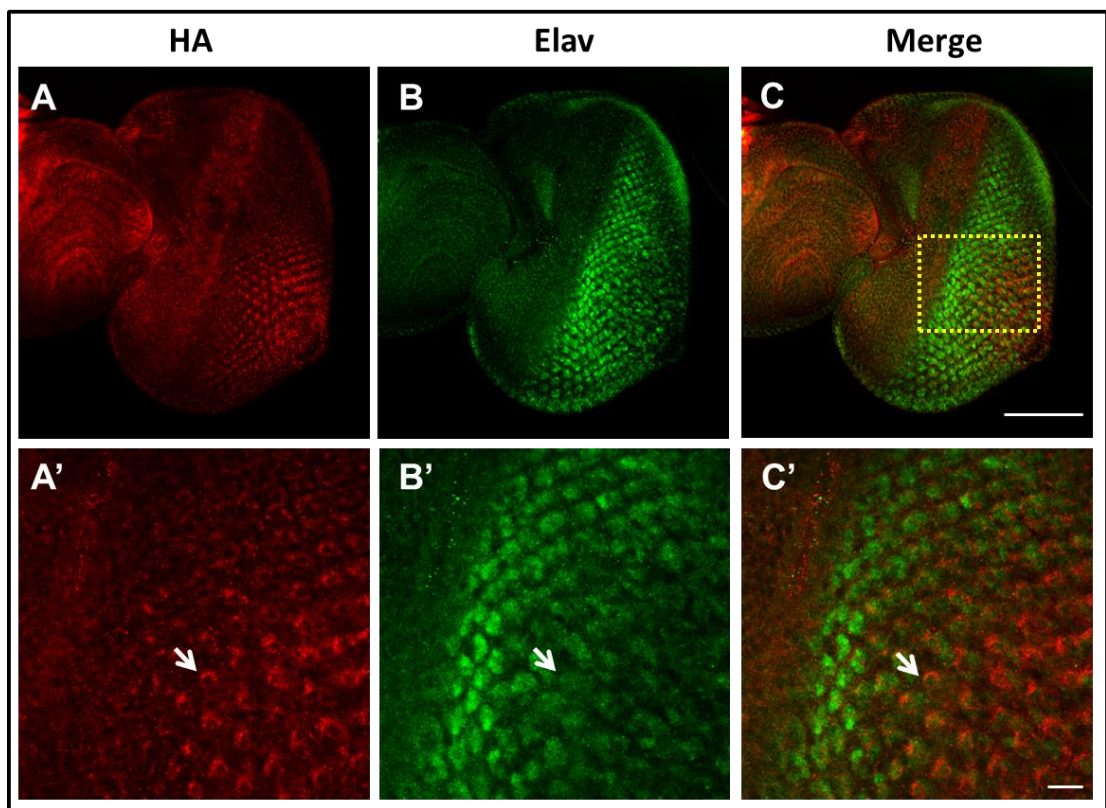
Figure 4.1. Expression analysis of FH::Uzip in 3rd instar larval eye discs. (A) α-HA staining is detected in cells posterior to the morphogenetic furrow. (B) α-elav antibody stains the nuclei of photoreceptor neurons. (C) FH::Uzip appears to surround the nuclei of some of the photoreceptor cells and seems to be excluded from the nuclei (white arrow). (A',B',C') Magnified view of A, B, and C, respectively. α-HA (red), α-Elav (green).

FH::Uzip expression was observed in early born photoreceptors posterior to the morphogenetic furrow (Figure 4.1). FH::Uzip appears to surround Elav-positive PR nuclei and its localization and thus could either be cytoplasmic or membranous. More detailed

analyses using antibodies that localize to the membrane are needed to determine its localization unequivocally. Uzip expression was not observed in all PRs of one ommatidium, rather it seemed to be expressed in one or a few of them. This expression pattern is consistent with the expression of the enhancer-trap line. Unfortunately, the staining was not homogenous as can be judged from the lacking Elav-staining at the posterior end of the imaginal disc. To evaluate the endogenous expression pattern of Unzipped further stainings with PR cell-specific markers are necessary. These require crossing in of marker lines and could not be accomplished in the framework of this thesis.

The enhancer-trap line for Uzip shows expression in both neurons and glial cells (Öztürk, 2010; Zülbahar, 2012). As the neuronal expression could not be evaluated further as discussed above we set out to determine whether the FH::Uzip expression resembles the enhancer-trap line expression in glial cells. For this purpose, FH::Uzip was co-stained in larval eye imaginal discs with α-HA and α-Repo antibodies (Figure 4.2).

The expression of FH::Uzip is observed in a regular pattern after the morphogenetic furrow and seems to stain one cell per ommatidium. As can be seen from the overlay with the Repo staining this signal does not co-localize with Repo and thus not appear to be glial. While Repo, similar to Elav, only stains the nuclei of glial cells we do not expect the exact co-localization, but the distribution of the HA signal is quite different from the Repo staining and thus clearly not coming from the glial cells. The HA signal comes rather from a layer beneath the glial layer, where PR cells reside. This is inconsistent with the expression pattern of the enhancer-trap line, which also shows expression in a subset of glial cells. In order to get a better understanding of the expression pattern, a triple staining should be performed. However, the triple staining with α-HA, α-Repo, and α-Elav could not be performed because these antibodies are not available in three different host species. An alternative could be to replace the Repo antibody with a reporter line, which can be crossed into the FH::Uzip line and analyzed with a triple staining. Also a simultaneous staining of FH::Uzip with the enhancer-trap line would be interesting to see how much the stainings overlap, which could be done after crossing the lines together.
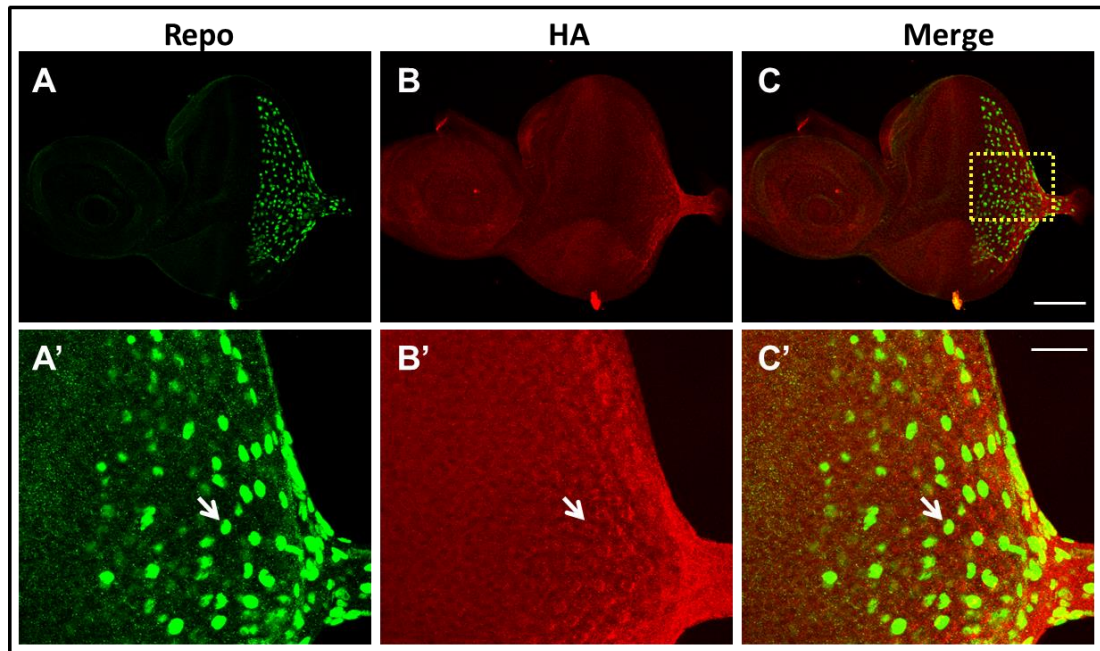
Figure 4.2. Expression analysis of FH::Uzip in third instar larva by double staining α-HA with α-Repo. (A) α-Repo stains the nuclei of glial cells. (B) α-HA staining is detected in cells posterior to the morphogenetic furrow. (C) FH::Uzip expression does not seem to originate from glial cells (white arrow). (A',B',C') Magnified views of A, B, and C respectively, taken from the yellow square. Rat-α-HA (red), mouse-α-Repo (green).

The stainings using the HA tag were difficult and did not work consistently in every experiment. As an alternative, we also tried α-Flag antibody to evaluate if this works better than the HA antibody. Additionally, as the FLAG antibody was raised in a different host species than α-Elav and α-Repo antibodies it was possible to perform a triple staining with these antibodies in FH::Uzip third instar larvae using WT larvae as control (Figure 4.3).

While a α-Flag signal was detected that looked very specific to the nucleus, it was distributed widely over the eye-antennal imaginal disc (Figure 4.3A). However, the same signal was also detected in control eye discs indicating that the observed signal cannot be specific to Uzip. Because of time constraints this staining was performed only once in the time course of this study. This staining could be repeated by performing several optimizations in the protocol including changing of the antibody concentration and pre-adsorption of the antibody with embryos of control imaginal discs before use.
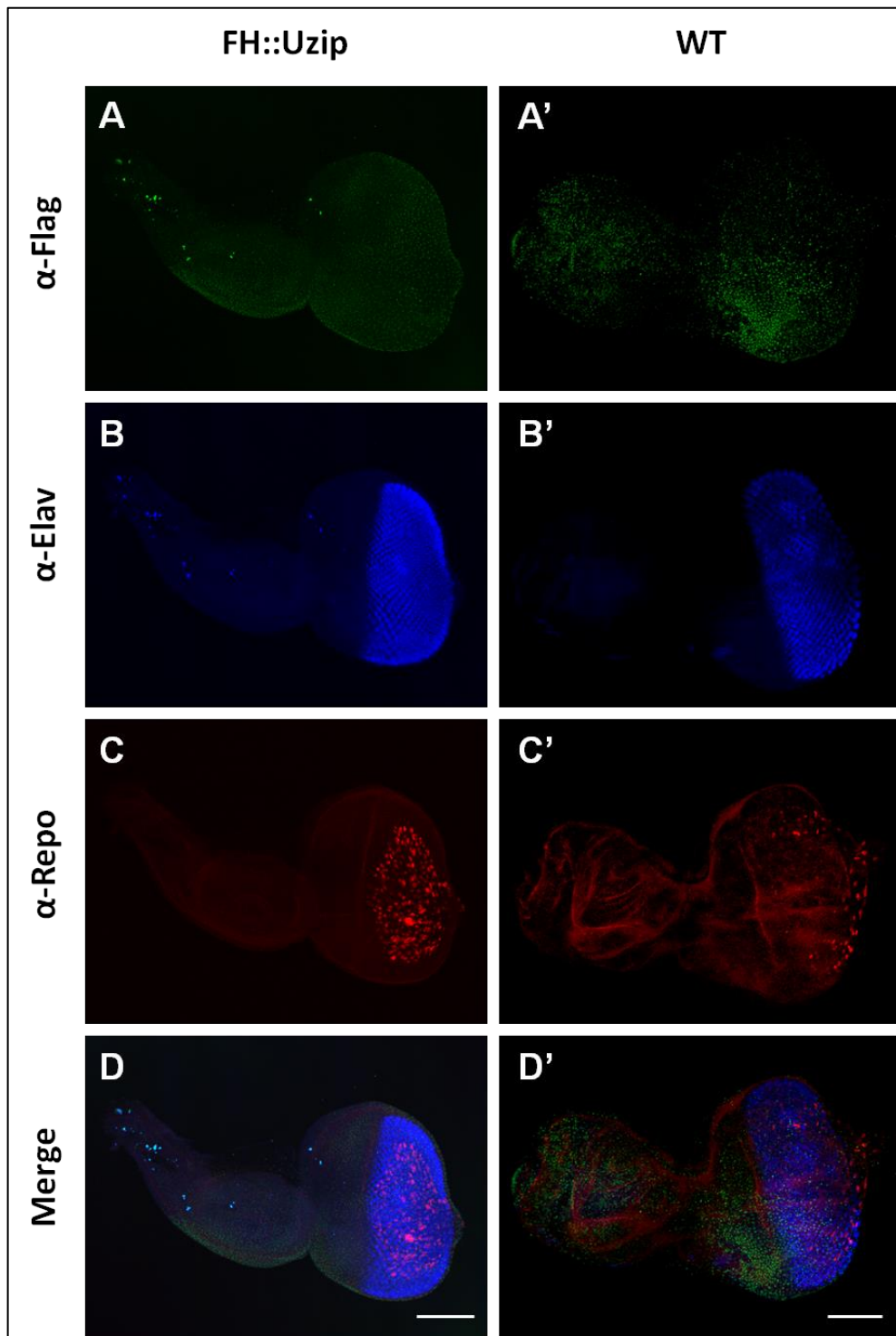
Figure 4.3. Expression analysis of FH::Uzip in third instar larva by triple staining with α-Flag, α-Elav, and α-Repo antibodies. α-Flag staining is detected all over the eye antennal imaginal disc in both FH::Uzip and WT flies. (A, B, C, D) Triple staining of FH::Uzip larval eye discs. (A) α-Flag staining did not result in a meaningful pattern. (A', B', C', D') Triple staining of WT larval eye discs. Anterior is to the left.

4.1.2. Uzip is Expressed in the Visual System during Pupal Development

Endogenous expression of Uzip was further analyzed at pupal stages where photoreceptors start to differentiate (Figure 4.4). Elav staining was again used to visualize neurons and HA staining used to label FH::Uzip expressing cells.
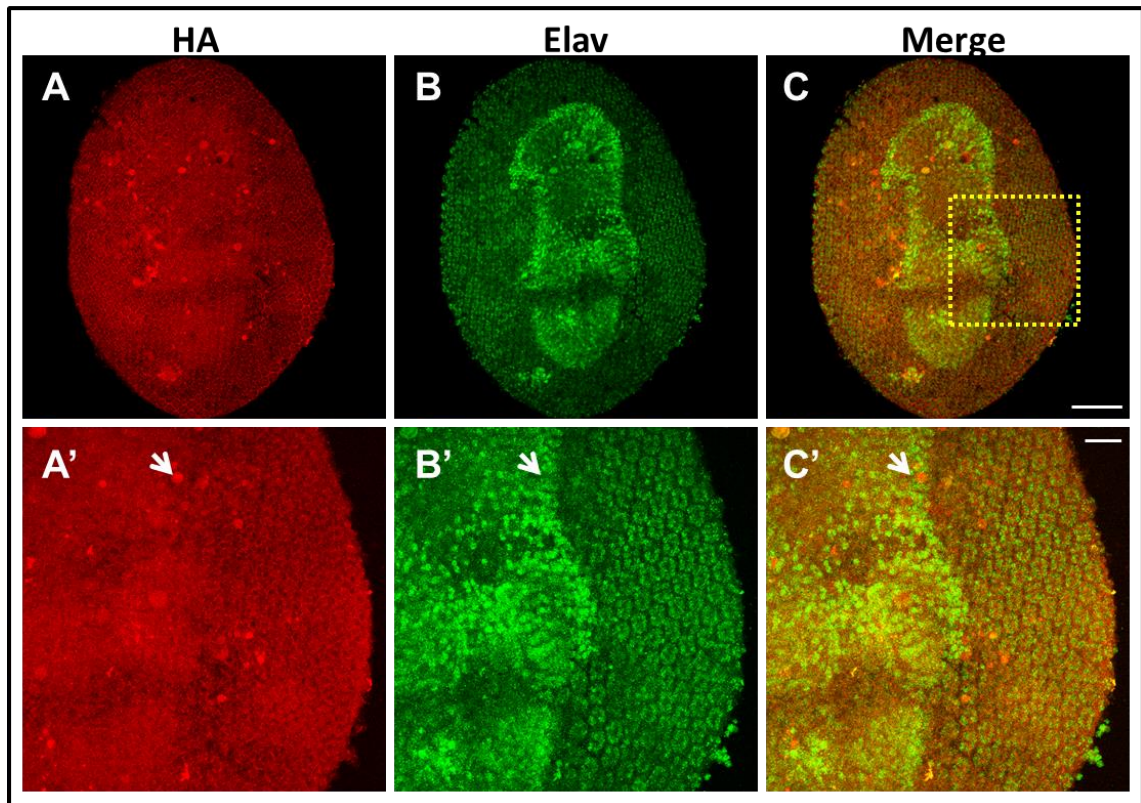
Figure 4.4. Uzip is expressed in the pupal retina. Immunostaining of FH::Uzip in pupal retinas 40h APF with α-HA (A, A') and α-Elav (B, B') antibodies. (C) Uzip expression is detected around Elav expressing nuclei, and in another source (see white arrow). (A', B', C') Magnified view of A, B, and C respectively, taken from the yellow square. α-HA (red), α-Elav (green).

Expression of FH::Uzip in the pupal retina shows a similar pattern as in the larval eye disc, surrounding the nuclei of photoreceptors. In addition some signal was detected in spots (see white arrow in Figure 4.4), which could be glial origin. Even though the enhancer-trap line expression co-localizes with the R8 specific marker senseless, the pupal expression of FH::Uzip did not appear to show such a specific pattern. Again more immunostainings will help to evaluate the localization of Unzipped. In Figure 4.4, it seems

that Uzip co-localizes with the neuronal nuclei staining of Elav. However, this is not a reasonable pattern for Uzip, which is found in membrane attached and secreted forms (Ding *et al.*, 2011).

4.1.3. Uzip is Expressed in the Adult Stage

Uzip expression using the enhancer-trap line was previously observed in the adult brain, in particular in the olfactory circuit. FH::Uzip transgenic fly brains were immunostained with antibodies against HA and Elav (Figure 4.5). In a second experiment we immunostained adult brains of FH::Uzip flies with α-Repo (data now shown). This experiment again did not give any specific pattern for FH::Uzip expression. No meaningful expression pattern for FH::Uzip was observed suggesting that the staining did not work properly.
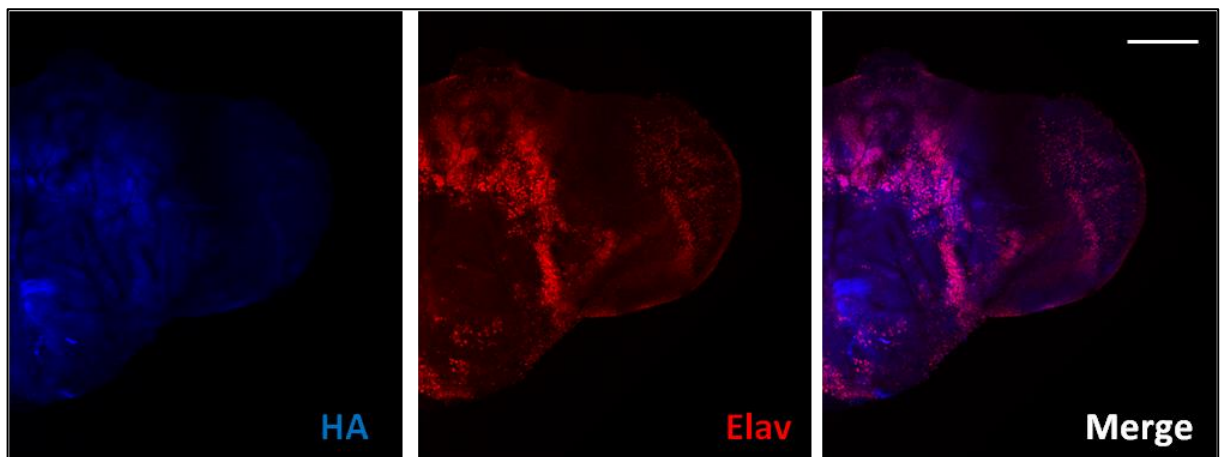
Figure 4.5. FH::Uzip expression in the adult fly brain. α-HA staining does not result in a specific expression pattern. Half of a brain is shown. α-HA (blue), α-Elav (red). Magnification: 20X. Scale bar: 100 μm.

The overall results of expression analyses of endogenous Uzip show us that Uzip is expressed in neurons but not glial cells, and it appears to be localized to the membrane of the neurons. The localization in the eye imaginal discs corresponds to the expression observed with the enhancer-trap line, while the extent of co-localization of glial expression needs to be investigated further using better tools. Detection of the HA tag turned out to be

difficult and a lot of optimization was necessary to get any kind of reasonable a-HA stainings, and it still does not work every time for reasons that are not very clear. As an alternative FLAG antibodies could be optimized to see if they work better than HA antibodies in tissues. Currently we are waiting for a transgenic line in which Unzipped expression can be monitored by looking at mcherry expression. Ultimately, the use of a functional Unzipped-specific antibody will be the best way to show Unzipped localization.

4.2. Co-immunoprecipitation of *Uzip* with its Possible Interaction Partners

In the visual system of *Drosophila,* our *Uzip* enhancer-trap line is only expressed in R8 photoreceptors and a subset of glia, and similarly in the olfactory system it is only expressed in a single subset of ORNs in the antenna, whose identity needs still to be determined (Zülbahar, 2012). It is known that R8 cells are the first neurons to differentiate (Jarman *et al*., 1994; Tomlinson and Ready, 1987) and antennal ORN axons are the first neurons to reach the antennal lobe and start to form glomeruli (Sweeney *et al*., 2007). This observation lead us to hypothesize that Uzip-expressing R8 neurons and ORNs have pioneering roles in establishing the neuronal circuitry in both sensory systems (Zülbahar, 2012). We suggest that glia-derived Uzip interacts with membrane-bound Uzip on pioneering axons, which in turn guides the follower axons via heterophilic interaction of Uzip.

In light of these data, we aimed to identify the interaction partners of Uzip by performing co-immunoprecipitation (co-IP) assays followed by Mass Spectrometry (MS) analysis.

4.2.1. Optimization of Co-IP Conditions for MS Analysis

In order to identify protein-protein interaction partners of Uzip, we performed co-IP followed by MS analysis of co-immunoprecipitated proteins. For this purpose, we extracted total protein from fly heads of the transgenic line FH::Uzip (Figure 4.6). Total protein extracts of fly heads were incubated with anti-HA agarose beads (Sigma) and FH::Uzip was co-immunoprecipitated together with its interaction partners. As a negative

control mouse IgG-agarose beads (Sigma) were used with protein lysates obtained from heads of the same transgenic fly line.
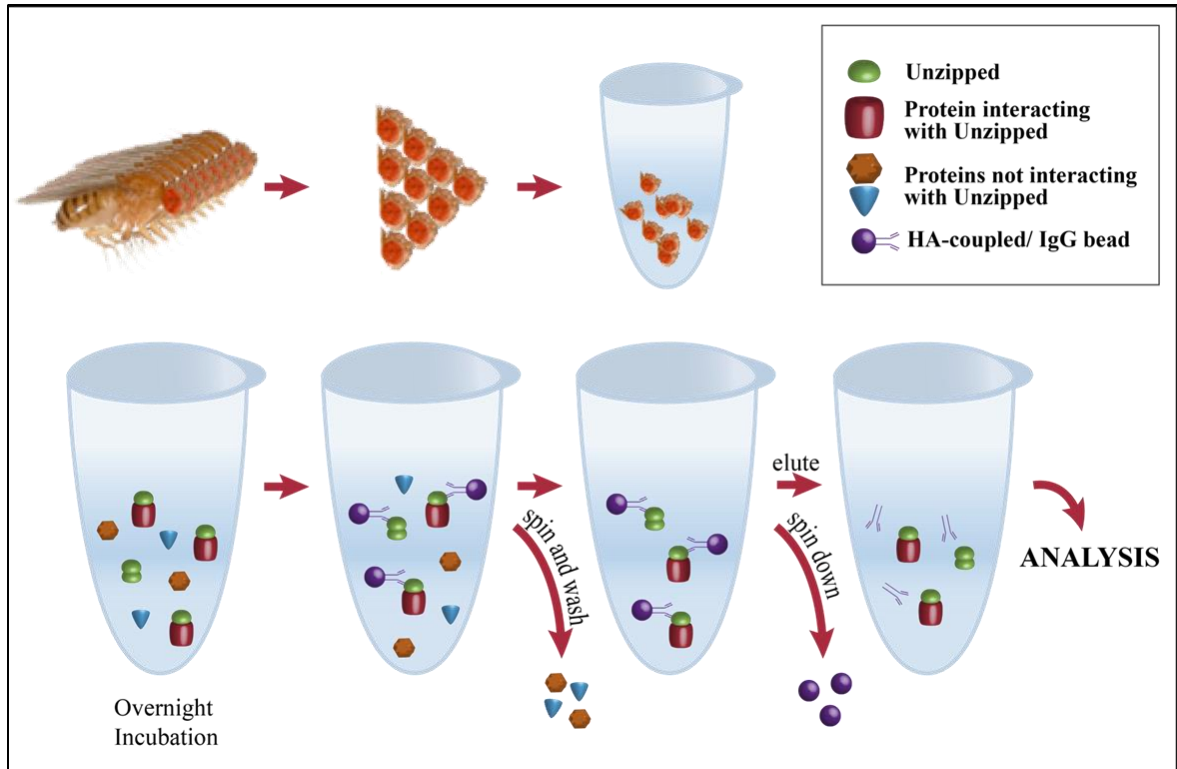
Figure 4.6. Schematic representation of the experimental outline starting from protein extraction from FH::Uzip *Drosophila* heads and co-immunoprecipitation using anti-HA and mouse IgG agarose beads.

First, it was necessary to establish and optimize co-IP conditions in our laboratory. We used the protocol suggested by Sigma for use of anti-HA agarose beads with minor adjustments. The most important step was the determination of the lysis buffer, since Uzip is found in both secreted and membrane-bound forms and we wanted to obtain both forms. Thus, we started by extracting FH::Uzip from the transgenic fly line by using three different lysis buffers: ionic, non-ionic, and denaturing. All of the lysis buffers were able to extract both forms of FH::Uzip as can be seen in the Figure 4.7. Two bands are observable on the blot corresponding to the membrane-bound (80 kD) and secreted (65 kD) forms of Unzipped. Actin was used as loading control. However, in order to preserve the interactions between Uzip and its partners as much as possible, we preferred to continue with the non-ionic lysis buffer, which is less stringent than the others.
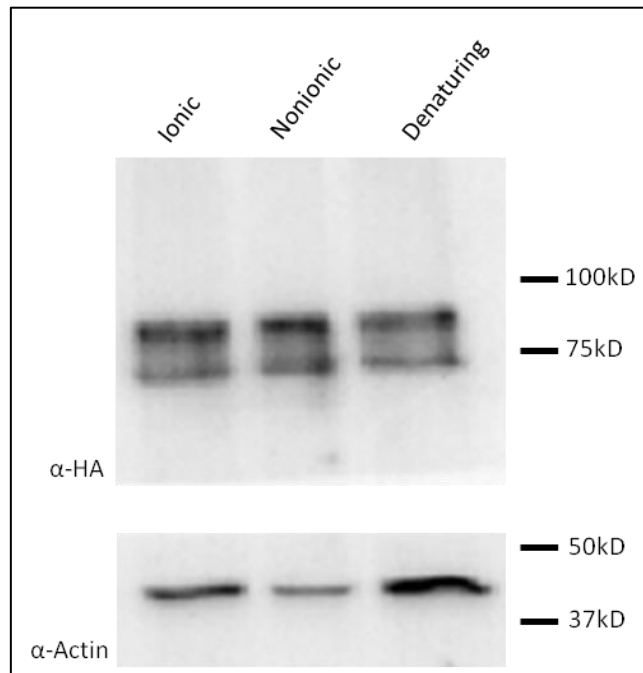
Figure 4.7. Western blot analysis of protein extracts isolated from the transgenic fly line FH::Uzip. Two bands of FH::Uzip, ~65 kD and ~80 kD were extracted by all three different lysis buffers. Actin was used as a loading control.

A few additional changes to the Sigma protocol were made, which are described as follows. The suggested centrifugation speed of the Sigma protocol was decreased from 12000 g to 2000 g and the timing was increased from 30 sec to 2 min, since the suggested speed caused the beads to stick to the tip of the tube. After decreasing the centrifugation speed we increased the timing of centrifugation in order to make sure that all beads were spinned down. The elution was performed in two steps differing from the Sigma protocol to obtain all of the bound proteins. In the first elution step, bound proteins were eluted at 70°C for 20 min with agitation and in the second step elution was performed at 99°C for 10 min with agitation.

At each spinning step, supernatants were collected and kept frozen for further use in Coomassie staining (Figure 4.8) and Western blotting. FH::Uzip proteins are expected to bind to the α-HA beads and thus decrease the amount of FH::Uzip bands in the blot after overnight incubation with the beads. In addition to that, FH::Uzip bands should be detectable in the IgG control lane. Therefore, the supernatant taken right after the overnight incubation was analyzed for the presence of FH::Uzip proteins (Figure 4.9). Moreover, the supernatants after the washes were checked for any loss of bound protein during the washing steps.
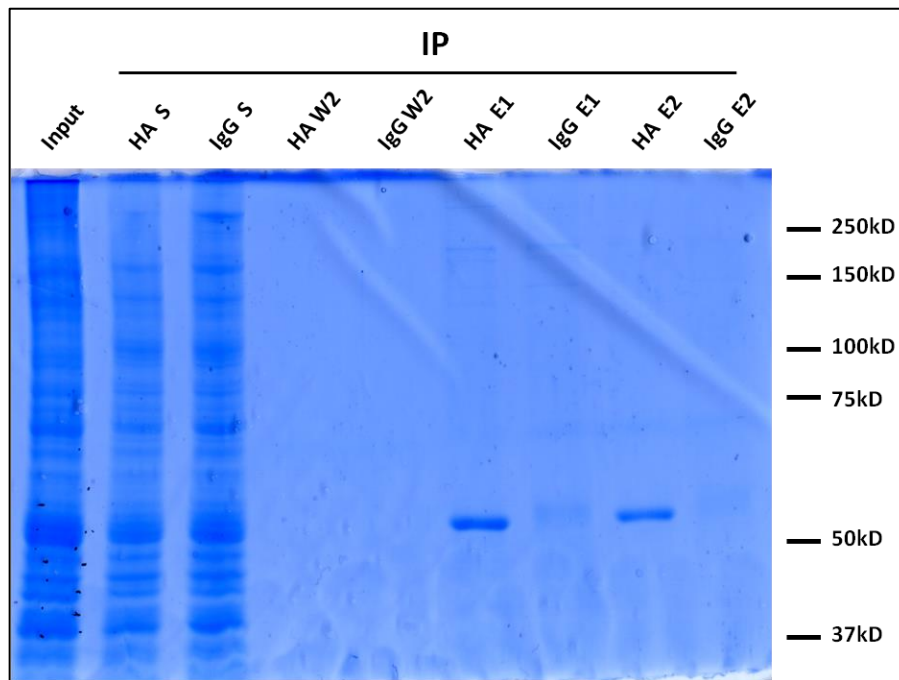
Figure 4.8. Coomassie blue stained SDS-PAGE gel. ~50 kD bands in eluates correspond to the heavy chain of HA. S: Supernatant, W: Wash, E: Eluate.

As can be seen in Figure 4.8, we were able to elute bound proteins from the beads and there was no detectable loss of protein during the washing steps. A band at ~50 kD in the eluate lanes corresponds to the heavy chain of HA antibody that is detached from the agarose beads.

As expected, we could not detect any band that corresponds to FH::Uzip in the supernatant taken right after the overnight incubation with the anti-HA beads (see lane HA S in Figure 4.9). In contrast, FH::Uzip proteins were not bound to IgG beads and were detected in the blot (see IgG S lane in Figure 4.9). In order to see any loss of protein during the washing steps, we used the supernatant of the second wash in the blot from a total of 4 washing steps. Luckily for us, there was no loss of FH::Uzip throughout the washing steps. As observed in the lane HA E1 in Figure 4.9, bound proteins were successfully eluted from the anti-HA beads and they were not present in the control lane.
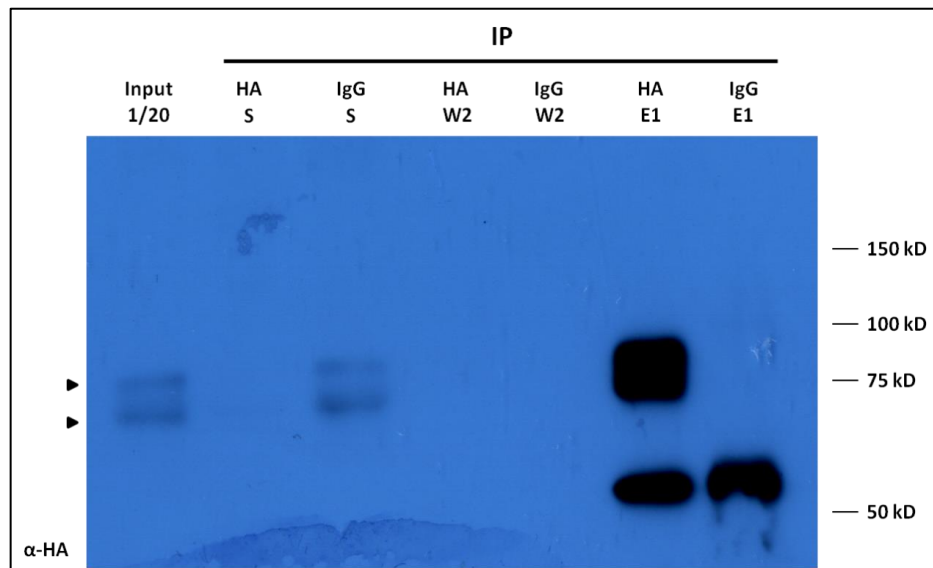
Figure 4.9. Western blotting of co-immunoprecipitated proteins with α-HA. The two Uzip bands, ~80 kD and ~65 kD (shown with arrowheads) are seen in Input and IgG S lanes. They are also detected in the HA eluate sample. The bands at ~50 kD in the eluate lanes correspond to the heavy chain of HA and IgG. Input is the total protein lysate of fly heads. S: Supernatant, W: Wash, E: Eluate.

4.3. Mass Spectrometry Analysis

Mass spectrometry (MS) is a powerful and versatile technique for studying protein-protein interactions. When it is coupled with co-immunoprecipitation and liquid chromatography, mass spectrometry allows rapid, sensitive, and reliable identification of members of protein complexes. This technique has been recently used in *Drosophila* protein research (Ohler *et al*., 2011; Guruharsha *et al*., 2012; Lee *et al*., 2012). Thus, we decided to use MS for the identification of protein interaction partners of Uzip.

4.3.1. Co-IP for Mass Spectrometry Analysis

As the first step, we obtained crude protein extract from fly heads of the FH::Uzip transgenic line as described in 4.2.1. After several trials to optimize number of flies in relation to the amount of protein that is extracted, we decided to use 100 fly heads for co-immunoprecipitation in order to have detectable amounts of protein for the MS analysis.

Then, the interaction partners of Uzip were co-immunoprecipitated with FH::Uzip by using anti-HA agarose beads using IgG-coated agarose beads as negative control. In the next step, the eluted samples from both anti-HA and IgG beads were run on an 8% Tris-Glycine gel. The gel was divided into three fractions and removed by a scalpel for further analysis (Figure 4.10). The fractions shown in Figure 4.10 were chosen according to following criteria. We aimed to avoid the heavy chain of the HA antibody that would mask low abundant proteins in our experimental sample. Since Uzip is a cell adhesion molecule, we expect to identify cell adhesion proteins as potential interaction partners of Uzip. Most of the cell adhesion molecules are heavy proteins, for instance NCad [347 kDa, (Uniprot ID: O15943)] and Gogo [139 kDa, (Uniprot ID: Q9VWA7)]. Therefore, we obtained our gel fractions from regions that are above the heavy chain of α-HA (~50 kDa). While the bands are not clearly visible, the amounts were sufficient to obtain meaningful data as will be described in section 4.3.2. MS analysis was performed at Koç University Proteomics Facility (Istanbul, Turkey) using LC-MS/MS device (Q Exactive Benchtop Orbitrap LC-MS/MS Mass Spectrometer).
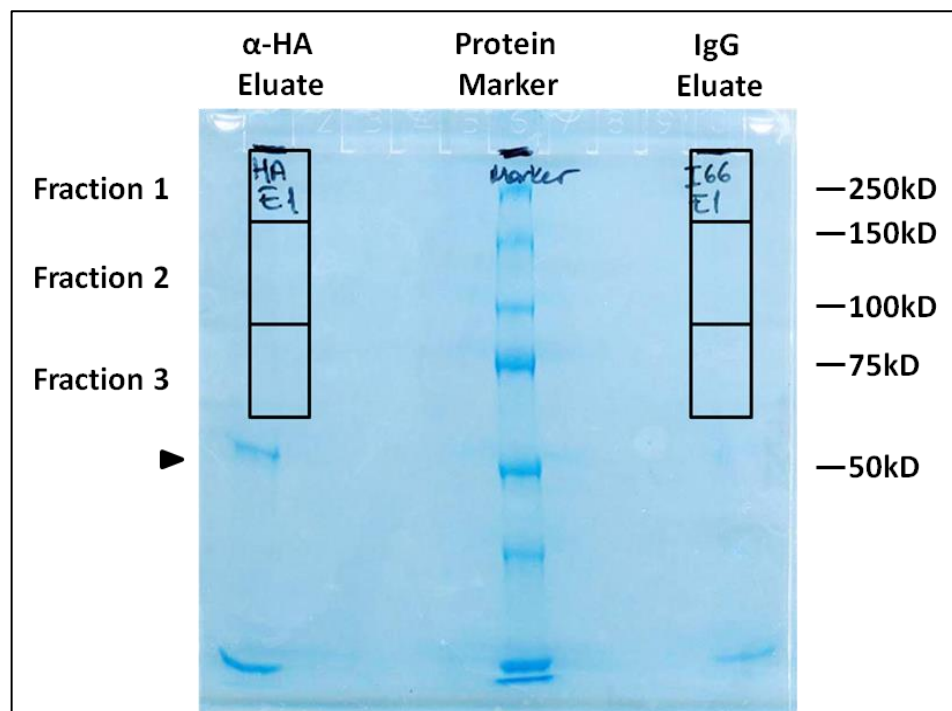
Figure 4.10. Coomassie blue staining of PAGE gel of eluates obtained from fly heads of FH::Uzip using both anti-HA and IgG beads of the first MS analysis. The gel fractions that were chosen for MS analysis were cut from the gel and are shown by rectangles. Arrowhead points to the heavy chain of α-HA.

After obtaining the results of the first round of MS analysis we performed a second experiment using a biological replicate in order to increase our confidence in the obtained data. Additionally, after analysis of the results we decided to increase the amount of protein input and doubled the number of fly heads from which the protein was extracted. Thus, in the second experiment total protein of 200 fly heads was extracted. The results of the gel are shown in Figure 4.11. As can be observed by comparing Figures 4.10 and 4.11 the amount of proteins bound to the beads is increased. This time two fractions from the gel was cut and used in MS analysis (Figure 4.11). As will be shown in Table 4.1. there is one OR protein (Or42b) in the first MS analysis result. Even though its coverage percent is lower than our threshold, it is possible that OR42b might be the only ORN that expresses Uzip. The molecular weight of Or42b is ~46 kD and the molecular weights of other olfactory receptor proteins are similar. With the hope to find Or42b again or another OR protein in the replicate MS analysis, we expanded the fraction size to below 50 kD.
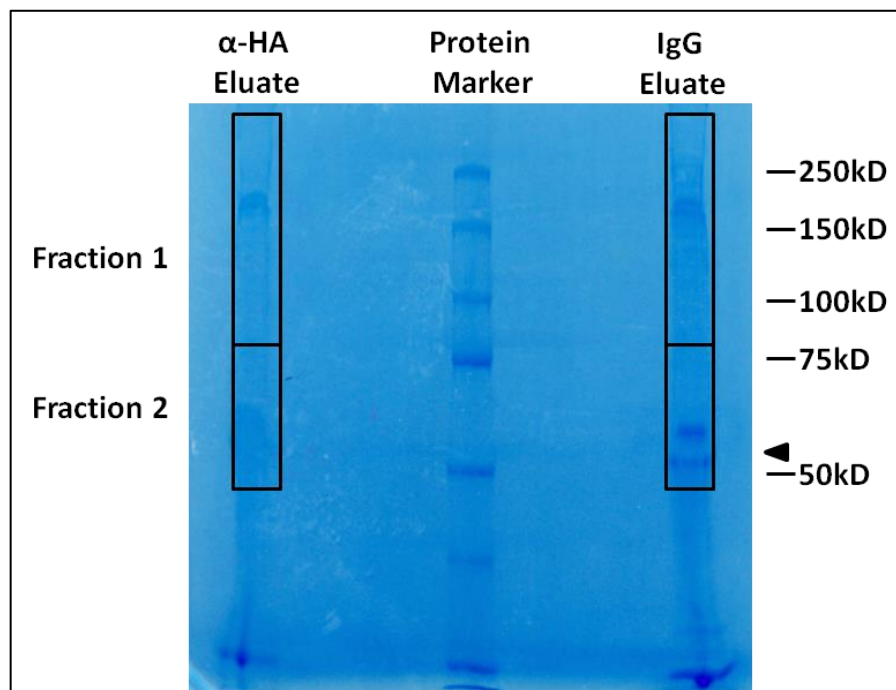
Figure 4.11. Coomassie blue staining of eluates obtained from fly heads of FH::Uzip using both anti-HA and IgG beads of the second MS analysis. The gel fractions that were chosen for MS analysis were cut from the gel and are shown by rectangles. Arrowhead points to the heavy chain of α-HA.

4.3.2. Mass Spectrometry Analysis of Co-immunoprecipitated Proteins

The first mass spectrometry analysis of co-immunoprecipitated partners of Uzip has resulted in the identification of 83 different possible interactor proteins, 12 of which also showed up in the control sample. These 12 proteins were excluded from further analysis. The remaining 71 proteins (Table 4.1) were then sorted according to their coverage and unique peptide number to peptide number ratio (Table 4.2). Protein coverage percent represents the abundance of a protein in a sample, while the unique peptide number of a protein shows the number of peptides that are unique for that protein. Proteins that have coverage above 5% and at least one unique peptide were chosen as possible interaction partners of Uzip.

Table 4.1. Possible interaction partners of Uzip identified by LC-MS/MS listed according to highest coverage.

Accession*	Description	Coverage	# Unique Peptides	# Peptides
A4V134	CaMKII, Isoform E	26.72	1	12
P91928	CG6455	25.98	7	18
D1YSG7	CaMKII, Isoform I	25.66	1	12
A4V364	CG17838	24.76	8	16
P10379	Uzip	23.98	7	11
Q9VEX6	Bor	22.35	5	13
Q8T4D1	Pasilla	20.04	6	9
A4V4U5	Sluggish A, isoform F	19.28	4	14
Q9VA73-3	Aralar1	18.56	7	11
Q0KHU2	IGF-II mRNA-binding protein, isoform I	18.2	4	9
O62619-2	PyK, Isoform B	17.19	5	7
Q02645-4	Hts, Isoform D	16.77	5	8
P21521-2	Syt1, Isoform B	15.68	5	8
P10676	NinaC	15.32	3	23
A1Z7S3	Lightoid, Isoform B	14.58	4	9
O97125	Hsp68	14.33	1	6
Q8T4G5	CG6512, isoform A	14.29	4	9
P10676-2	NinaC, Isoform A	14.1	1	16
P13607-3	Atpα	13.23	4	8
Q7KU78	CG10077, Isoform C	12.71	1	6
Q95U20	Opa1-like	12.54	5	12
P29844	Hsc70-3	12.2	1	10
Q24560	βTub56D	12.08	2	4

Table 4.1. Possible interaction partners of Uzip identified by LC-MS/MS listed according to highest coverage (cont.)

P91926	AP-2α	11.91	4	10
Q2PDR9	Varicose, isoform C	11.73	2	5
Q09103-3	RdgA	10.91	5	9
E1JJ68	Rm62, isoform H	10.78	4	5
Q9NFU0-3	dFMR1	9.33	3	6
E1JJL2	Flotillin 2, isoform G	9.12	1	3
P06002	Rh1	9.12	1	2
Q7K5K0	CG2183	8.46	1	3
Q8INN7	Unc-115, isoform D	8.16	1	6
Q86PA0	CG17816, isoform D	7.25	1	4
Q04047-2	NonA	6.73	1	4
A4V3Q6	Ef1α100E	6.71	1	2
P22700-2	Ca-P60A	6.19	3	5
Q9VIE8	Aconitase, isoform B	6.1	1	4
E2QCG7	eIF3-S9	6.09	1	5
Q9V431	Aac11	5.97	2	3
A1ZBJ2	CG7461	5.74	3	4
Q8MMD3	Eps-15	5.61	1	6
Q9W3M7	CG10777	5.61	2	5
Q9VVH0	CG12229	5.43	1	2
Q9VHC7	Rump	5.38	2	3
Q24253	AP-1-2β	5.21	1	5
Q9VPJ9	CG3164, isoform B	5.16	1	3
P52034	Pfk	5.08	2	3
A4V449	ND75	5.06	1	3
Q24008	InaD	4.9	3	5
Q9VHP0	Bel	4.76	3	4
P02828	Hsp83	4.6	2	3
Q9VFC8	CG6904	4.51	2	3
Q07327	Rop	4.36	1	2
A1ZAK9	Psi	4.05	1	2
Q9V7Y2	Sply	4.04	1	2
P35381	Blw	3.99	2	2
Q7K569	Gpo-1	3.59	1	2
O77283	Ec	3.15	1	4
Q9VZ49	CG2145	3.04	1	1
Q00963	Beta-Spec	2.97	1	4
Q9W0F6	FucTD	2.46	1	1
Q9V9I4	Or42b	2.26	1	1
Q9VCC0	CHORD	2.26	1	2
Q9I7S4	CG42629	2.22	1	1

Table 4.1. Possible interaction partners of Uzip identified by LC-MS/MS listed according to highest coverage (cont.)

Q09103-2	RdgA, Isoform C	2.15	1	1
Q24546	Syn	2.15	1	2
Q9W003	Spn	1.77	1	3
Q9W0I6	Sac1	1.69	1	1
A8JQX3	Nocturnin, isoform D	1.56	1	1
Q9Y163	Hoe1	1.37	1	1
Q8IRV7	Trol, Isoform B	0.31	1	1

*Uniprot ID number.

Even though there was not much visible protein detection in the Coomassie blue staining of co-immunoprecipitated samples (Figure 4.10), the LC-MS/MS device is able to detect peptides that are present in nano scales.

The most expected protein in the MS analysis results was Uzip, since it had been previously shown in *in vitro* experiments to bind itself homophilically (Ding *et al*., 2011). Uzip is present in the results with a high coverage percent and unique peptide number (Table 4.1). Unfortunately, by the analysis tools it cannot be determined whether this protein is the Flag-HA-tagged transgenic Uzip or endogenous Uzip that interacts with the transgenic protein.

We expected to identify several cell adhesion molecules in the MS analysis since Uzip is a cell adhesion molecule (Ding *et al*., 2011). However, the only cell adhesion associated protein in our results is Flotillin 2 (Stuermer and Plattner, 2005). There might be two reasons behind that. First, the nonionic lysis buffer we used may not be strong enough to extract transmembrane cell adhesion proteins. Second, cell adhesion interactions are transient and may not have been caught at the time of immunoprecipitation.

Even though there is not much cell adhesion molecule in the first MS analysis results, there are two proteins that have functions in axon guidance, which is shown to be the role of Uzip in *Drosophila* nervous system (Ding *et al*., 2011; Zülbahar, 2012). The proteins that are associated with axon guidance process are Hts (Ohler *et al*., 2011) and dFMR1 (Morales *et al*., 2002).

Table 4.2. MS results filtered according to coverage percent and unique peptide number.

Accession	Description	Coverage	# Unique Peptides	# Peptides
A4V134	CaMKII, Isoform E	26.72	1	12
P91928	CG6455	25.98	7	18
D1YSG7	CaMKII, Isoform I	25.66	1	12
A4V364	Syncrip, Isoform F	24.76	8	16
P10379	Unzipped	23.98	7	11
Q9VEX6	Bor	22.35	5	13
Q8T4D1	Pasilla	20.04	6	9
A4V4U5	Sluggish A	19.28	4	14
Q9VA73-3	Aralar1	18.56	7	11
Q0KHU2	IGF-II mRNA-binding protein, Isoform I	18.2	4	9
O62619-2	PyK, Isoform B	17.19	5	7
Q02645-4	Hts, Isoform D	16.77	5	8
P21521-2	Syt1, Isoform B	15.68	5	8
A1Z7S3	Lightoid, Isoform B	14.58	4	9
O97125	Hsp68	14.33	1	6
Q8T4G5	CG6512	14.29	4	9
P10676-2	ninaC	14.1	1	16
P13607-3	Atpα	13.23	4	8
Q7KU78	CG10077	12.71	1	6
Q95U20	opa1-like	12.54	5	12
P29844	Hsc70-3	12.2	1	10
Q24560	βTub56D	12.08	2	4
P91926	AP-2α	11.91	4	10
Q2PDR9	Varicose	11.73	2	5
Q09103-3	Retinal degeneration A	10.91	5	9
E1JJ68	Rm62, Isoform H	10.78	4	5
Q9NFU0-3	dFMR1	9.33	3	6
E1JJL2	Flotillin 2, Isoform G	9.12	1	3
P06002	ninaE/Rh1	9.12	1	2
Q7K5K0	CG2183	8.46	1	3
Q8INN7	Unc-115b	8.16	1	6
Q86PA0	CG17816	7.25	1	4
Q04047-2	nonA	6.73	1	4
A4V3Q6	Ef1α100E	6.71	1	2
P22700-2	Ca-P60A	6.19	3	5
Q9VIE8	Aconitase, Isoform B	6.1	1	4
E2QCG7	eIF3-S9	6.09	1	5

Table 4.2. MS results filtered according to coverage percent and unique peptide number
(cont.).

Q9V431	Aac11	5.97	2	3
A1ZBJ2	CG7461	5.74	3	4
Q8MMD3	Eps-15	5.61	1	6
Q9W3M7	CG10777	5.61	2	5
Q9VVH0	CG12229	5.43	1	2
Q9VHC7	Rump	5.38	2	3
Q24253	AP-1-2β	5.21	1	5
Q9VPJ9	CG3164	5.16	1	3
P52034	Pfk	5.08	2	3
A4V449	ND75	5.06	1	3

Possible interaction partners of Uzip in Table 4.2 were categorized according to the biological processes they are involved in, with the help of the GeneCodis tool (Carmona-Saez *et al*., 2007; Nogales-Cadenas *et al*., 2009; Tabas-Madrid *et al*., 2012). GeneCodis was able to associate 41.5% of the proteins with at least one gene ontology (GO) term (Figure 4.12A). Some of these GO terms are associated with nervous system functioning (see Figure 4.12B). For the remaining proteins we searched for GO terms by using the UniProt protein database (www.uniprot.org). These GO terms were divided into six main categories (Table 4.3). Proteins that are associated with any biological processes in neurons and the nervous system were collected under one main category (*Neuronal function / Nervous system associated* column in Table 4.3) since we are interested in the nervous system. The other proteins were categorized into five other categories, namely: translation / protein processing, behavior, development / morphogenesis, cytoskeleton-associated and others.
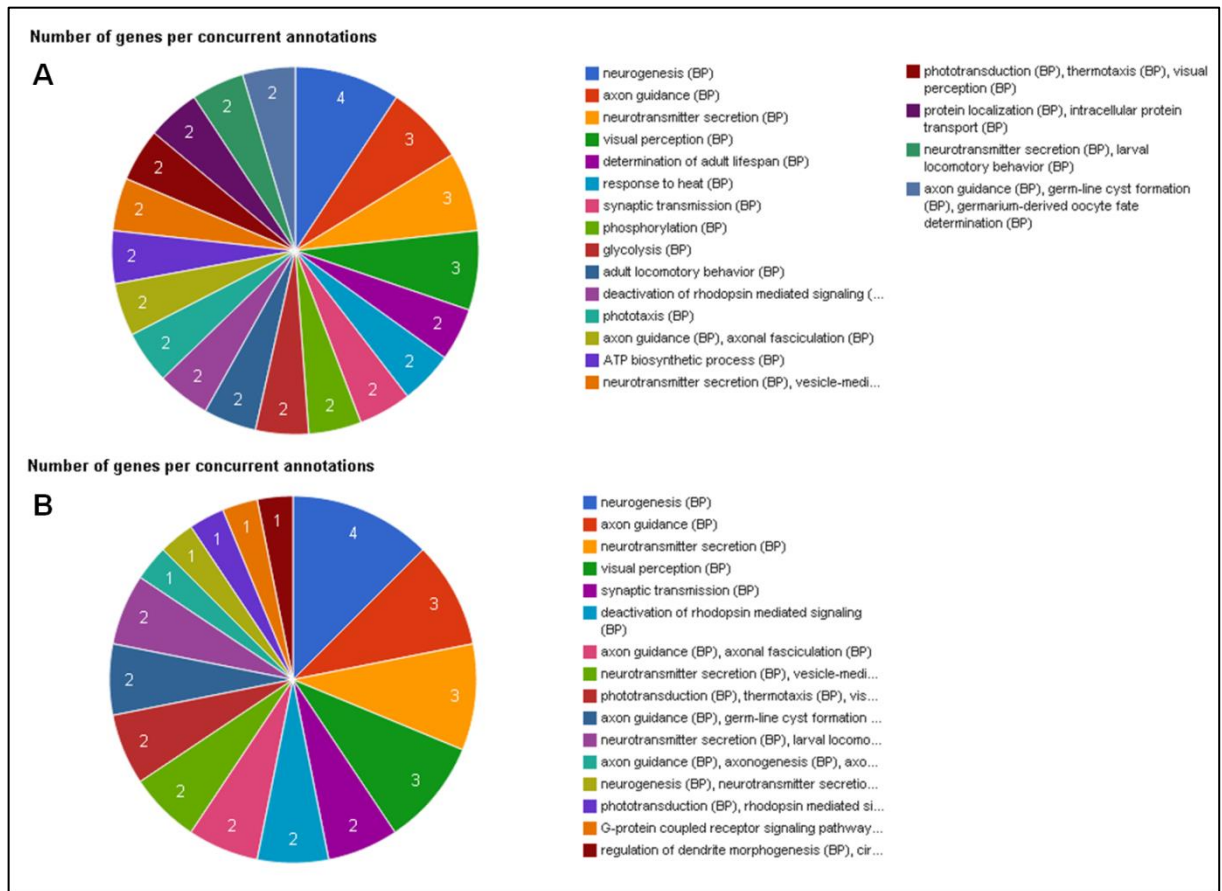
Figure 4.12. Gene Ontology (GO) analysis of MS results. (A) Number of genes per GO term, indicated by different colors. (B) Number of genes per GO terms associated with the nervous system. (http://genecodis.cnb.csic.es/)

Proteins that are categorized under 'Neuronal function / Nervous system associated' (Table 4.3) have functions in many different biological processes: nervous system development, axonal transport, axon guidance, phototransduction, synaptic transmission, synaptic vesicle endocytosis, etc.

Table 4.3. Proteins in Table 4.2 are categorized according to the GO terms.

Neuronal Function/ Nervous System Associated		Translation/ Protein Processing		Behavior		Development/ Morphogenesis		Cytoskeleton associated		Others	
P91928	CG6455	Q8T4D1	Pasilla	A4V4U5	Sluggish A	A4V364	Syncrip, Isoform F	Q24560	βTub56D	Q9VEX6	Bor
P10379	Unzipped	O62619-2	PyK, Isoform B	A1Z7S3	Lightoid, Isoform B	P13607-3	Atpα	Q8INN7	Unc-115b	Q9VA73-3	Aralar1
Q0KHU2	IGF-II mRNA-binding protein, Isoform I	O97125	Hsp68	P22700-2	Ca-P60A					Q8T4G5	CG6512
Q02645-4	Hts, Isoform D	Q7KU78	CG10077							Q95U20	opa1-like
P21521-2	Syt1, Isoform B	P29844	Hsc70-3							Q7K5K0	CG2183
P10676-2	ninaC	Q2PDR9	Varicose							Q86PA0	CG17816
P91926	AP-2α	E1JJ68	Rm62, Isoform H							Q9VIE8	Aconitase, Isoform B
Q09103-3	Retinal degeneration A	A4V3Q6	Ef1α100E							Q9V431	Aac11
Q9NFU0-3	dFMR1	E2QCG7	eIF3-S9							A1ZBJ2	CG7461
E1JJL2	Flotillin 2, Isoform G	P52034	Pfk							Q9W3M7	CG10777
P06002	ninaE/Rh1									Q9VVH0	CG12229
Q04047-2	nonA									Q9VHC7	Rump
Q8MMD3	Eps-15									Q9VPJ9	CG3164
Q24253	AP-1-2β									A4V449	ND75
A4V134	CaMKII, Isoform E										
D1YSG7	CaMKII, Isoform I										

From these, several proteins were selected for further analysis according to following criteria:

- previously identified role in nervous system development and function,
- availability of analysis tools (antibodies, reporter lines).

Thus, we focused on four candidate proteins: Hts, dFMR1, EPS15 and Syt1 (*detailed explanation in* Section 4.4).

In the meantime, we repeated the MS analysis and received the results, which were analyzed in the same way as described above. Doubling the sample size in the second MS experiment resulted in the identification of a higher number of possible interaction partners for Uzip. Here, 316 proteins were identified, 99 of which were also present in the control sample. The remaining 217 possible interaction proteins (Table 4.4) were filtered according to the coverage percent and unique peptide number to peptide number ratio (Table 4.5). Proteins that were identified by only one peptide were excluded, since one peptide is unreliable to identify a protein.

Table 4.4. Possible interaction partners of Uzip identified by the second MS analysis listed according to highest coverage.

Accession	Description	Coverage	# Unique Peptides	# Peptides
A4V4F2	Flo-2, isoform F	51.53	17	21
O61491-2	Flotillin-1	38.60	17	20
E1JIR4	Atpalpha, isoform I	35.13	23	29
A4V134	CaMKII, isoform E	29.47	1	13
Q9VWH4-2	l(1)G0156, isoform A	29.10	5	8
D1YSG7	CaMKII, isoform I	28.30	1	13
E1JJ68	Rm62, isoform H	27.48	6	13
P50887	RpL22	25.75	3	6
Q9VA73-2	Aralar1, isoform 2	22.29	6	12
Q8MMD3	Eps-15, isoform C	21.97	9	16
P10379	Unzipped	21.93	8	9
B7YZQ3	Prominin, isoform D	21.86	14	22
P09180	RpL4	18.70	4	6
Q24212	stnB	18.23	8	14
E1JIT0	how, isoform E	17.82	2	6
Q9VCI3	Lsd-1	17.63	4	8
O61380	eIF4G, isoform A	17.35	16	22

Table 4.4. Possible interaction partners of Uzip identified by the second MS analysis listed according to highest coverage (cont.).

Q9W596	futsch	17.03	26	43
Q86BS7	CG9485, isoform C	16.24	15	22
P41073	Pep	15.92	6	10
E1JGN7	Bancal, isoform E	15.42	4	6
Q8T4G5	CG6512, isoform A	15.25	2	13
Q1WWC9	Dap160, isoform C	15.05	12	14
Q9VPQ2	CG4164	14.97	2	3
P19334	trp	14.82	9	14
Q9VJ86	bsf	14.59	9	16
Q86PA0	CG17816, isoform D	14.51	4	7
Q9V4C7	PMCA, isoform I	14.43	8	18
Q9VTG8	CG7607	14.37	1	1
A8DZ10	CG34313	14.23	1	5
Q9VUQ5	AGO2	14.00	2	7
Q9VN25	eIF3-S10	13.77	10	17
Q9W3E2	PIP82	13.56	10	17
Q9VDI8	CG17838, isoform D	13.44	5	11
P17210	Khc	13.33	5	11
Q9VCK0	eIF-3p66	12.86	3	6
Q9VSU8	nwk	12.70	8	10
P38979-2	sta, isoform A	11.85	1	3
Q8IR16	nonA, isoform B	11.59	1	6
Q9W0A8	RpL23A	11.55	1	3
A8JQV3	CG17816, isoform G	11.34	4	6
O16797	RpL3	11.30	4	5
P91926	alpha-Adaptin	11.17	3	9
Q9V397	Mtpalpha	10.86	3	7
O77410	eIF3-S6	10.34	2	5
P41073-3	Pep, isoform C	10.25	2	5
Q8MSV2	shep	10.21	2	5
Q1RKY1	CG10737, isoform U	10.10	5	6
Q0E8Y1	PIP5K59B, isoform D	10.02	3	8
Q9VV75	CG4169	9.77	3	4
Q02645-2	hts, isoform B	9.75	2	6
Q9VYW4	CG1703	9.66	1	8
Q24008	inaD	9.64	3	5
Q9VEH0	alt, isoform A	9.50	4	9
P16554	numb	9.17	2	5
Q9VZV8	CG16753	9.04	1	1
Q9VU43	SRm160	8.91	1	9
Q24546	Syn	8.88	3	7

Table 4.4. Possible interaction partners of Uzip identified by the second MS analysis listed according to highest coverage (cont.).

A1Z7V1	Bruchpilot, isoform D	8.79	3	13
A1ZAX1	eIF3-S8	8.79	2	7
Q7KT16	vari	8.65	4	5
Q9VTZ0	tral	8.59	2	3
P26686-3	B52, isoform B	8.51	1	4
P15215	LanB2	8.18	6	12
P28668	Aats-glupro	8.17	5	13
Q9VTB4	CG6463	8.06	1	1
Q8SWR8	Atx2	7.75	4	6
P08928	Lam	7.72	3	5
O96553-2	pug,isoform A	7.71	1	7
P15372	Arr1	7.69	1	3
Q7JQN4	Rs1	7.67	1	6
Q59E58	Zipper, isoform C	7.66	2	12
Q9Y102	rgn	7.63	1	7
Q95U20	opa1-like	7.61	4	7
P91928	CG6455	7.58	1	5
Q7JMZ7	sm	7.58	1	3
A1Z9E3	EfTuM	7.57	1	2
Q9NJH0	Ef1gamma	7.42	1	2
Q26365-2	sesB, isoform A	7.36	1	2
P23226-2	Map205, isoform C2	7.21	4	6
E1JJH6	dlg1, isoform N	7.19	1	6
Q9VUH8	CG13472	7.18	2	6
Q9W406	CG15894, isoform A	7.13	5	7
Q9I7I8	CG5077	7.11	1	5
Q8MZI3	CG10077, isoform A	6.85	3	5
Q7JS69	nrv3	6.75	1	2
A1Z7H3	Acsl	6.51	2	5
E1JH90	Patronin	6.46	1	9
Q9VGQ1	CG5214	6.41	1	3
Q7KU92	Ank2, isoform L	6.37	8	24
E1JJH5	dlg1, isoform M	6.31	1	6
Q9VF03	mor	6.29	2	7
A8DZ06	CG4587, isoform C	6.19	1	6
A4V383	ND42, isoform B	6.14	1	2
L0MLQ9	CG32016, isoform H	6.13	1	6
P07909-3	Hrb98DE, isoform E	6.11	1	2
Q9VEN9	Patr-1	6.10	1	5
Q0E996	NAT1, isoform A	5.88	1	5
Q03042	Pkg21D	5.86	1	3

Table 4.4. Possible interaction partners of Uzip identified by the second MS analysis listed according to highest coverage (cont.).

E1JJK8	rdgB, isoform G	5.82	2	6
Q00174	LanA	5.77	10	18
P04052	RpII215	5.72	1	10
Q9VEX2	Gilgamesh, isoform A	5.69	1	1
Q24478	Cp190	5.47	4	6
Q7JWR9	CG8635	5.45	2	2
A1Z9J3	shot, isoform H	5.41	6	44
Q0KHS8	eag, isoform B	5.28	1	6
Q8MLN9	prom	5.27	1	4
Q9VPJ9	CG3164, isoform B	5.16	2	3
Q86BI3	Zn72D, isoform B	5.09	2	3
L0MN72	Asator, isoform J	5.08	2	6
Q24208	Su(var)3-9	5.05	1	2
Q7KT48	CLIP-190, isoform H	5.01	1	7
P11046	LanB1	4.98	3	8
Q7KVT3	Stardust, isoform E	4.97	2	6
Q9VSY1	CG4022	4.90	1	2
Q9VZY4	CG16976	4.80	1	1
Q9W1Y2	PIP5K59B	4.80	1	3
Q9VE79	CG14309	4.76	1	3
Q9VBA2	SIP2-RE	4.69	1	1
Q9VZ49	CG2145	4.56	2	2
P07486	Gapdh1	4.52	1	1
Q9VYS4	wisp	4.52	1	5
Q9VJH2	mdy	4.44	1	4
Q9U9Q4	eIF-3p40	4.44	1	2
Q9VAW5-1	larp, isoform C	4.42	2	5
Q9W0C9	CG12105	4.37	1	5
Q8IN01	CG31161	4.36	1	2
Q7KLW9	Prp19	4.36	2	3
Q7KQM6-2	CG11148	4.34	2	6
Q7PLL3	eIF-4B	4.14	1	2
A1Z843	CG1371	4.09	1	4
Q9VXR5	CG9281, isoform B	4.09	1	3
Q9W3M7	CG10777	4.02	1	3
A8JV00	CG34417, isoform H	4.00	2	21
A4V364	Syp, isoform F	3.97	1	2
Q9W4M7	tyf, isoform B	3.87	1	6
Q27237	l(2)tid	3.85	1	2
E1JJD5	norpA, isoform E	3.84	1	4
O62621	beta'Cop	3.72	1	4

Table 4.4. Possible interaction partners of Uzip identified by the second MS analysis listed according to highest coverage (cont.).

A1Z7T0	Pkn	3.70	1	4
Q9V455	Kap-alpha3	3.70	1	1
A8JNP1	Argk, isoform F	3.65	1	1
A1Z877	Ndg	3.63	1	4
E1JI46	Mi-2, isoform C	3.63	1	6
Q8MLV1-2	LBR, isoform A	3.63	2	2
P41374	eIF-2alpha	3.52	1	1
Q9VD58	CG6439, isoform A	3.51	1	1
Q9VVH0	CG12229	3.50	1	1
E1JIT7	Efa6, isoform E	3.49	1	4
Q8MSS1	lva	3.42	3	10
Q9VF87	Sra-1	3.41	1	4
Q9NFU0-4	dFMR1, isoform B	3.40	1	2
A4V1B2	Patj, isoform B	3.33	2	4
Q9VHN8	CG8032	3.26	1	2
B5RIU6	endoA	3.25	1	2
Q9I7T7-2	CG11505, isoform A	3.22	1	3
Q94526	Ork1	3.20	2	3
Q9V431	Aac11	3.17	2	2
P25159-2	stau, isoform B	3.06	1	3
Q9VBU7	Nup358	3.04	1	8
Q9NBD7	chb	2.95	1	4
Q9W425	Rbcn-3A	2.90	2	8
P25455-2	Plc21C , isoform 1	2.84	1	3
E1JJN9	Set2, isoform B	2.81	1	7
P98081	Dab	2.79	1	6
Q9W0D3	CG13917	2.77	1	4
O62530	AP-50, isoform A	2.75	1	1
Q9VN68	Cdep, isoform C	2.72	1	1
Q7PLL6	CG17514, isoform A	2.70	1	6
Q9V9V7	pasha	2.65	1	1
Q9W0S9	DIP2	2.59	1	5
P29844	Hsc70-3	2.59	1	2
Q95RN0-2	CG10038, isoform B	2.59	1	1
A4V101	Ef2b, isoform C	2.52	1	2
Q9VB55	woc, isoform A	2.49	1	4
A4V449	ND75, isoform B	2.46	1	1
P20478	Gs2	2.44	1	1
Q9VFK2	cv-c, isoform A	2.36	1	3
O77062	Eaat1, isoform A	2.30	1	1
Q9VXY3	CG5599	2.16	1	1

Table 4.4. Possible interaction partners of Uzip identified by the second MS analysis listed according to highest coverage (cont.).

Q9VHC7	rump	2.06	1	1
P48994	trpl	2.05	2	2
Q9VX63	CG8915-RA	2.05	1	1
P52034-2	Pfk, isoform A	2.00	1	2
Q9VKK1	Ge-1	1.99	2	3
P46824	Klc	1.97	1	1
Q9W002	msn, isoform A	1.93	1	2
Q9VCA8	mask	1.92	4	6
Q9VXY0	Cyp4s3	1.82	1	1
Q868Z9-2	ppn, isoform F	1.77	1	4
P29845	Hsc70-5	1.60	1	1
A1ZBJ2	CG7461	1.59	1	1
P56079	CdsA	1.57	1	1
Q9VNR7	CG11241, isoform A	1.57	1	1
O18645	SNF1A	1.55	1	1
Q8IN24	GABA-B-R2, isoform A	1.48	1	2
Q8INN5	Unc-115, isoform B	1.47	1	1
Q9VS37	Cdc27	1.33	1	1
A8JNJ9	enc, isoform E	1.29	1	3
Q9VFR2	CG9297, isoform A	1.18	1	1
E2QCG7	eIF3-S9	1.16	1	1
Q24253	Bap	1.09	1	1
Q8IPP4	Canoe, isoform C	0.80	1	1
Q9U1H0-2	cic, isoform A	0.78	1	1
Q9VWP8	CG42450	0.72	1	1
Q9W2X2	CG34408, isoform A	0.65	1	1
Q961B8	CG8290, isoform B	0.62	1	1
Q9W0L7	CG32479	0.53	1	1
Q9VEZ2	CG10185	0.46	1	1
Q9VJ35	ssp3	0.46	1	1
Q9W437	Raptor	0.43	1	1
Q9VC45	asp	0.41	1	1
Q9VXY2	rab3-GEF	0.39	1	1
A1Z713	Vps13	0.27	1	1
Q4ABH0	Msp-300, isoform B	0.24	1	2
Q9VPL9	kis, long isoform	0.13	1	1

As explained above, we expect cell adhesion molecules as possible interaction partners for Uzip. In the repeat MS analysis the only ones associated with cell adhesion are Flotillin 1 and Flotillin 2 (Stuermer and Plattner, 2005).

Similar to the first analysis, there are several axon guidance proteins in the second MS analysis: dFMR1 (Morales *et al*., 2002), Hts (Ohler *et al*., 2011), Laminin A (Stevens and Jacobs, 2002) and Khc (Berger *et al*., 2008).

Table 4.5. Results of second MS analysis filtered according to coverage percent and unique peptide number.

Accession	Description	Coverage	#Unique Peptides	# Peptides
A4V4F2	Flo-2, isoform F	51.53	17	21
O61491-2	Flotillin-1	38.6	17	20
E1JIR4	Atpalpha, isoform I	35.13	23	29
A4V134	CaMKII, isoform E	29.47	1	13
Q9VWH4-2	l(1)G0156, isoform A	29.1	5	8
D1YSG7	CaMKII, isoform I	28.3	1	13
E1JJ68	Rm62, isoform H	27.48	6	13
P50887	RpL22	25.75	3	6
Q9VA73-2	Aralar1, isoform 2	22.29	6	12
Q8MMD3	Eps-15, isoform C	21.97	9	16
P10379	Unzipped	21.93	8	9
B7YZQ3	Prominin, isoform D	21.86	14	22
P09180	RpL4	18.7	4	6
Q24212	stnB	18.23	8	14
E1JIT0	how, isoform E	17.82	2	6
Q9VCI3	Lsd-1	17.63	4	8
O61380	eIF4G, isoform A	17.35	16	22
Q9W596	futsch	17.03	26	43
Q86BS7	CG9485, isoform C	16.24	15	22
P41073	Pep	15.92	6	10
E1JGN7	Bancal, isoform E	15.42	4	6
Q8T4G5	CG6512, isoform A	15.25	2	13
Q1WWC9	Dap160, isoform C	15.05	12	14
Q9VPQ2	CG4164	14.97	2	3
P19334	trp	14.82	9	14
Q9VJ86	bsf	14.59	9	16
Q86PA0	CG17816, isoform D	14.51	4	7
Q9V4C7	PMCA, isoform I	14.43	8	18
A8DZ10	CG34313	14.23	1	5
Q9VUQ5	AGO2	14	2	7
Q9VN25	eIF3-S10	13.77	10	17
Q9W3E2	PIP82	13.56	10	17
Q9VDI8	CG17838, isoform D	13.44	5	11
P17210	Khc	13.33	5	11
Q9VCK0	eIF-3p66	12.86	3	6

Table 4.5. Results of second MS analysis filtered according to coverage percent and unique peptide number (cont.).

Q9VSU8	nwk	12.7	8	10
P38979-2	sta, isoform A	11.85	1	3
Q8IR16	nonA, isoform B	11.59	1	6
Q9W0A8	RpL23A	11.55	1	3
A8JQV3	CG17816, isoform G	11.34	4	6
O16797	RpL3	11.3	4	5
P91926	alpha-Adaptin	11.17	3	9
Q9V397	Mtpalpha	10.86	3	7
O77410	eIF3-S6	10.34	2	5
P41073-3	Pep, isoform C	10.25	2	5
Q8MSV2	shep	10.21	2	5
Q1RKY1	CG10737, isoform U	10.1	5	6
Q0E8Y1	PIP5K59B, isoform D	10.02	3	8
Q9VV75	CG4169	9.77	3	4
Q02645-2	hts, isoform B	9.75	2	6
Q9VYW4	CG1703	9.66	1	8
Q24008	inaD	9.64	3	5
Q9VEH0	alt, isoform A	9.5	4	9
P16554	numb	9.17	2	5
Q9VU43	SRm160	8.91	1	9
Q24546	Syn	8.88	3	7
A1Z7V1	Bruchpilot, isoform D	8.79	3	13
A1ZAX1	eIF3-S8	8.79	2	7
Q7KT16	vari	8.65	4	5
Q9VTZ0	tral	8.59	2	3
P26686-3	B52, isoform B	8.51	1	4
P15215	LanB2	8.18	6	12
P28668	Aats-glupro	8.17	5	13
Q8SWR8	Atx2	7.75	4	6
P08928	Lam	7.72	3	5
O96553-2	pug,isoform A	7.71	1	7
P15372	Arr1	7.69	1	3
Q7JQN4	Rs1	7.67	1	6
Q59E58	Zipper, isoform C	7.66	2	12
Q9Y102	rgn	7.63	1	7
Q95U20	opa1-like	7.61	4	7
P91928	CG6455	7.58	1	5
Q7JMZ7	sm	7.58	1	3
A1Z9E3	EfTuM	7.57	1	2
Q9NJH0	Ef1gamma	7.42	1	2
Q26365-2	sesB, isoform A	7.36	1	2

Table 4.5. Results of second MS analysis filtered according to coverage percent and unique peptide number (cont.).

P23226-2	Map205, isoform C2	7.21	4	6
E1JJH6	dlg1, isoform N	7.19	1	6
Q9VUH8	CG13472	7.18	2	6
Q9W406	CG15894, isoform A	7.13	5	7
Q9I7I8	CG5077	7.11	1	5
Q8MZI3	CG10077, isoform A	6.85	3	5
Q7JS69	nrv3	6.75	1	2
A1Z7H3	Acsl	6.51	2	5
E1JH90	Patronin	6.46	1	9
Q9VGQ1	CG5214	6.41	1	3
Q7KU92	Ank2, isoform L	6.37	8	24
E1JJH5	dlg1, isoform M	6.31	1	6
Q9VF03	mor	6.29	2	7
A8DZ06	CG4587, isoform C	6.19	1	6
A4V383	ND42, isoform B	6.14	1	2
L0MLQ9	CG32016, isoform H	6.13	1	6
P07909-3	Hrb98DE, isoform E	6.11	1	2
Q9VEN9	Patr-1	6.1	1	5
Q0E996	NAT1, isoform A	5.88	1	5
Q03042	Pkg21D	5.86	1	3
E1JJK8	rdgB, isoform G	5.82	2	6
Q00174	LanA	5.77	10	18
P04052	RpII215	5.72	1	10
Q24478	Cp190	5.47	4	6
Q7JWR9	CG8635	5.45	2	2
A1Z9J3	shot, isoform H	5.41	6	44
Q0KHS8	eag, isoform B	5.28	1	6
Q8MLN9	prom	5.27	1	4
Q9VPJ9	CG3164, isoform B	5.16	2	3
Q86BI3	Zn72D, isoform B	5.09	2	3
L0MN72	Asator, isoform J	5.08	2	6
Q24208	Su(var)3-9	5.05	1	2
Q7KT48	CLIP-190, isoform H	5.01	1	7

For the second MS experiment we again performed a GO analysis. The GeneCodis tool was able to associate 40% of the proteins that are listed in Table 4.5 with a GO term (Figure 4.13). Some of these GO terms are again associated with nervous system function (see Figure 4.13B). For the remaining proteins we used the UniProt protein database for

the determination of their GO terms. These GO terms were also categorized into the same main categories as previously described (Table 4.6).
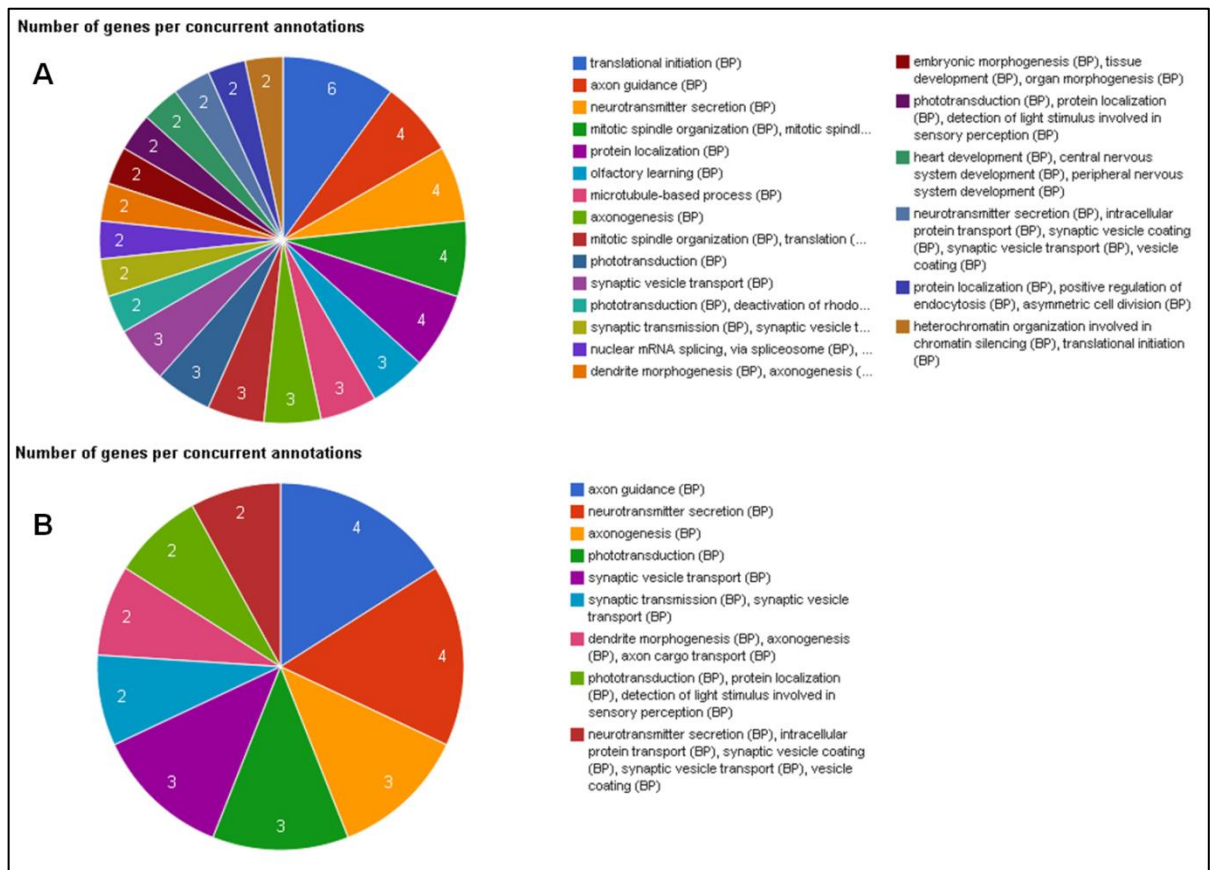

Figure 4.13. Gene Ontology (GO) analysis of second MS experiment. (A) Number of genes per GO term are indicated by different colors. (B) Number of genes per GO term associated with the nervous system. (http://genecodis.cnb.csic.es/)

Table 4.6. Proteins in Table 4.5 are categorized according to the GO terms.

Neuronal Function/ Nervous System Associated		Translation/Protein Processing		Behaviour		Development/ Morphogenesis		Cytoskeleton Associated		Others	
P91926	alpha-Adaptin	Q9VCK0	eIF-3p66	Q8MSV2	shep	P08928	Lam	Q1WWC9	Dap160, isoform C	P38979-2	sta, isoform A
Q24212	stnB	Q24208	Su(var)3-9	Q7JS69	nrv3	O61491-2	Flotillin-1	Q9VV75	CG4169	Q24478	Cp190
P19334	trp	O77410	eIF3-S6			E1JIR4	Atpalpha, isoform I	P23226-2	Map205, isoform C2	P04052	RpII215
Q24008	inaD	Q9VN25	eIF3-S10			E1JGN7	Bancal, isoform E	Q9VTZ0	tral	P26686-3	B52, isoform B
P16554	numb	A1ZAX1	eIF3-S8			Q9VDI8	CG17838, isoform D	E1JH90	Patronin	P28668	Aats-glupro
Q00174	LanA	Q9VUQ5	AGO2			Q59E58	Zipper, isoform C	Q7KT48	CLIP-190, isoform H	Q9VCI3	Lsd-1
P15215	LanB2	P50887	RpL22			Q9VF03	mor			Q9VA73-2	Aralar1, isoform 2
Q9W596	futsch	O16797	RpL3							O96553-2	pug,isoform A
P17210	Khc	P41073	Pep							Q9VWH4-2	l(1)G0156, isoform A
Q26365-2	sesB, isoform A	Q9NJH0	Ef1gamma							Q86BS7	CG9485, isoform C
Q24546	Syn	P07909-3	Hrb98DE, isoform E							Q9VYW4	CG1703
P15372	Arr1	P09180	RpL4							Q9VJ86	bsf
P10379	Unzipped	E1JJ68	Rm62, isoform H							Q86PA0	CG17816, isoform D
Q02645-2	hts, isoform B	O61380	eIF4G, isoform A							Q9V4C7	PMCA, isoform I
Q8SWR8	Atx2	Q8T4G5	CG6512, isoform A							A8DZ10	CG34313
A4V4F2	Flo-2, isoform F	Q9VPQ2	CG4164							Q9W3E2	PIP82
Q8MMD3	Eps-15, isoform C	Q9W0A8	RpL23A							A8JQV3	CG17816, isoform G
B7YZQ3	Prominin, isoform D	P41073-3	Pep, isoform C							Q9V397	Mtpalpha
E1JIT0	how, isoform E	Q9VU43	SRm160							Q1RKY1	CG10737, isoform U
Q9VSU8	nwk	Q7KT16	vari							Q9VEH0	alt, isoform A
Q8IR16	nonA, isoform B	Q7JQN4	Rs1							Q9Y102	rgn
Q0E8Y1	PIP5K59B, isoform D	A1Z9E3	EfTuM							Q95U20	opa1-like
A1Z7V1	Bruchpilot, isoform D	Q9VEN9	Patr-1							P91928	CG6455

Table 4.6. Proteins in Table 4.5 are categorized according to the GO terms (cont.).

Q7JMZ7	sm									Q9W406	CG15894, isoform A
E1JJH6	dlg1, isoform N									Q9I7I8	CG5077
Q9VUH8	CG13472									Q8MZI3	CG10077, isoform A
A1Z7H3	Acsl									Q9VGQ1	CG5214
E1JJH5	dlg1, isoform M									A8DZ06	CG4587, isoform C
Q7KU92	Ank2, isoform L									A4V383	ND42, isoform B
E1JJK8	rdgB, isoform G									L0MLQ9	CG32016, isoform H
A1Z9J3	shot, isoform H									Q0E996	NAT1, isoform A
Q8MLN9	prom									Q03042	Pkg21D
A4V134	CaMKII, isoform E									Q7JWR9	CG8635
D1YSG7	CaMKII, isoform I									Q0KHS8	eag, isoform B
										Q9VPJ9	CG3164, isoform B
										Q86BI3	Zn72D, isoform B
										L0MN72	Asator, isoform J

From the proteins that are listed in Table 4.6, several proteins were selected according to the criteria explained above and thus we decided to focus on three proteins: Hts, EPS15, and Syn (*detailed explanation in* Section 4.4).

The results of the first and second MS analysis were compared. One of the proteins that we determined as a candidate after the first round of MS analysis, Syt1, was present in the IgG control of the second MS analysis. Therefore, we excluded this protein from our candidate list. Furthermore, dFMR1 was filtered out when the proteins were filtered according to their coverage percent because the percent coverage of dFMR1 in the second MS analysis was only 3.4%. However, we did not exclude this protein from our candidate list because it was present in both MS analysis results. Even though its coverage was lower in the second one, the presence of dFMR1 in both analyses gave us some contidence and we continued to think of this protein as a candidate partner for Uzip. Similar to dFMR1 the percent coverage of Synapsin (Syn) was below 5% in the first MS analysis. So, we did not include this protein into our initial candidate protein list. However, Syn showed up in the second MS analysis and resulted in 8.8% coverage percent. Therefore, we decided to add it into our list. Hts and EPS15 were above threshold level of coverage percent in the results of both MS analyses.

As a result we chose four proteins Hts, dFMR1, EPS15, and Syn as candidate interaction partner candidates of Uzip for analysis in co-IP experiments and immunohistochemical analysis of their localization.

4.4. Candidate Interaction Partners of *Uzip*

Among the possible interaction partners that were identified by MS (Table 4.3 and Table 4.6) four proteins have readily available antibodies: Hts, dFMR1, EPS15, and Syn. Therefore, these proteins were chosen for further analysis. MS analysis is a large scale screening method to identify possible biochemical interaction partners of a protein of interest. However, the validity of the predicted interactions has to be confirmed with other, more direct methods. In order to validate the MS results using four of the most promising predicted candidates we performed direct co-IP experiments with the antibodies against these proteins that were obtained from commercial sources. Furthermore, we examined the

expression pattern of these candidates in *Drosophila* adult brain and larval eye imaginal disc.

4.4.1. Hts

Hu li tai shao (Hts) is the homolog of mammalian Adducin in the fruit fly. Adducin is a membrane-skeletal protein located in spectrin-actin junctions in axonal growth cones. Adducin is ubiquitously expressed and required for the proper Actin-Spectrin architecture (Matsuoka *et al*., 2000). *Drosophila* Hts was first found to be an important component of ring canals and fusomes, which are required for oogenesis (Yue and Spradling, 1992), and it is required for the organization of the early embryonic cytoskeleton (Zaccai *et al*., 1996b). Hts contributes to synapse stability by stabilizing the Spectrin skeleton and has a function in presynaptic nerve growth (Pielage *et al*., 2011). Hts has been shown to have a role in PR axon guidance by interacting with the axon guidance receptor Gogo (Ohler *et al.,* 2011).

There are four different spliced forms of Hts encoded by a single gene: Add1, Add2, Ovhts and ShAdd (Petrella *et al.,* 2007). All isoforms are expressed in the *Drosophila* head except for Ovhts, which is restricted to the ovaria of females (Telonis-Scott *et al*., 2009). Hts is ubiquitously expressed in 3rd instar larval optic lobes, localized to the PR axons and R1-R6 terminals in the lamina plexus (Ohler *et al.,* 2011).

Hts was shown to be required for R7 and R8 targeting to their proper layers and for the formation of a regular array of axons in the medulla (Ohler *et al.,* 2011). Furthermore, Hts interacts with the R8-specific axon guidance receptor Gogo. Uzip, on the other hand, was shown to be expressed in R8 cells (Zülbahar, 2012). In the light of these data and our MS analysis results, Hts appeared as a strong candidate interaction partner of Uzip.

4.4.1.1. Co-immunoprecipitation of Hts with FH::Uzip. Hts isoforms Add1 and Add2 are detected as a doublet band around 100 kD by α-Hts antibody 1B1 (DSHB) in the larval eye-brain complex extract. 1B1 antibody also detects additional bands around 95, 90, and 80 kD and it does not detect a band corresponding to the ShAdd isoform (Ohler *et al*., 2011). In Western blotting experiments, we used a protein extract obtained from adult fly

heads and probed this extract with α-Hts antibody. In our blot, we detected a doublet around 95 kD, a thick band around 90 kD, a doublet around 80 kD and a faint band around 70 kD (Figure 4.14A). This observation is consistent with previously published data for Hts.
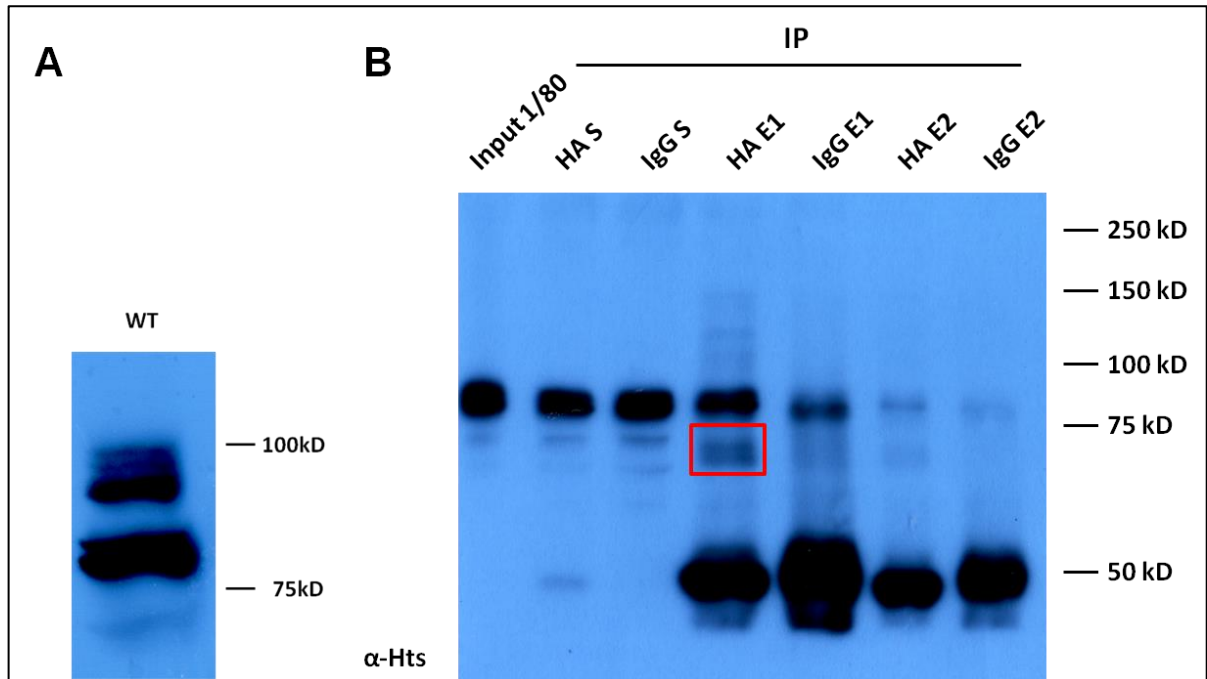

Figure 4.14. Hts interacts with Uzip. (A) Total protein lysate of WT fly heads was blotted with α-Hts. (B) Western blotting of co-IP samples from FH::Uzip adult heads incubated with α-HA or IgG agarose beads probed with α-Hts. S: Supernatant; E: Eluate; WT: Wild type.

To analyze the predicted interaction between Hts and Uzip, co-immunoprecipitated proteins were run on a SDS-PAGE gel and probed with α-Hts antibody (Figure 4.14). The supernatants taken right after overnight incubation were kept for Western blotting analysis and bound proteins were eluted twice from the beads. If there is an interaction between Uzip and Hts, no bands corresponding to Hts in the HA S lane should be observed. However, Hts did not seem to bind to FH::Uzip, since we observe bands that are similar to the ones seen in the input lane. On the other hand, there are bands detected in eluates of both HA and IgG beads. A doublet below 75 kD appears to be present only in the HA eluate samples (*red rectangle in* Figure 4.14B). This result might indicate that only one of the Hts isoforms interacts with Uzip.

4.4.1.2. Co-immunoprecipitation of FH::Uzip with Hts. The previous result appeared promising and thus we wanted to move one step further and perform a cross co-IP assay, which should work as well if Hts and Uzip are true interaction partners. In this experiment we tried to co-immunoprecipitate FH::Uzip together with Hts by using α-Hts antibody-attached agarose beads. The samples obtained from the experiment were run on an SDS-PAGE gel (Figure 4.15).
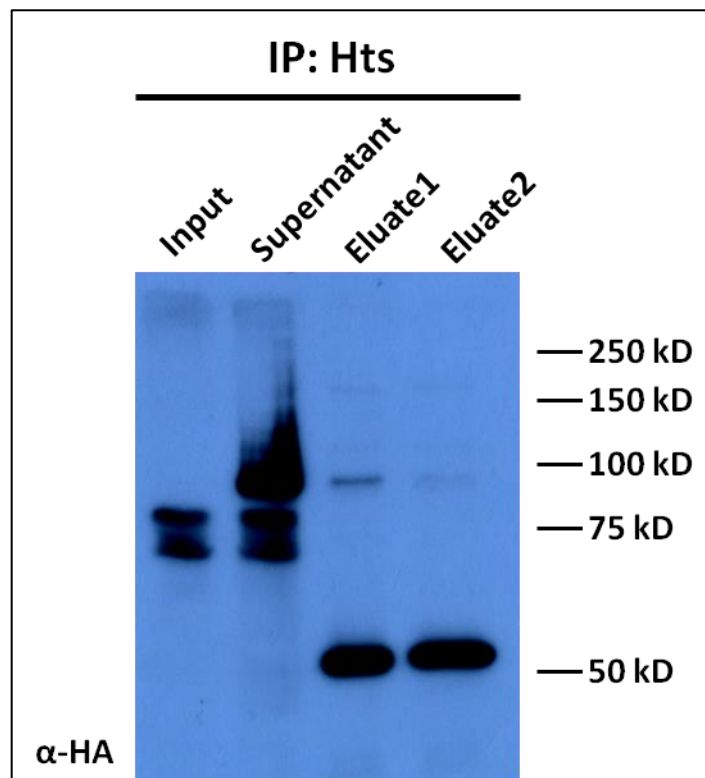

Figure 4.15. Co-Immunoprecipitation of FH::Uzip with α-Hts samples were blotted with α-HA.

As can be seen in Figure 4.15, when the membrane was blotted with α-HA the 65 kD and 80 kD bands corresponding to Uzip in the eluates were not observed. This means that Hts does not interact with Uzip. The thick smear around 100 kD in the supernatant lane corresponds to Hts. Even though we used α-HA antibody for detection, α-Hts antibody detached from the beads could bind to Hts proteins on the membrane.

4.4.1.3. Expression Pattern of Hts. In order to analyze the expression pattern of Hts, we immunostained third instar larval eye disc-brain complexes (Figure 4.16) and adult brains (Figure 4.17) with α-Hts antibody.
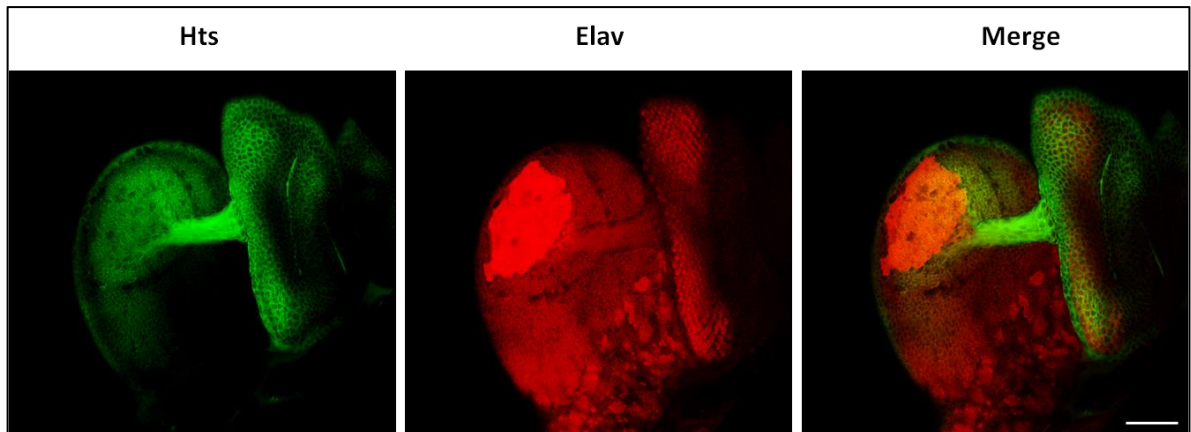

| Hts | Elav | Merge |

Figure 4.16. Hts is expressed in third instar optic lobe and eye discs. α-Hts (green), α-Elav (red). Anterior is to the right. Magnification: 20X. Scale bar: 50 μm.

Hts was ubiquitously expressed in the larval optic lobe, localizing to the PR axons (Ohler *et al*., 2011). Similarly, we observed axonal localization of Hts in the eye disc-brain complex (Figure 4.16). α-Hts antibody stains the PR axons elongating from the eye disc to the optic lobe through the optic stalk. Hts protein seems to localize to the membranes of the cells it is expressed in, which is in accordance with its function on the cytoplasmic side of the membrane (Zaccai and Lipshitz, 1996b).

Next, the adult fly brains were immunostained with α-Hts and α-NCad antibodies for the staining of neuropil structures (Figure 4.17). Neuropils are the structures that are formed mostly by axons and dendrites. Hts expression in the adult brain was observed in the medulla of the optic lobe. In the third instar larvae, the medulla shows a diffusible expression of Hts. However, the layer of expression could not be determined in the adult medulla from this staining. More detailed analyses are needed to understand its exact localization.
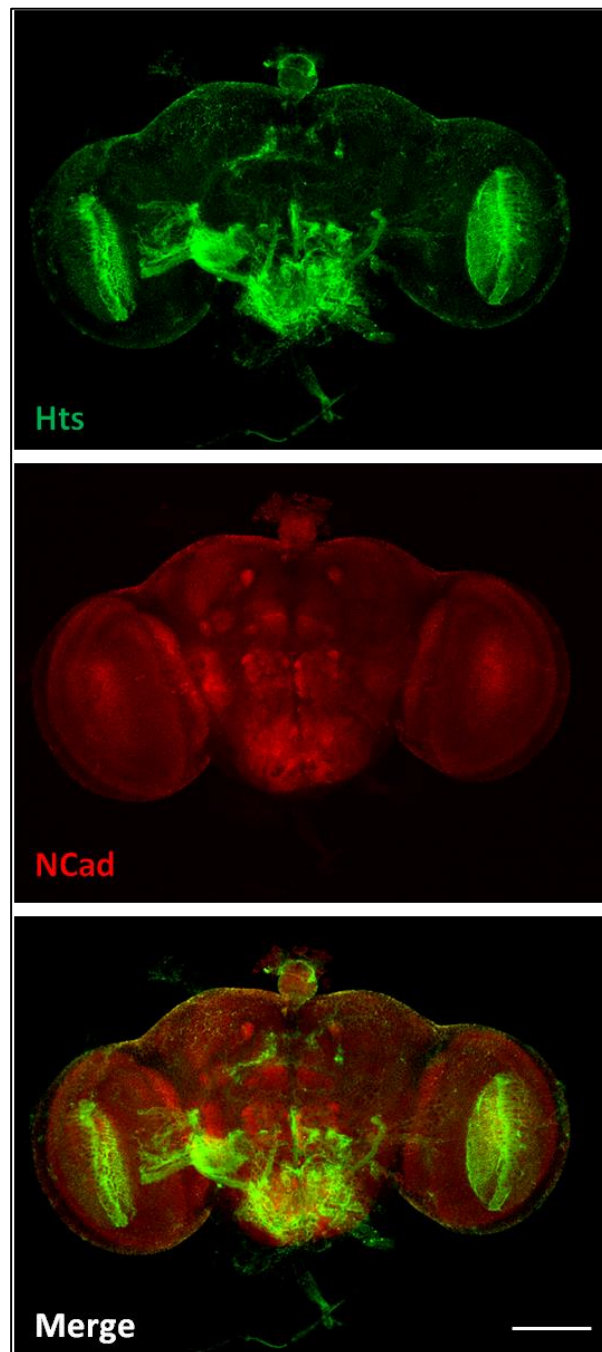
Figure 4.17. Hts is expressed in the adult optic lobe and SOG. It is also localized to the medulla. α-Hts (green), α-Elav (red). Magnification: 20X. Scale bar: 100 μm.

4.4.2. dFMR1

dFMR1 is the *Drosophila* homolog of mammalian fragile X mental retardation protein (FMRP). Loss of function of FMRP causes an X-linked neurodevelopmental disorder called Fragile X Syndrome (Wan *et al.,* 2000). FMRP is known to have the ability

to bind mRNA (Laggerbauer *et al*., 2001) and to form homomers and heteromers (with other fragile X syndrome proteins (FXRs)) (Zhang *et al.,* 1995). FMRP negatively regulates translation (Laggerbauer *et al*., 2001), acts as an adaptor between RNA granules and motor proteins (Kanai *et al*., 2004), controls microtubule (MT) stability (Lu *et al*., 2004) and has several roles in neuronal development (Callan and Zarnescu, 2011). Similar to its vertebrate counterpart, dFMR1 has the ability to regulate mRNA translation (Ascano *et al*., 2012), controls synaptic structure and function (Zhang *et al*., 2001), regulates neuronal morphology and function of the brain (Morales *et al.,* 2002), also regulates neuronal elaboration and synaptic differentiation (Pan *et al.,* 2004), contributes to eye development and circadian behavior (Sofola *et al*., 2008) and regulates MT network formation and axonal transport of mitochondria (Yao *et al.,* 2011).

dFMR1 expression is enriched in the central nervous system, muscles and gonads in the developing embryo. In addition to these sites it is present in eye imaginal discs and the mushroom body in third instar larvae (Schenck *et al*., 2002). In the pupal and adult fly brain dFMR1 is expressed in all neurons, located in the cytoplasm of the cells, but restricted to the soma (Morales *et al.,* 2002). dFMR1 is found in two forms: 85 and 92 kDa.

dFMR1 expression was shown to be localized to the R8 cells in the larval eye imaginal discs and mushroom bodies of the larval brain (Schenck *et al*., 2002). Uzip shows a similar expression pattern and is localized to R8 cells and mushroom bodies (Zülbahar, 2012). Since it has functions in neuronal development and MT network formation and interacts with various cytoskeletal proteins (Zhang *et al*., 2001), dFMR1 was chosen as a candidate interaction partner of Uzip.

4.4.2.1. Co-immunoprecipitation of dFMR1 with FH::Uzip. dFMR1 is detected as two forms in tissue extracts: 85 and 92 kD. In Western blots of WT fly head protein extracts with α-dFMR1 (5A11, DSHB), two bands corresponding to these isoforms were detected (Figure 4.18A). Additionally, four other bands ranging from 50 kD to 75 kD were also observed.
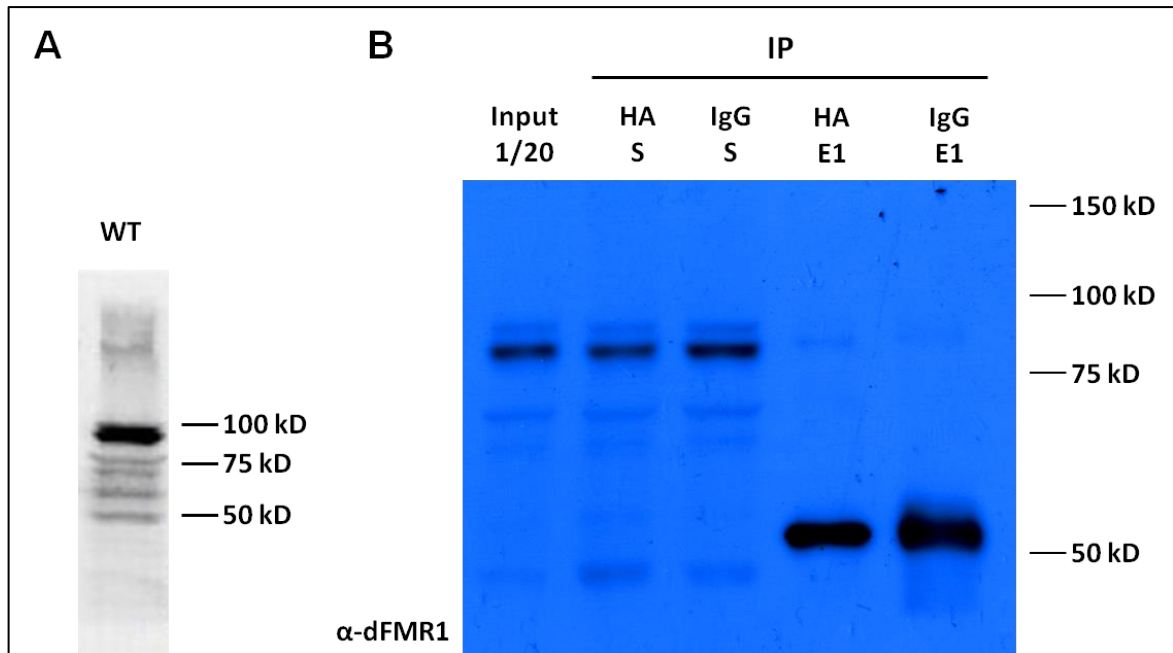
Figure 4.18. dFMR1 does not interact with FH::Uzip. (A) Total protein lysate of WT fly heads was blotted with α-dFMR1. (B) Western blotting of co-IP samples probed with α-dFMR1. S: Supernatant; E: Eluate; WT: Wild type.

We performed a co-IP assay in order to evaluate the interaction between dFMR1 and Uzip and run the collected samples on an SDS-PAGE gel (Figure 4.18B). If dFMR1 interacts with HA, no bands should be observed in the HA S lane. However, a faint band in the HA eluate lane also showed up in the control lane. Thus, the results indicate that dFMR1 protein does not bind to the HA beads and we conclude that dFMR1 does not appear to be interacting with Uzip.

4.4.2.2. Expression Pattern of dFMR1. Co-IP experiments and expression analyses were performed in parallel. dFMR1 is shown to be expressed in the third instar eye antennal disc, with a suggested localization to R8 (Schenck *et al.*, 2002). In our immunostainings we used a different antibody against α-FMR1 as the antibody generated in the Schenck et al. paper is not available any more, and observed ubiquitous expression in the eye disc (Figure 4.19). Even though we could not observe a R8-specific localization, the cellular location of dFMR1 seems to be cytoplasmic, which is consistent with previous data (Pan *et al.*, 2004).
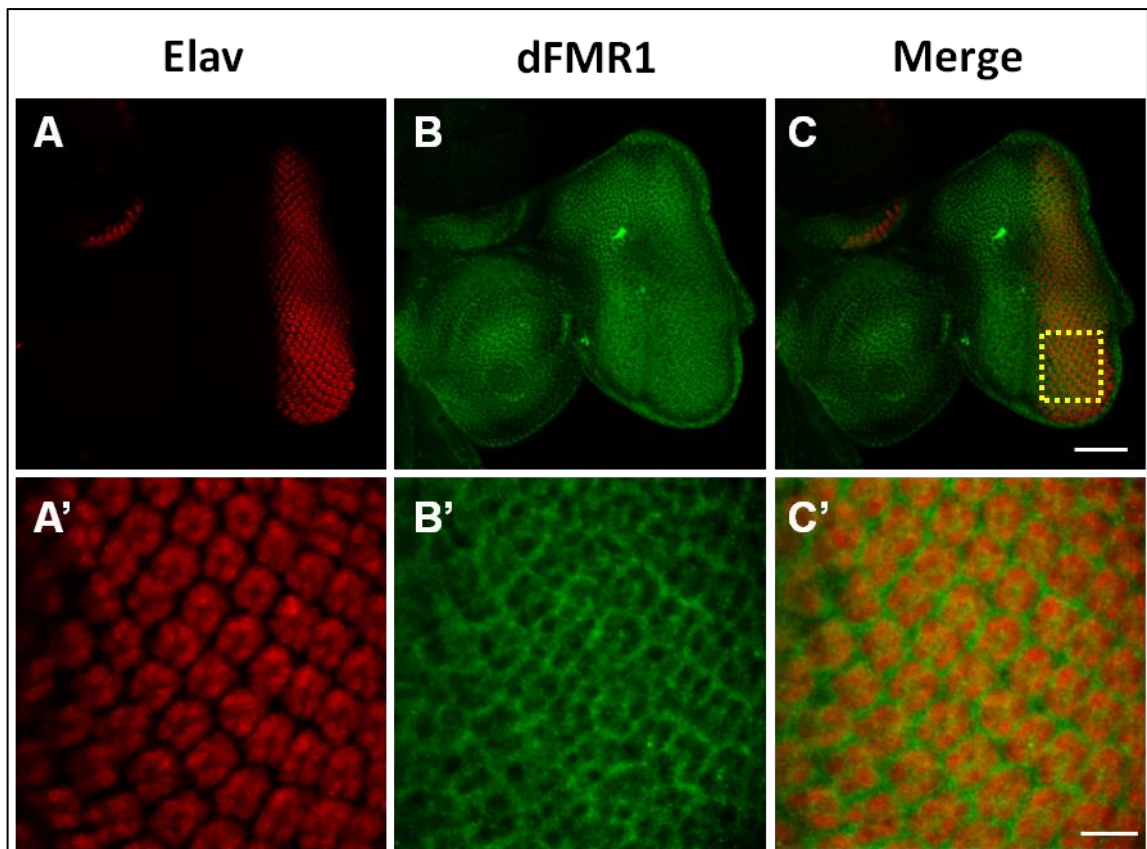
Figure 4.19. dFMR1 is expressed in third instar larval eye disc. It seems to be located in the cytoplasm of PRs, surrounding the nuclei. α-dFMR1 (green), α-Elav (red). Anterior is to the left. Magnifications: Upper row 20X, Lower row 40X. Scale bar: Upper row 50 µm; Lower row 10 µm.

dFMR1 is ubiquitously expressed in the adult fly brain with a specific localization to the mushroom body. Its expression is restricted to the cytoplasm of soma, not detectable in the axons or dendrites (Pan *et al.*, 2004). Similarly, we observe the ubiquitous expression of dFMR1 and its localization does not overlap with neuropil structures (Figure 4.20). However, we could not detect any mushroom body specific expression.
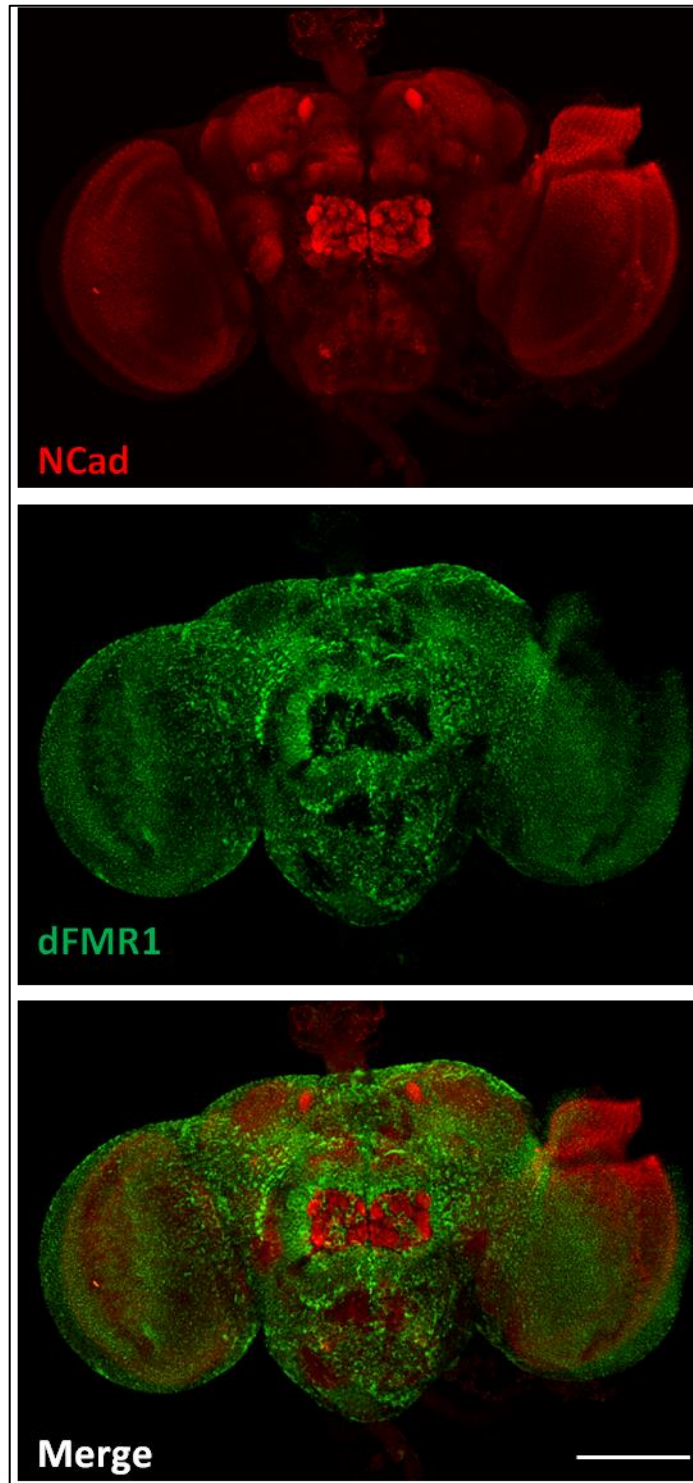
Figure 4.20. dFMR1 is expressed in the adult brain. It is distributed ubiquitously throughout the brain and does not co-localize with neuropil structures. α-dFMR1 (green), α-NCad (red). Magnification: 20X. Scale bar: 100 μm.

4.4.3. EPS15

Epidermal growth factor receptor pathway substrate clone 15 (EPS15) was identified as a substrate for tyrosine kinase activity of mammalian epidermal growth factor receptor (EGFR) (Fazioli *et al*., 1993). It has been found to interact with various components of the endocytic machinery (Benmerah *et al*., 1996 and 1998; Koh *et al*., 2007) and is involved in endocytosis during synaptic vesicle recycling, endosomal protein sorting and cytoskeletal organization (Koh *et al*., 2007). The *Drosophila* homolog of EPS15 localizes to the lamina and the medulla neuropils, in addition to the central brain neuropils and co-localizes with Dynamin to the R1-R6 terminals (Hamanaka and Meinertzhagen, 2010). EPS15 has been shown to interact with Dynamin, Stoned B, α-Adaptin (Majumdar *et al*., 2006) and Dap160 (Koh *et al*., 2007), which are known to function in endocytosis. It has been suggested that EPS15 and Dap160 have a role in synaptic development by regulating cytoskeletal organization and/or signal transduction pathways (Koh *et al*., 2007).

The role of EPS15 in cytoskeletal organization and synaptic vesicle recycling have led us to think that it may be involved in the secretory processes of the secreted form of Uzip. Therefore we determine this protein as our third candidate.

4.4.3.1. Co-immunoprecipitation of EPS15 with FH::Uzip. EPS15 is observed in immunoblots as a band around 100 kD. In immunoblots of WT protein extracts we noticed the same band with an additional ~70 kD band (Figure 4.21A).

As previously described the MS analysis results were evaluated by testing a possible physical interaction of Uzip and EPS15 by performing co-IP and Western blotting with the α-EPS15 antibody. When the samples were blotted we observed that EPS15 did not bind to the beads and so it is not present in the eluate samples (Figure 4.20B). According to this result, EPS15 is not an interaction partner for Uzip.
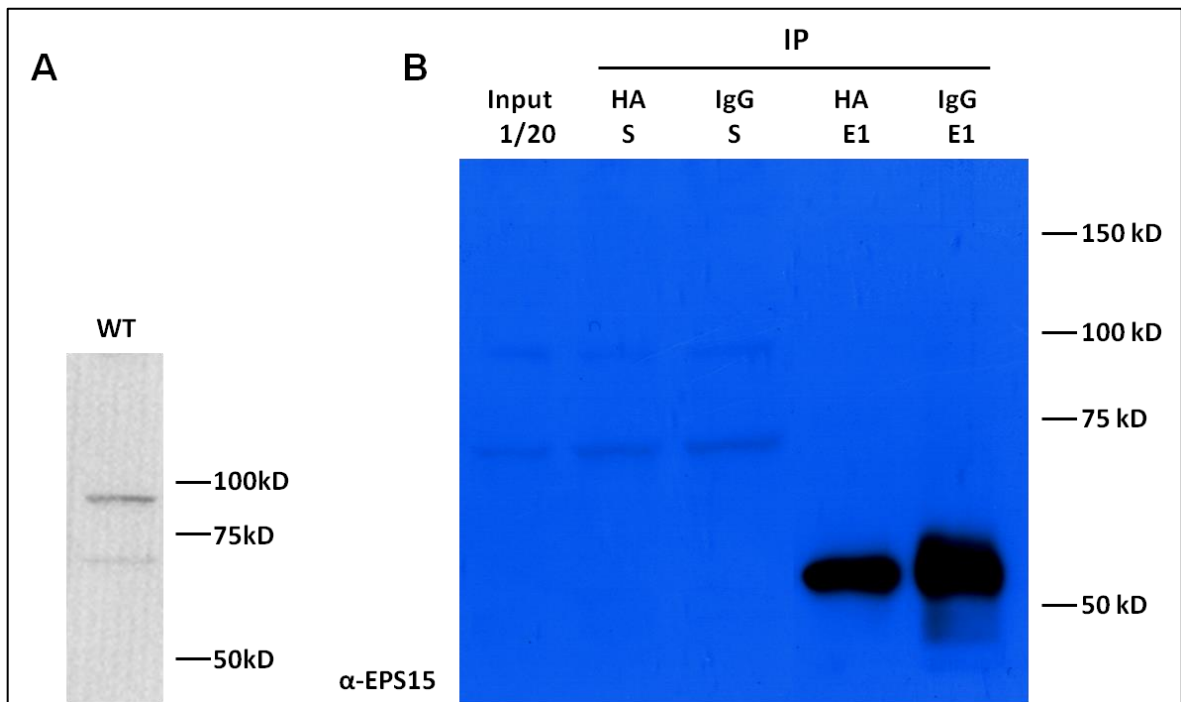
Figure 4.21. EPS15 does not interact with FH::Uzip. (A) Total protein lysate of WT fly heads was blotted with α-EPS15. (B) Western blot of co-IP samples with α-EPS15. S: Supernatant; E: Eluate; WT: Wild type.

4.4.3.2. Expression Pattern of EPS15. Immunostaining experiments to determine the expression profile of EPS15 were performed in parallel with the Western blots and co-IP experiments on third instar larval eye discs (Figure 4.22) and adult brain (Figure 4.23). Third instar larval eye-antennal discs were stained with α-EPS15 and α-Elav for the staining of PR cell nuclei (Figure 4.22). The immunostaining results indicate that they might be co-localizing with one or a few PRs (see white arrow in Figure 4.22). Further analysis is necessary to determine which cell-type EPS15 is localizing to, and if this cell type might be the R8 cell.
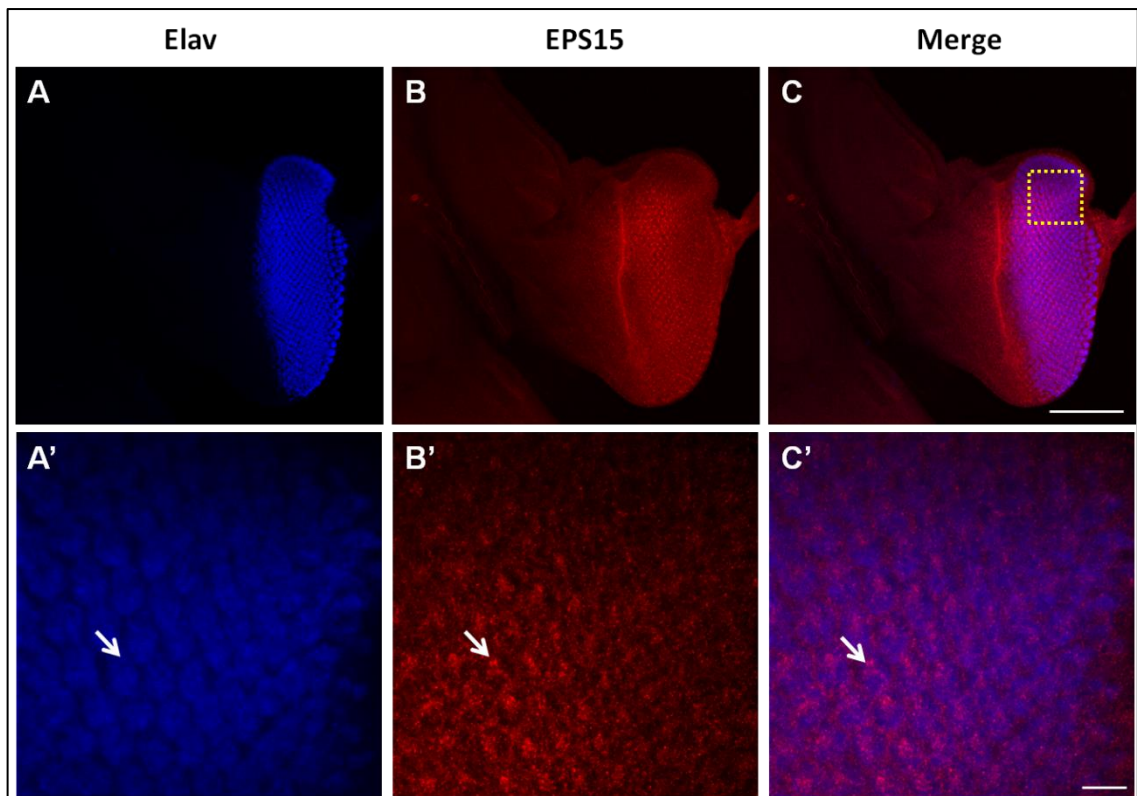
Figure 4.22. EPS15 is expressed in third instar eye imaginal disc. α-EPS15 (red), α-Elav (blue). (A', B', C') Magnified view of A, B, and C respectively, taken from the yellow square Anterior is to the left. Magnifications: Upper row 20X; Lower row 63X. Scale bar: Upper row 75 µm; Lower row 7.5 µm.

The expression of EPS15 in the adult brain was also analyzed. Similar to previously published expression data obtained in adult brain sections (Halder *et al*., 2011), we observed ubiquitous expression of EPS15 in brain neuropils (Figure 4.23) and EPS15 expression is not observed in the soma of neurons. From previous publications it is known that EPS15 localizes to the synaptic terminal of axons (Halder *et al*., 2011).

EPS15 may still be a possible interaction candidate fro Uzip. In order to show the interaction between Uzip and EPS15, further analyses are necessary.
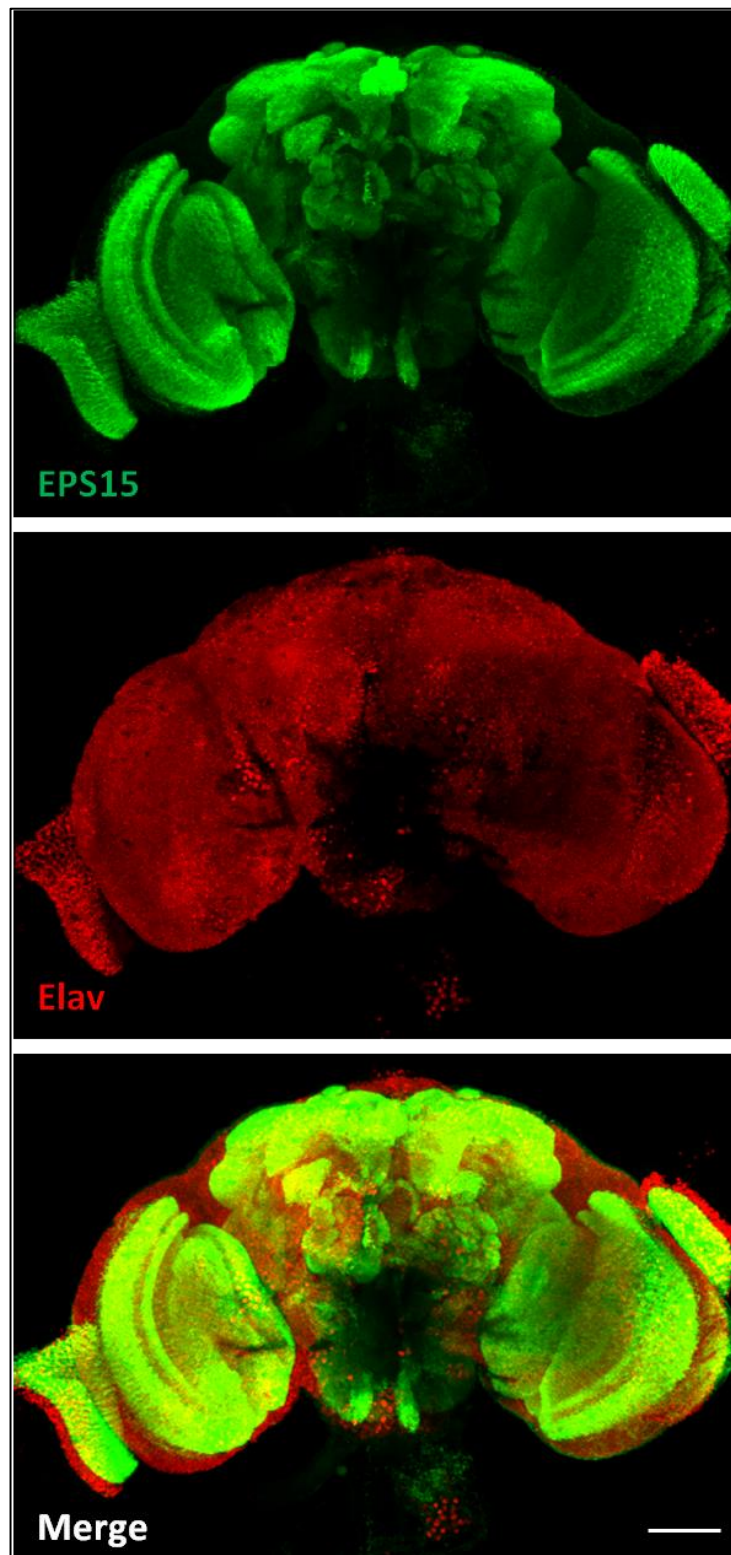
Figure 4.23. EPS15 is ubiquitously expressed in the adult brain. α-EPS15 (green), α-Elav (red). Magnification: 20X. Scale bar: 50 μm.

4.4.4. Synapsin

Synapsins are synaptic vesicle-associated phosphoproteins, conserved through evolution from invertebrates to vertebrates. While vertebrates have three *synapsin* genes, the fruit fly has only one. Each gene codes for several proteins by means of alternative splicing (Klagges *et al.*, 1996). In *Drosophila*, five Synapsin proteins were found to be expressed: three proteins around 70, 74, and 80 kDa and two proteins around 143 kDa (Klagges *et al.*, 1996). Synapsin functions in regulating the balance between different synaptic vesicle pools, binding them to the cytoskeleton and modulating neurotransmitter release (Greengard *et al.*, 1993). Synapsins have been associated with axon elongation, synaptogenesis, synaptic plasticity and olfactory learning and memory (Lu *et al.*, 1992; Greengard *et al.*, 1993; Ferreira *et al.*, 1994; Godenschwege *et al.*, 2004; Knapek *et al.*, 2010). Synapsins are expressed widely in the nervous system, localizing to presynaptic membranes of neurons (Klagges *et al.*, 1996). Synapsin activity is regulated by CaMKII and PKA and through phosphorylation it is able to modulate synaptic vesicle release (Cesca *et al.*, 2010).

Synapsin is a vesicle-associated protein, which binds to Golgi-derived vesicles. It interacts with many proteins on the vesicles and in the cytoskeleton. Syn may function in the secretory pathway of 65kD Uzip.

4.4.4.1. Co-immunoprecipitation of Synapsin with FH::Uzip. Syn is found in five forms in *Drosophila* (as described in section 4.4.4). In protein extracts obtained from WT fly heads all five forms could be observed (Figure 4.24A).

In order to confirm the predicted interaction between Syn and Uzip, we performed a co-IP assay and immunoblotted the samples with antibody against Syn (Figure 4.24B). If the interaction predicted by the MS analysis is real, it is not expected to observe the Syn corresponding bands in the HA S lane. The experimental results indicate that some binding seems to occur, since there are bands detected in the eluates. However, the same proteins were also eluted from the IgG control beads.
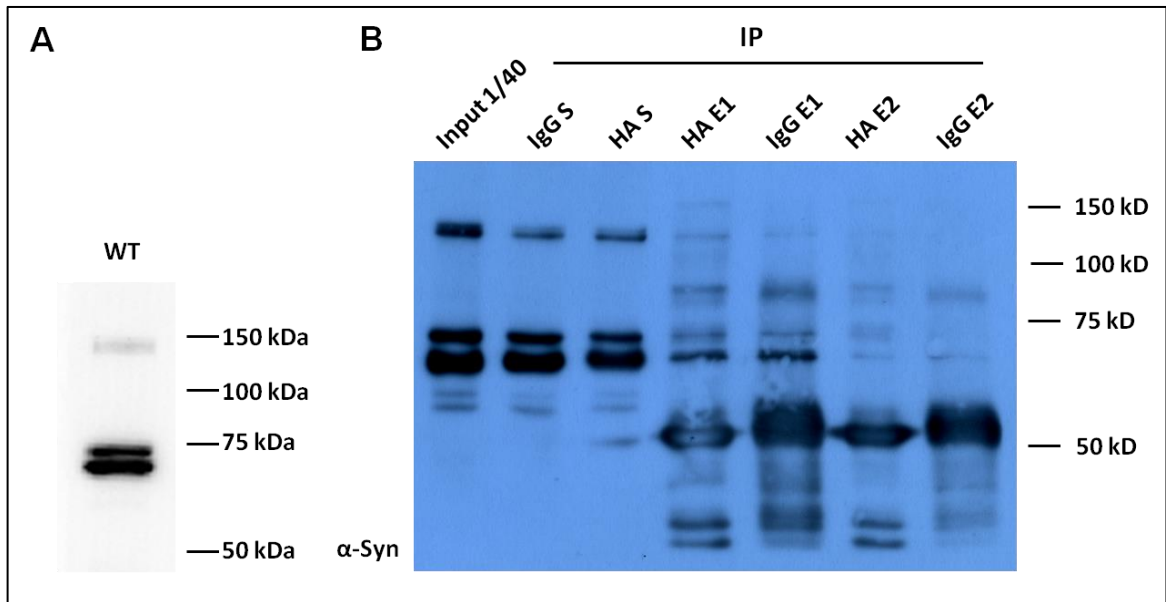
Figure 4.24. Syn does not interact with FH::Uzip. (A) Total protein lysate of WT fly heads was blotted with α-Syn. (B) Western blotting of co-IP samples with α-Syn. S: Supernatant; E1: Eluate 1; E2: Eluate 2; WT: Wild type.

4.4.4.2. Expression Pattern of Syn. We investigated the expression pattern of Syn in the adult brain (Figure 4.25). Syn expression was observed in all neurons, localizing in particular to the axons. In correlation with these data, we observed that Syn is expressed in the brain neuropils, perfectly co-localizing with NCad.
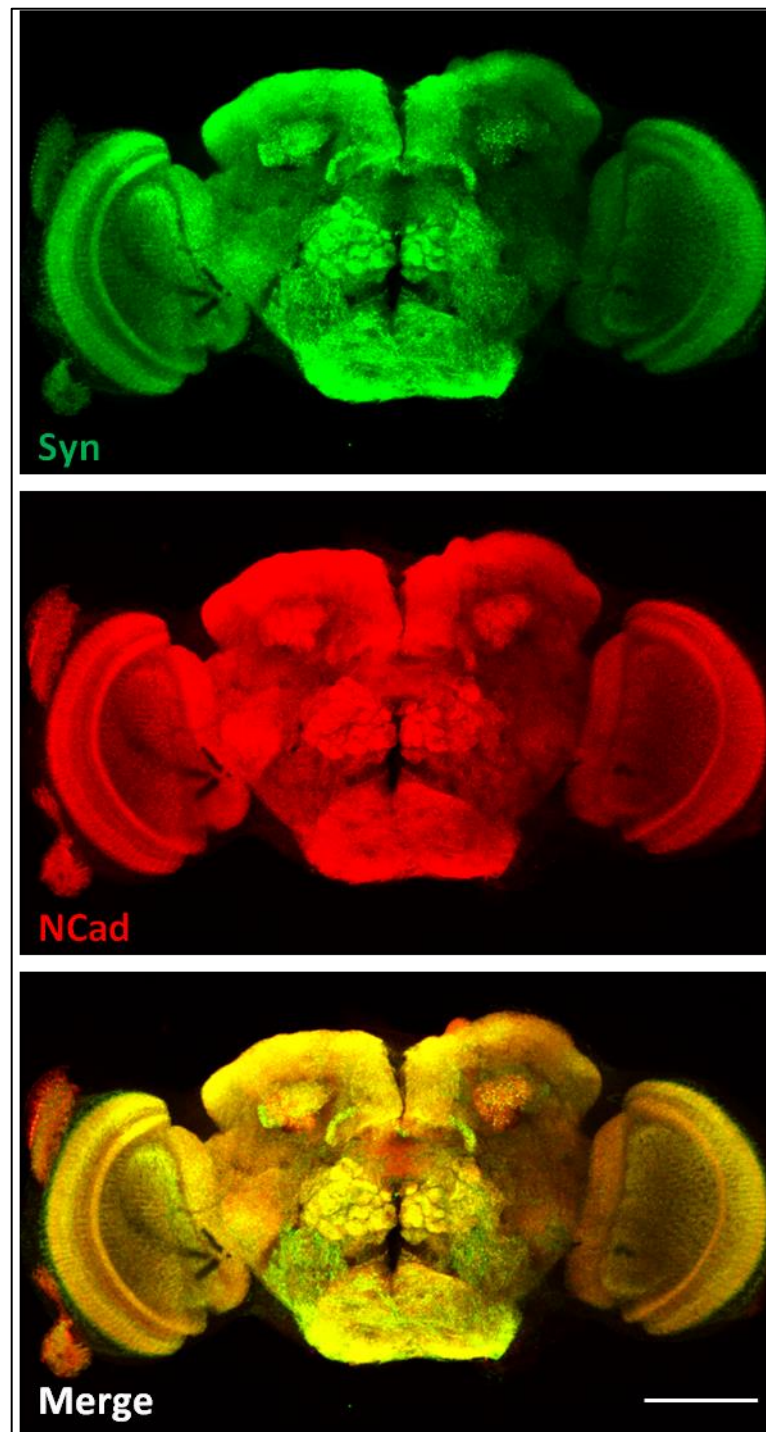
Figure 4.25. Syn is expressed in the adult brain, perfectly co-localizing to the neuropils. α-Syn (green), α-NCad (red). Magnification: 20X. Scale bar: 100 μm.

5. DISCUSSION

Axons travel along long distances with the help of guidance cues provided by other cells and synapse to their correct targets. The properties of guidance cues, providing attractive or repulsive cues, help axons find their ways. There are many types of guidance cues. Uzip is a recently identified cell adhesion molecule, which has no homology to previously identified cell adhesion molecules (Ding *et al*., 2011). Unzipped has been identified in our lab and shown to have a role in axon guidance of ORNs (Zülbahar, 2012). We hypothesize that it acts through homophilic and heterophilic interactions.

In the framework of this study, we aimed to identify interaction partners of Uzip through a mass spectrometry approach. Identified interaction partners were analyzed by co-IP and immunohistochemistry. At the same time we tried to describe the endogenous expression pattern of Uzip making use of a BAC transgenic line generated in our laboratory.

5.1. Expression Analysis of FH::Uzip

While the generation of Uzip-specific antibodies in our lab is in process a transgenic fly line expressing Flag-HA tagged Uzip under endogenous promoter control was generated (Zülbahar, 2012). The peptide sequences of Flag and HA were introduced into the coding sequence of *Uzip*. Uzip has a secreted and a membrane-bound form, and we intended to tag both of them. Uzip is known for being cleaved at the C-terminus upon secretion (Ding *et al*., 2011). In order to prevent cleavage of the tags and not to interfere with the proper secretion of Uzip, it was tagged at the N-terminus right after the predicted signal peptide (Zülbahar, 2012).

This transgenic fly line was used in expression analyses in order to confirm that the enhancer trap line for Uzip generated in our lab reflects endogenous Uzip expression. Since Uzip expression using the enhancer trap line was observed in larval eye imaginal

discs (Öztürk, 2010), in the pupal retina and in the adult brain (Zülbahar, 2012), we analyzed endogenous Uzip expression in these developmental stages.

Uzip expression was observed posterior to the morphogenetic furrow in the early born PR cells (Figure 4.1). One or a few PR cell nuclei per ommatidium appear to be surrounded by Uzip, but not all. Uzip signal appeared to be localized to the membrane, which is consistent with its predicted function as cell adhesion molecule. The immunostainings with α-HA antibody turned out to be difficult, probably due to the fact that this small tag is not easily accessible in the tissue context. Thus, in the best staining that is shown here the posterior end of the eye disc was not stained properly especially with the neuronal marker α-Elav. This prevents us from determining the exact localization of FH::Uzip. Uzip was shown before to co-localize with the R8-specific marker Senseless towards the end of larval development (Zülbahar, 2012). For the correct evaluation of PRs positive for endogenous Uzip expression, PR-specific markers, using Senseless in particular will be useful. As crossing in PR marker lines necessary for this purpose would take long it could not be carried out in the time course of this study, but will be done as soon as these crosses are done.

Uzip enhancer-trap expression was also detected in the glial cells of larval eye imaginal discs (Zülbahar, 2012). We co-stained larval eye discs of our transgenic fly line with α-HA and α-Repo antibodies (Figure 4.2) in order to see the glial expression pattern of endogenous Uzip. Unfortunately, Uzip expression does not appear to originate from glial cells. The only expression observed seems to belong to a layer beneath the glial layer, where PR cells are found. Even though Repo is a nuclear marker and Uzip is not a nuclear protein, we expect expression in a subset of these cells. In the model generated in our lab, glial cells are suggested to be the source of the secreted form of Uzip and the neurons are the source of the membrane-attached form (Zülbahar, 2012). Therefore, the cellular localization of endogenous Uzip is expected to be cytoplasmic in glial cells or it might be secreted to the external environment. For the better understanding of this expression pattern triple staining of HA, Repo, and Elav should be performed, which could not be accomplished due to the lack of available antibodies for these markers in three different host species. Alternatively, the FH::Uzip line can be crossed with a fly line that expresses a

LacZ-tagged version of Repo and larval eye discs of the generated line can be stained with α-HA, α-Elav, and βGal antibodies to resolve this issue.

Since triple staining with α-HA, α-Elav and α-Repo could not be achieved; we set out to immunostain larval eye discs with α-Flag antibody. This antibody was raised in a different species than α-Elav and α-Repo antibodies, allowing us to perform triple stainings (Figure 4.3). For this purpose we followed the same protocol that we used for α-HA stainings. Unfortunately, a uniform α-Flag signal was observed in the eye antennal disc, thus, it did not give a meaningful pattern. Furthermore, in WT eye discs stained as controls α-Flag signal was detected as well. However, this staining was only performed once due to time constrains. Since we have not encountered any α-Flag whole mount staining protocol in the literature, the staining protocol could be optimized for better analysis.

The enhancer trap expression of Uzip was previously observed in neurons and glial cells in the pupal retina (Zülbahar, 2012). Here, we showed that endogenous Uzip expression is localized to PRs in 40 h pupal discs (Figure 4.5). Again the Uzip signal surrounds the nuclei of PRs like in the case of eye imaginal discs. Even though the retinas were not stained with α-Repo antibody, there is some non-neuronal signal that might be originating from glial cells. This should be investigated further with α-Repo staining.

Previously, Uzip expression was detected in the adult nervous system, especially in the olfactory circuit (Zülbahar, 2012). However, in this study we could not observe any specific expression pattern of Uzip in the adult brain (Figure 4.5). α-Repo staining of adult fly brains also gave no clue about the glial expression of Uzip (*data not shown*). We conclude that the HA staining protocol for adult brains needs to be optimized further.

As a result, endogenous Uzip expression was detected in photoreceptors in larval eye discs and pupal retinas. For understanding of glial expression, further stainings need to be performed. Unfortunately, the optimization of α-HA staining was difficult and required a harsh fixation, which inhibits other antibodies from working properly (as in Figure 4.1). An alternative approach would be to optimize the staining against the Flag tag to see if it gives a reasonable expression pattern. Furthermore, recently a mCherry-tagged version of Uzip was generated in our lab and is in the process of injection into *Drosophila* embryos.

Hopefully, this transgenic line will give us a better idea of the endogenous expression profile of Uzip. Ultimately, the best way of showing endogenous Uzip expression is the use of an Uzip-specific antibody, which we will hopefully have soon.

In the previous study, the enhancer-trap line of Uzip was shown to drive expression in R8 cells using a nuclear GFP reporter (Zülbahar, 2012). Even though we could not perform Senseless staining of larval eye discs for FH::Uzip, we can speculate that it does not localize to nuclei by analyzing α-Elav and α-FH double stainings. Since Uzip is a membrane-bound protein we expect it to localize to the cell membrane. The use of a nuclear reporter only helps to identify the cells expressing the protein of interest, but not their subcellular localization. Therefore, we do not expect perfect co-localization of expression patterns of the enhancer trap line and FH::Uzip line.

In the adult brain, the enhancer trap expression of Uzip was shown in the antennal lobe and the mushroom body by using a membrane-bound GFP reporter (Zülbahar, 2012). As stated before, Uzip is expected to localize to membranes of the cells. Therefore, the enhancer-trap driven membrane-bound GFP expression detected in the adult brain represents its possible localization. In order to understand the localization of endogenous Uzip, we performed immunostainings in the adult brain of FH::Uzip transgenic flies. Unfortunately, we could not detect any localization to the antennal lobe or mushroom body due to the technical problems of α-HA staining. Therefore, we are unable to compare adult expression of Uzip with the previous study.

5.2. Co-IP and MS Analysis of FH::Uzip with its Possible Interaction Partners

Uzip is a cell adhesion molecule implicated in axon guidance (Ding *et al*., 2011; Zülbahar, 2012). In the visual system it is expressed only in R8 photoreceptors and glia. In the olfactory system it is only expressed in one subset of ORNs in the antenna (Zülbahar, 2012). R8 cells are the first photoreceptors to differentiate and send their axons to the optic lobe and thus have a pioneering role as the other axons follow these axons to reach the optic lobe (Jarman *et al*., 1994; Tomlinson and Ready, 1987). Similarly, axons of antennal ORNs are the first to reach the antennal lobe and have a pioneering role in the projection of maxillary palp axons to the antennal lobe by the repulsive interactions of Sema-1a

(Sweeney *et al*., 2007). In light of these data, we suggested a model for Uzip function in both sensory systems. In this model Uzip expressing axons (PR / ORN) have pioneering roles in the establishment of the neuronal circuitry in these systems. These neurons are the first neurons to interact and receive guidance cues from glia. The secreted form of Uzip might be one of these cues, which guide Uzip expressing neurons via homophilic interaction. Uzip expressing pioneer axons, in turn lead the way to the follower axons via heterophilic interactions of Uzip (Zülbahar, 2012). In light of these data, we aimed to identify protein-protein interaction partners of Uzip by co-IP assays followed by MS analysis.

To achieve this purpose, we needed to establish a co-IP protocol in our lab. One of the most important steps in the optimization was the choice of a proper tissue lysis buffer. Thus, three different lysis buffers were employed in order to extract proteins from FH::Uzip transgenic fly line. Even though all tested buffers were able to extract both Uzip isoforms (Figure 4.7), in order to preserve interactions of the proteins we decided to continue with the non-ionic lysis buffer, which is the least stringent. As control of the co-IP experiment, we used mouse-IgG beads to exclude any non-specific binding of the proteins to the agarose beads or the IgG domain of α-HA. Alternatively, mouse-IgG beads could be used as a pre-clearing agent in order to get rid of unwanted interactions. When the co-IP assay was performed, we observed that both forms of FH::Uzip were successfully bound to α-HA beads and could be eluted (Figure 4.9).

To identify the interaction partners of Uzip, LC-MS/MS analysis was performed twice using eluates of two different co-IP experiments. After obtaining the raw data of the MS analyses, the proteins were filtered according to their coverage percent and unique peptide-to-peptide number in order to exclude possible false positives (Table 4.2 and Table 4.5). One of our expectations was to observe the presence of Uzip, since it was previously shown *in vitro* to bind itself by homophilic interactions. However, LC-MS/MS analysis could not distinguish between the endogenous Uzip and the FH::Uzip fusion protein. Thus, although Uzip was observed in the results we were not able to determine unequivocally that it is there because it is a binding partner or if this signal belongs to FH::Uzip fusion protein that is present in excess amount in the eluate.

The proteins that were filtered according to the criteria explained above were analyzed according to their biological functions using the GeneCodis tool to find the associated GO terms of possible interaction partners. These proteins were categorized according to their GO terms (Table 4.3 and Table 4.6) and the ones that have a known function in the nervous system were collected under one category. Several proteins were selected as candidates for further analyses.

Since Uzip is a cell adhesion molecule (Ding *et al.,* 2011), we expect it to interact with other cell adhesion proteins. Interestingly, Flotillin 1 and Flotillin 2 were the only proteins identified that are associated with cell adhesion in our MS analyses. Previously predicted partners like the cell adhesion protein N-Cadherin and Wnt5 did not appear in our experiments. This is not so surprising as these interaction partners were shown to be genetically interacting with Uzip in the embryo and no physical interaction was determined. The same interactions are not necessarily present in the brain.

One reason for not identifying more cell adhesion proteins could also be technical, eg. low stringency of non-ionic lysis buffer. The lysis buffer might be strong enough to extract membrane-attached Uzip but not be strong enough to extract transmembrane adhesion proteins. Another reason might be the transient nature of cell adhesion interactions that could be broken at the time of protein extraction.

As stated before, Uzip has a function in axon guidance in the *Drosophila* olfactory system (Zülbahar, 2012). Therefore, there is a high possibility that it interacts with proteins functioning in axon guidance. As a result of both MS analyses, four proteins were identified that have known functions in axon guidance: Hts, dFMR1, Laminin A, and Khc, and thus represent interesting candidates for further analysis.

The analysis revealed the presence of a number of vesicle-associated endocytosis or exocytosis proteins. Syn, EPS15, α-adaptin, stnB, and Syt1 are the identified proteins associated with synaptic vesicle functioning. The identification of these kinds of proteins as interaction partners is not surprising as Uzip is a secreted and a membrane-bound

protein and to be properly processed and localized it is interacting with many proteins during this process, which is reflected here.

Four proteins were chosen for further analysis from this long list of candidates according to the availability of analysis tools (antibodies, reporter lines, etc.). These were Hts, dFMR1, EPS15, and Syn. Initially, the interaction between Uzip and these candidate proteins were analyzed for confirmation of the validity of MS analysis using direct co-IP. Additionally, the expression pattern of the candidates in adult brain and larval eye discs were analyzed to identify if they show a similar localization to unzipped and could represent true interaction partners.

Among those, Hts was the most promising candidate since it interacts with the R8 specific axon guidance molecule Gogo and contributes to the targeting of R7 and R8 axons (Ohler *et al.,* 2011). Immunoblots of co-IP eluates with α-Hts antibody revealed promising results (Figure 4.14). However, a cross co-IP assay did not result in the detection of a physical interaction of Hts with Uzip. However, the cross co-IP assay was only performed once and a better result might be obtained if the protocol is optimized. Additionally, the reason for this negative result might be the previously reported poor immunoprecipitation properties of α-Hts antibody (Wang *et al*., 2011). The expression analysis of Hts in larva showed that it localizes to R axons elongating to the optic lobe (Figure 4.16), which is in accordance with previous findings (Ohler *et al*., 2011). The adult staining of Hts was not previously reported, and we determined a Hts signal in the medulla and SOG of the adult brain (Figure 4.17). While the medulla layers that display Hts localization need to be determined in more detail, it would not be surprising if the layers correspond to the M3 and M6 layers, where R8 and R7 axons terminate. Thus, Hts remains as an interesting candidate and we will analyze mutants of *hts* to determine if the loss of Hts function resembles the loss of function phenotypes of Uzip, which is expected if they are interacting partners.

dFMR1 was chosen as a possible interaction partner for Uzip due to its functions in neuronal development and axon guidance (Morales *et al.,* 2002). Furthermore, its expression in R8 cells and mushroom bodies was previously reported (Schenck *et al*., 2002), regions where Uzip is expressed as well (Zülbahar, 2012 and *unpublished data*).

Unfortunately, an interaction between dFMR1 and Uzip was not observed in the co-IP experiments. This suggests that these proteins do not interact physically. The low coverage percent of dFMR1 in the second MS analysis might be indicating that this is a pseudo-interaction. In expression analyses dFMR1 was detected in the larval eye disc, with an apparent localization to the cytoplasm of PR cells (Figure 4.19). Even though the previous report suggested R8 localization, we could not observe any R8-specific expression. This might be due to the fact that the antibody raised in the Schenck *et al*. (2002) study was not available and a different antibody for dFMR1 was used. This is in accordance with the observation of different bands in the immunoblot of WT protein extracts. It was also previously reported that dFMR1 localizes to the mushroom body in the adult brain (Pan *et al*., 2004). Again, we did not observe expression in the mushroom body, and dFMR1 appears to be localized to the soma of neurons (Figure 4.20). Since the origin of the antibody used in Pan *et al*. (2004) is not stated properly, we cannot speculate about the reason for this difference in expression. From these results we do not think of dFMR1 as a good candidate that should be pursued further.

EPS15 functions in synaptic development and synaptic vesicle endocytosis (Koh *et al*., 2007). It interacts with Numb, Dap160, stnB, and α-adaptin (Tang *et al.,* 2005; Majumdar *et al*., 2006; Koh *et al*., 2007), all of which were detected in the second MS analysis. These proteins are probably found in a complex with EPS15 and were co-immunoprecipitated together with EPS15. We thought that EPS15 might be in interaction with the secreted form of Uzip. However, EPS15 was not detected in immunoblots of co-IP eluates (Figure 4.21). Judging from the low WT expression level, the antibody might not have detected immunoprecipitated EPS15, which is present in much lower levels compared to WT expression, since Uzip also binds other proteins. Larval eye disc expression of the protein shows localization to one or more PR. Further analysis is needed to understand which of the PRs expresses it. Adult expression analysis resulted in the same pattern that was reported before (Halder *et al*., 2011). Thus, EPS15 still might be a good candidate but further analyses are necessary to prove the interaction between Uzip and EPS15.

Syn is also a synaptic vesicle-associated protein, which we suggested to interact with secreted Uzip. Contrary to our expectations, Syn did not co-immunoprecipitate with Uzip (Figure 4.24). On the other hand, the Syn expression pattern that we observed in

neuropils in the adult brain is in correlation with previous reports (Figure 4.25). Thus Syn does not represent a good candidate for further analysis.

MS is a powerful technique for the initial examination of interacting molecules, yet the identified proteins need to be confirmed with other analyses. Among the candidates only Hts gave promising results, but these could not be verified with further analysis. This could be a result of pseudo-interactions, which can occur when the tissue is crushed for lysis. Lysis would bring proteins together from separate cellular compartments (nucleus, cytoplasm, mitochondria, etc.) and generate an environment for interactions that would not occur under normal circumstances.

The unexpected results bring up the question of the functionality of the FH::Uzip fusion protein. Even though both forms of Uzip can be detected in Western blots, it may not be functional *in vivo*. In order to test the functionality of FH::Uzip a rescue experiment has been performed (Zülbahar, 2012). In this analysis the phenotype caused by the absence of Uzip could not be rescued by the presence of one copy of FH::Uzip. The signal peptide domain of Uzip was only predicted based on the amino acid sequence, which could represent an improper prediction. Introducing the tags after this predicted sequence might cause a disruption in the folding of Uzip. For further understanding of the situation, rescue experiments should be repeated using more copies of the transgene.

This study provides preliminary data for the identification of protein interactors of Uzip. Several proteins were selected as candidates from the results of MS analyses. For the direct validation of MS analyses, co-IP samples were blotted with antibodies against these candidates. Unfortunately, these experiments did not confirm most of the predicted physical interactions. However, these techniques have been established and performed in our lab for the first time. More experiments are needed to optimize co-IP protocols and MS analysis could be repeated once we have a functional Unzipped antibody at hand, to exclude technical problems. Similarly, another set of MS experiments could be performed using the mcherry-tagged version of membrane-bound Unzipped once this line is generated.

In future experiments, the candidates should be tested for interaction with functional analyses. The phenotypes caused by the mutant forms of these proteins should be compared with the phenotypes caused by mutant Uzip and genetic interaction experiments should be performed. These experiments will give us a clue about the interactions between our candidates and Uzip.

Moreover, different candidates can be selected from the results of our MS analysis. Flotillin 1 and 2 and Laminin A would be promising candidates with their known functions in cell adhesion and axon guidance. We have considered these proteins but the lack of available tools did not allow us to analyze them further.

While this work has not yielded the best results in terms of concrete identification of interaction partners of Unzipped and insights into its signaling mechanism, we have opened a new avenue of research into the biochemistry of *Drosophila*, which is not widely used. In the long run we hope that with better tools we will be able to identify and confirm some of the predicted interactions.

REFERENCES

Ascano, M., Jr., N. Mukherjee, P. Bandaru, J. B. Miller, J. D. Nusbaum, D. L. Corcoran, C. Langlois, M. Munschauer, S. Dewell, M. Hafner, Z. Williams, U. Ohler, and T. Tuschl, 2012, "Fmrp Targets Distinct Mrna Sequence Elements to Regulate Protein Expression", *Nature*, Vol. 492, No. 7429, pp.382-6.

Ayoob, J. C., J. R. Terman, A. L. Kolodkin, 2006, "Drosophila Plexin B is a Sema-2a Receptor Required for Axon Guidance", *Development*, Vol. 133, pp. 2125–2135.

Bagnard D., M. Lohrum, D. Uziel, A. Puschel, J. Bolz, 1998, "Semaphorins Act as Attractive and Repulsive Guidance Signals During the Development of Cortical Projections", *Development*, Vol. 125, pp. 5043–53.

Battye, R., A. Stevens, J. R. Jacobs, 1999, "Axon Repulsion from the Midline of the Drosophila CNS Requires Slit Function", *Development*, Vol. 126, No. 11, pp. 2475-2481.

Berger, J., K. A. Senti, G. Senti, T. P. Newsome, B. Asling, B. J. Dickson, and T. Suzuki, 2008, "Systematic Identification of Genes That Regulate Neuronal Wiring in the Drosophila Visual System", *PLoS Genetics*, Vol. 4, No. 5, pp. e1000085.

Benmerah, A., C. Lamaze, B. Begue, S. L. Schmid, A. Dautry-Varsat, and N. Cerf-Bensussan, 1998, "Ap-2/Eps15 Interaction Is Required for Receptor-Mediated Endocytosis", *Journal of Cell Biology*, Vol. 140, No. 5, pp. 1055-62.

Callan, M. A., and D. C. Zarnescu, 2011, "Heads-Up: New Roles for the Fragile X Mental Retardation Protein in Neural Stem and Progenitor Cells", *Genesis*, Vol. 49, No. 6, pp. 424-40.

Carmona-Saez, P., M. Chagoyen, F. Tirado, J. M. Carazo, and A. Pascual-Montano, 2007, "Genecodis: A Web-Based Tool for Finding Significant Concurrent Annotations in Gene Lists", *Genome Biology*, Vol. 8, No. 1, pp. R3.

Castellani, V., A. Chédotal, M. Schachner, C. Faivre-Sarrailh, G. Rougon, 1998, "Roundabout Controls Axon Crossing of the CNS Midline and Defines a Novel

Subfamily of Evolutionarily Conserved Guidance Receptors", *Cell*, Vol. 92, No. 2, pp. 205-215.

Castellani, V., A. Chédotal, M. Schachner, C. Faivre-Sarrailh, G. Rougon, 2000, "Analysis of the L1-deficient Mouse Phenotype Reveals Cross-Talk Between Sema3A and L1 Signaling Pathways in Axonal Guidance", *Neuron*, Vol. 27, No. 2, pp. 237-49.

Cesca, F., P. Baldelli, F. Valtorta, and F. Benfenati, 2010, "The Synapsins: Key Actors of Synapse Function and Plasticity", *Progress in Neurobiology*, Vol. 91, No. 4, pp. 313-48.

Choe, K. M., S. Prakash, A. Bright, and T. R. Clandinin, 2006, "Liprin-alpha is Required for Photoreceptor Target Selection in Drosophila", *Proceeding of the National Academy of Sciences of the USA*, Vol. 103, pp. 11601-11606.

Choi, K. W., and S. Benzer, 1994, "Migration of Glia along Photoreceptor Axons in the Developing Drosophila Eye", *Neuron*, Vol. 12, pp. 423-431.

Clandinin, T. R., S. L. Zipursky, 2000, "Afferent Growth Cone Interactions Control Synaptic Specificity in the Drosophila Visual System", *Neuron*, Vol. 28, No. 2, pp. 427‑436.

Clandinin, T. R., C. H. Lee, T. Herman, R. C. Lee, A. Y. Yang, S. Ovasapyan, and S. L. Zipursky, 2001, "Drosophila Lar Regulates R1-R6 and R7 Target Specificity in the Visual System", *Neuron*, Vol. 32, No. 2, pp.237-48.

Ding, Z. Y., Y. H. Wang, Z. K. Luo, H. F. Lee, J. Hwang, C. T. Chien, and M. L. Huang, 2011, "Glial Cell Adhesive Molecule Unzipped Mediates Axon Guidance in Drosophila", *Developmental Dynamics*, Vol. 240, No. 1, pp. 122-34.

Drescher, U., C. Kremoser, C. Handwerker, J. Löschinger, M. Noda, and F. Bonhoeffer, 1995, "In Vitro Guidance of Retinal Ganglion Cell Axons by RAGS, a 25 kDa Tectal Protein Related to Ligands for Eph Receptor Tyrosine Kinases", *Cell*, Vol. 82, No. 3, pp. 359-370.

Fazioli, F., L. Minichiello, B. Matoskova, W. T. Wong, and P. P. Di Fiore, 1993, "Eps15, a Novel Tyrosine Kinase Substrate, Exhibits Transforming Activity", *Molecular and Cellular Biol*ogy, Vol. 13, No. 9, pp. 5814-28.

Ferreira, A., K. S. Kosik, P. Greengard, and H. Q. Han, 1994, "Aberrant Neurites and Synaptic Vesicle Protein Deficiency in Synapsin Ii-Depleted Neurons", *Science*, Vol. 264, No. 5161, pp. 977-9.

Fischbach, K. F., and P. R. Hiesinger, 2008, "Optic Lobe Development", *Advances in Experimental Medicine and Biology*, Vol.628, No. 115-36.

Gonzalo-Gomez, A., E. Turiegano, Y. Leon, I. Molina, L. Torroja, and I. Canal, 2012, "Ih Current Is Necessary to Maintain Normal Dopamine Fluctuations and Sleep Consolidation in Drosophila", *PLoS One*, Vol. 7, No. 5, pp. e36477.

Greengard, P., F. Valtorta, A. J. Czernik, and F. Benfenati, 1993, "Synaptic Vesicle Phosphoproteins and Regulation of Synaptic Function", *Science*, Vol. 259, No. 5096, pp.780-5.

Guruharsha K.G., R.A. Obar, J. Mintseris, K. Aishwarya, R.T. Krishnan, and K. Vijay Raghavan, 2012, "*Drosophila* Protein interaction Map", *Fly*, Vol. 6, pp. 246-253.

Hadjieconomou, D., K. Timofeev and I. Salecker, 2011, "A Step-by-Step Guide to Visual Circuit Assembly in Drosophila", *Current Opinion in Neurobiology*, Vol. 21, pp. 76–84.

Halder, P., Y. C. Chen, J. Brauckhoff, A. Hofbauer, M. C. Dabauvalle, U. Lewandrowski, C. Winkler, A. Sickmann, and E. Buchner, 2011, "Identification of Eps15 as Antigen Recognized by the Monoclonal Antibodies Aa2 and Ab52 of the Wuerzburg Hybridoma Library against Drosophila Brain", *PLoS One*, Vol. 6, No. 12, pp. e29352.

Hamanaka, Y., and I. A. Meinertzhagen, 2010, "Immunocytochemical Localization of Synaptic Proteins to Photoreceptor Synapses of Drosophila Melanogaster", *Journal of Comparative Neurology*, Vol. 518, No. 7, pp. 1133-55.

Hansson, B. S., M. Knaden, S. Sachse, M. C. Stensmyr, and D. Wicher, 2010, "Towards Plant-Odor-Related Olfactory Neuroethology in Drosophila", *Chemoecology*, Vol. 20, No. 2, pp. 51-61.

Harris, R., L. M. Sabatelli, and M. A. Seeger, 1996, "Guidance Cues at the *Drosophila* CNS Midline: Identification and Characterization of Two *Drosophila* Netrin/UNC-6 Homologs", *Neuron*, Vol. 17, pp. 217-228.

Hindges, R., T. McLaughlin, N. Genoud, and M. Henkemeyer, D. O'Leary, 2002, "EphB Forward Signaling Controls Directional Branch Extension and Arborization Required for Dorsal-ventral Retinotopic Mapping", *Neuron*, Vol. 35, No. 3, pp. 475-487.

Hummel, T., and S. L. Zipursky, 2004, "Afferent Induction of Olfactory Glomeruli Requires N-Cadherin", *Neuron*, Vol. 42, No. 1, pp. 77-88.

Hummel, T., M. L. Vasconcelos, J. C. Clemens, Y. Fishilevich, L. B. Vosshall, and S. L. Zipursky, 2003, "Axonal Targeting of Olfactory Receptor Neurons in Drosophila Is Controlled by Dscam", *Neuron*, Vol. 37, No. 2, pp.221-31.

Hynes, R. O., and A. D. Lander, 1992, "Contact and Adhesive Specificities in the Associations, Migrations, and Targeting of Cells and Axons", *Cell*, Vol. 68, No. 2, pp. 303-22.

Iwai Y, T. Usui, and S. Hirano, 1997, "Axon Patterning Requires DN-cadherin, a Novel Neuronal Adhesion Receptor, in the Drosophila Embryonic CNS", *Neuron*, Vol. 19, pp. 77–89.

Jarman, A.P., E.H. Grell, L. Ackerman, L.Y. Jan, and Y.N. Jan, 1994, "Atonal is the Proneural Gene for Drosophila Photoreceptors", *Nature*, Vol. 369, No. 6479, pp. 398-400.

Kanai, Y., N. Dohmae, and N. Hirokawa, 2004, "Kinesin Transports Rna: Isolation and Characterization of an Rna-Transporting Granule", *Neuron*, Vol. 43, No. 4, pp. 513-25.

Karen, L. W. S., J. P. Correia and T. E. Kennedy, 2011, "Netrins: Versatile Extracellular Cues with Diverse Functions", *Development*, Vol. 138, pp. 2153-2169.

Koh, T. W., V. I. Korolchuk, Y. P. Wairkar, W. Jiao, E. Evergren, H. Pan, Y. Zhou, K. J. Venken, O. Shupliakov, I. M. Robinson, C. J. O'Kane, and H. J. Bellen, 2007,

"Eps15 and Dap160 Control Synaptic Vesicle Membrane Retrieval and Synapse Development", *Journal of Cell Biology*, Vol. 178, No. 2, pp. 309-22.

Kolodziej, P. A., L. C., Timpe, K. J., Mitchell, S. R., Fried, C. S., Goodman, L. Y. Jan, and Y. N. Jan, 1996, "Frazzled Encodes a Drosophila Member of the DCC Immunoglobulin Subfamily and is Required for CNS and Motor Axon Guidance" *Cell*, Vol. 87, pp. 197-204.

Keleman, K. and B. J. Dickson, 2001, "Short- and long-range Repulsion by the Drosophila Unc5 Netrin Receptor", *Neuron*, Vol. 32, pp. 605-617.

Kidd, T., K. S. Bland, and C. S. Goodman, 1999, "Slit is the Midline Repellent for the Robo Receptor in Drosophila", *Cell*, Vol. 96, No. 6, pp. 785-794.

Kidd, T., K. Brose, K. J. Mitchell, R. D. Fetter, M. Tessier-Lavigne, C. S. Goodman, and G. Tear 1988, "Roundabout Controls Axon Crossing of the CNS Midline and Defines a Novel Subfamily of Evolutionarily Conserved Guidance Receptors", *Cell*, Vol. 92, No. 2, pp. 205-215.

Klagges, B. R., G. Heimbeck, T. A. Godenschwege, A. Hofbauer, G. O. Pflugfelder, R. Reifegerste, D. Reisch, M. Schaupp, S. Buchner, and E. Buchner, 1996, "Invertebrate Synapsins: A Single Gene Codes for Several Isoforms in Drosophila", *Journal of Neuroscience*, Vol. 16, No. 10, pp. 3154-65.

Knapek, S., B. Gerber, and H. Tanimoto, 2010, "Synapsin Is Selectively Required for Anesthesia-Sensitive Memory", *Learning and Memory*, Vol. 17, No. 2, pp. 76-9.

Laggerbauer, B., D. Ostareck, E. M. Keidel, A. Ostareck-Lederer, and U. Fischer, 2001, "Evidence That Fragile X Mental Retardation Protein Is a Negative Regulator of Translation", *Human Molecular Genetics*, Vol. 10, No. 4, pp. 329-38.

Lee, C.H., T. Herman, T. R. Clandinin, R. Lee, and S. L. Zipursky, 2001, "N-cadherin Regulates Target Specificity in the Drosophila Visual System", *Neuron*, Vol. 30, pp. 437-450.

Lee, R. C., T. R. Clandinin, C. H. Lee, P. L. Chen, I. A. Meinertzhagen, and S. L. Zipursky, 2003, "The Protocadherin Flamingo Is Required for Axon Target

Selection in the Drosophila Visual System", *Nature Neuroscience*, Vol. 6, No. 6, pp.557-63.

Lee T, S. Huang, C. Lee, H. Lee, H. Chan, K. Lin, H. Chan, and P. Lyu, 2012, "Proteome reference map of *Drosophila melanogaster* head", *Proteomics*, Vol. 12, pp. 1875-1878.

Long, H., C. Sabatier, L. Ma, A. Plump, W. Yuan, D. M. Ornitz, A. Tamada, F. Murakami, C. S. Goodman, and M. Tessier-Lavigne, 2004, "Conserved Roles for Slit and Robo Proteins in Midline Commissural Axon Guidance", *Neuron*, Vol. 42, No. 2, pp. 213-23.

Lu, B., P. Greengard, and M. M. Poo, 1992, "Exogenous Synapsin I Promotes Functional Maturation of Developing Neuromuscular Synapses", *Neuron*, Vol. 8, No. 3, pp. 521-9.

Lu, R., H. Wang, Z. Liang, L. Ku, T. O'Donnell W, W. Li, S. T. Warren, and Y. Feng, 2004, "The Fragile X Protein Controls Microtubule-Associated Protein 1b Translation and Microtubule Stability in Brain Neuron Development", *Proceedings of the National Academy of Sciences of the USA*, Vol. 101, No. 42, pp. 15201-6.

Majumdar, A., S. Ramagiri, and R. Rikhy, 2006, "Drosophila Homologue of Eps15 Is Essential for Synaptic Vesicle Recycling", *Experimental Cell Research*, Vol. 312, No. 12, pp. 2288-98.

Matsuoka, Y., X. Li, and V. Bennett, 2000, "Adducin: Structure, Function and Regulation", *Cellular and Molecular Life Sciences*, Vol. 57, No. 6, pp. 884-95.

Morales, J., P. R. Hiesinger, A. J. Schroeder, K. Kume, P. Verstreken, F. R. Jackson, D. L. Nelson, and B. A. Hassan, 2002, "Drosophila Fragile X Protein, Dfxr, Regulates Neuronal Morphology and Function in the Brain", *Neuron*, Vol. 34, No. 6, pp. 961-72.

Morgan, T. H., 1910, "Sex Limited Inheritance in Drosophila", *Science*, Vol. 32, No. 812, pp. 120-2.

Nogales-Cadenas, R., P. Carmona-Saez, M. Vazquez, C. Vicente, X. Yang, F. Tirado, J. M. Carazo, and A. Pascual-Montano, 2009, "Genecodis: Interpreting Gene Lists through Enrichment Analysis and Integration of Diverse Biological Information", *Nucleic Acids Research*, Vol. 37, No. Web Server issue, pp. W317-22.

Ohler S., S. Hakeda-Suzuki, and T. Suzuki, 2011, "Hts, the *Drosophila* homologue of Adducin, physically interacts with the transmembrane receptor Golden Goal to guide photoreceptor axons", *Developmental Dynamics*, Vol. 240, pp. 135-148.

Oland, L. A., G. Orr, and L. P. Tolbert, 1990, "Construction of a Protoglomerular Template by Olfactory Axons Initiates the Formation of Olfactory Glomeruli in the Insect Brain", *Journal of Neuroscience*, Vol. 10, No. 7, pp. 2096-112.

Öztürk, A., 2010, *Characterization of Genes Involved in Photoreceptor Differentiation*, M.S. Thesis, Boğaziçi University.

Pan, L., Y. Q. Zhang, E. Woodruff, and K. Broadie, 2004, "The Drosophila Fragile X Gene Negatively Regulates Neuronal Elaboration and Synaptic Differentiation", *Current Biology*, Vol. 14, No. 20, pp. 1863-70.

Petrella, L. N., T. Smith-Leiker, and L. Cooley, 2007, "The Ovhts Polyprotein Is Cleaved to Produce Fusome and Ring Canal Proteins Required for Drosophila Oogenesis", *Development*, Vol. 134, No. 4, pp. 703-12.

Pielage, J., V. Bulat, J. B. Zuchero, R. D. Fetter, and G. W. Davis, 2011, "Hts/Adducin Controls Synaptic Elaboration and Elimination", *Neuron*, Vol. 69, No. 6, pp. 1114-31.

Rajasekharan, S. and T. E. Kennedy, 2009, "The Netrin Protein Family", *Genome Biology* 10, No. 9, p. 239.

Reichert, H., 2009, "Evolutionary Conservation of Mechanisms for Neural Regionalization, Proliferation and Interconnection in Brain Development", *Biology Letters*, Vol. 5, No. 1, pp. 112-6.

Sakurai, M., T. Aoki, S. Yoshikawa, L. A. Santschi, H. Saito, K. Endo, K. Ishikawa, K. Kimura, K. Ito, J. B. Thomas, and C. Hama, 2009, "Differentially Expressed Drl

and Drl-2 Play Opposing Roles in Wnt5 Signaling During Drosophila Olfactory System Development", *Journal of Neuroscience*, Vol. 29, No. 15, pp. 4972-80.

Seeger, M., G. Tear, D. Ferres-Marco, C. S. Goodman, 1993, "Mutations Affecting Growth Cone Guidance in Drosophila: Genes Necessary for Guidance Toward or Away From the Midline", *Neuron*, Vol. 10, No. 3, pp. 409-426.

Schenck, A., V. Van de Bor, B. Bardoni, and A. Giangrande, 2002, "Novel Features of Dfmr1, the Drosophila Orthologue of the Fragile X Mental Retardation Protein", *Neurobioloy of Disease*, Vol. 11, No. 1, pp. 53-63.

Schmucker D., J. C. Clemens, H. Shu, 2000, "Drosophila Dscam is an Axon Guidance receptor exhibiting extraordinary molecular diversity", *Cell*, Vol. 101, pp. 671–684.

Soba, P., S. Zhu, K. Emoto, 2007, "Drosophila Sensory Neurons Require Dscam for Dendritic Self-avoidance and Proper Dendritic Field Organization", *Neuron*, Vol. 54, pp. 403–416.

Sofola, O., V. Sundram, F. Ng, Y. Kleyner, J. Morales, J. Botas, F. R. Jackson, and D. L. Nelson, 2008, "The Drosophila Fmrp and Lark Rna-Binding Proteins Function Together to Regulate Eye Development and Circadian Behavior", *Journal of Neuroscience*, Vol. 28, No. 41, pp. 10200-5.

Stevens, A., and J. R. Jacobs, 2002, "Integrins Regulate Responsiveness to Slit Repellent Signals", *Journal of Neuroscience*, Vol. 22, No. 11, pp. 4448-55.

Stuermer, C. A., and H. Plattner, 2005, "The 'Lipid Raft' Microdomain Proteins Reggie-1 and Reggie-2 (Flotillins) Are Scaffolds for Protein Interaction and Signalling", *Biochemical Society Symposium* 72, pp.109-18.

Sun, M. K., W. Xie, "Cell Adhesion Molecules in Drosophila Synapse Development and Function", *Science China Life Sciences*, Vol. 55, pp. 20–26, 2012.

Schwabe, T., A. C. Gontang, and T. R. Clandinin, 2009, "More Than Just Glue: The Diverse Roles of Cell Adhesion Molecules in the Drosophila Nervous System", *Cell Adhesion and Migration*, Vol. 3, No. 1, pp. 36-42.

Shinza-Kameda, M., E. Takasu, K. Sakurai, S. Hayashi, and A. Nose, 2006, "Regulation of Layer-Specific Targeting by Reciprocal Expression of a Cell Adhesion Molecule, Capricious", *Neuron*, Vol. 49, No. 2, pp. 205-13.

Sweeney, L.B., A. Couto, Y.H. Chou, D. Berdnik, B.J. Dickson, L. Luo, and T. Komiyama, 2007, "Temporal Target Restriction of Olfactory Receptor Neurons by Semaphorin-1a/Plexina-Mediated Axon-Axon Interactions", *Neuron*, Vol. 53, No. 2, pp. 185-200.

Raper, J. A., 2000, "Semaphorins and their receptors in vertebrates and invertebrates", *Current Opinion in Neurobiology*, Vol. 10, pp. 88–94.

Tabas-Madrid, D., R. Nogales-Cadenas, and A. Pascual-Montano, 2012, "Genecodis3: A Non-Redundant and Modular Enrichment Analysis Tool for Functional Genomics", *Nucleic Acids Research*, Vol. 40, No. Web Server issue, pp.W478-83.

Tamagnone, L., S. Artigiani, H. Chen, Z. He, G. Ming, H. Song, A. Chedotal, M. L. Winberg, C. S. Goodman, M. Poo, M. Tessier-Lavigne, P. M. Comoglio, 1999, "Plexins Are a Large Family of Receptors for Transmembrane, Secreted, and GPI-Anchored Semaphorins in Vertebrates", *Cell*, Vol. 99, No. 1, pp. 71-80.

Tang, H., S. B. Rompani, J. B. Atkins, Y. Zhou, T. Osterwalder, and W. Zhong, 2005, "Numb Proteins Specify Asymmetric Cell Fates Via an Endocytosis- and Proteasome-Independent Pathway", *Molecular and Cellular Biology*, Vol. 25, No. 8, pp. 2899-909.

Telonis-Scott, M., A. Kopp, M. L. Wayne, S. V. Nuzhdin, and L. M. McIntyre, 2009, "Sex-Specific Splicing in Drosophila: Widespread Occurrence, Tissue Specificity and Evolutionary Conservation", *Genetics*, Vol. 181, No. 2, pp. 421-34.

Ting, C. Y., S. Yonekura, P. Chung, S. N. Hsu, H. M. Robertson, A. Chiba, and C. H. Lee, 2005, "Drosophila N-Cadherin Functions in the First Stage of the Two-Stage Layer-Selection Process of R7 Photoreceptor Afferents", *Development*, Vol. 132, No. 5, pp. 953-63.

Ting, C. and C. Lee, 2007, "Visual circuit development in Drosophila", *Current Opinion in Neurobiology*, Vol. 17, pp. 65–72.

Tomasi, T., S. Hakeda-Suzuki, S. Ohler, A. Schleiffer, and T. Suzuki, 2008, "The Transmembrane Protein Golden Goal Regulates R8 Photoreceptor Axon-Axon and Axon-Target Interactions", *Neuron*, Vol. 57, No. 5, pp. 691-704.

Tomlinson, A., and D.F. Ready, 1987, "Neuronal Differentiation in Drosophila Ommatidium", *Developmental Biology*, Vol. 120, No. 2, pp. 366-376.

Wan, L., T. C. Dockendorff, T. A. Jongens, and G. Dreyfuss, 2000, "Characterization of Dfmr1, a Drosophila Melanogaster Homolog of the Fragile X Mental Retardation Protein", *Molecular and Cellular Biology*, Vol. 20, No. 22, pp. 8536-47.

Wilkinson, D. G., 2001, "Multiple Roles of EPH Receptors and Ephrins in Neural Development", *Natural Review Neuroscience*, Vol. 2, No. 3, pp. 155-164.

Winberg, M. L. et al., 1998, "Plexin A is a Neuronal Semaphorin Receptor That Controls Axon Guidance", *Cell*, Vol. 95, pp. 903–916.

Yao, Y., Y. Wu, C. Yin, R. Ozawa, T. Aigaki, R. R. Wouda, J. N. Noordermeer, L. G. Fradkin, and H. Hing, 2007, "Antagonistic Roles of Wnt5 and the Drl Receptor in Patterning the Drosophila Antennal Lobe", *Nature Neuroscience*, Vol. 10, No. 11, pp. 1423-32.

Yao, A., S. Jin, X. Li, Z. Liu, X. Ma, J. Tang, and Y. Q. Zhang, 2011, "Drosophila Fmrp Regulates Microtubule Network Formation and Axonal Transport of Mitochondria", *Human Molecular Genetics*, Vol. 20, No. 1, pp. 51-63.

Yonekura, S., L. Xu, C. Y. Ting, and C. H. Lee, 2007, "Adhesive but Not Signaling Activity of Drosophila N-Cadherin Is Essential for Target Selection of Photoreceptor Afferents", *Developmental Biology*, Vol. 304, No. 2, pp. 759-70.

Yue, L., and A. C. Spradling, 1992, "Hu-Li Tai Shao, a Gene Required for Ring Canal Formation During Drosophila Oogenesis, Encodes a Homolog of Adducin", *Genes and Development*, Vol. 6, No. 12B, pp. 2443-54.

Zaccai, M., and H. D. Lipshitz, 1996, "Role of Adducin-Like (Hu-Li Tai Shao) Mrna and Protein Localization in Regulating Cytoskeletal Structure and Function During Drosophila Oogenesis and Early Embryogenesis", *Developmental Genetics*, Vol. 19, No. 3, pp. 249-57.

Zhang, Y., J. P. O'Connor, M. C. Siomi, S. Srinivasan, A. Dutra, R. L. Nussbaum, and G. Dreyfuss, 1995, "The Fragile X Mental Retardation Syndrome Protein Interacts with Novel Homologs Fxr1 and Fxr2", *EMBO Journal*, Vol. 14, No. 21, pp. 5358-66.

Zhang, Y. Q., A. M. Bailey, H. J. Matthies, R. B. Renden, M. A. Smith, S. D. Speese, G. M. Rubin, and K. Broadie, 2001, "Drosophila Fragile X-Related Gene Regulates the Map1b Homolog Futsch to Control Synaptic Structure and Function", *Cell*, Vol. 107, No. 5, pp. 591-603.

Zülbahar, S., 2012, *Identification of The Role of a Novel Cell Adhesion Molecule, Unzipped, in Mediating Neuron-Glia Interactions in Drosophila*, M.S. Thesis, Boğaziçi University.